1-1-1991

Potential effects of increased atmospheric CO2 and climate change on thermal and water regimes affecting wheat and corn production in the Great Plains.

Cynthia Rosenzweig
University of Massachusetts Amherst

POTENTIAL EFFECTS OF INCREASED ATMOSPHERIC CO_2 AND CLIMATE CHANGE ON THERMAL AND WATER REGIMES AFFECTING WHEAT AND CORN PRODUCTION IN THE GREAT PLAINS

A Dissertation Presented

by

CYNTHIA ROSENZWEIG

Submitted to the Graduate School of the
University of Massachusetts in partial fulfillment
of the requirements for the degree of

DOCTOR OF PHILOSOPHY

May 1991

Department of Plant and Soil Sciences

POTENTIAL EFFECTS OF INCREASED ATMOSPHERIC CO_2
AND CLIMATE CHANGE ON THERMAL AND WATER REGIMES
AFFECTING WHEAT AND CORN PRODUCTION IN THE GREAT PLAINS

A Dissertation Presented

by

CYNTHIA ROSENZWEIG

Approved as to style and content by:

Daniel Hillel, Chairperson of Committee

John H. Baker, Member

Raymond S. Bradley, Member

Lyle E. Craker, Member

Lyle E. Craker, Department Head
Department of Plant & Soil Sciences

ACKNOWLEDGMENTS

In the course of the effort which has culminated in this doctoral degree, I have been accorded the generous assistance of the following people. I especially wish to thank my advisor, Dr. Daniel Hillel, for the privilege of being his student. I am grateful to the members of my dissertation committee, Dr. Lyle E. Craker, Dr. John H. Baker, and Dr. Raymond S. Bradley for their expert guidance on the path of research; to Dr. James Hansen, Dr. David Rind, and Dr. Frank Abramopoulos at the NASA/Goddard Institute for Space Studies for their exemplary scientific standards and long-standing support; and to Dr. Joe T. Ritchie of Michigan State University for his generous collaboration in the use of the crop models for climate change prediction. The ebullient encouragement of the late Dr. Sergej Lebedeff still reverberates in my office at GISS.

I also acknowledge Mr. Richard Goldberg for his computer programming assistance and Mr. Christopher Shashkin for his desk-top publishing skills.

My parents, George and Catherine Ropes, have been steadfast in their support of this endeavor; so they have been for all my efforts. Finally, I thank my husband, Arthur, and our children, Hannah and Jacob, for their gifts of time and love.

ABSTRACT

POTENTIAL EFFECTS OF INCREASED ATMOSPHERIC CO_2
AND CLIMATE CHANGE ON THERMAL AND WATER REGIMES
AFFECTING WHEAT AND CORN PRODUCTION IN THE GREAT PLAINS

MAY 1991

CYNTHIA ROSENZWEIG, B.S., COOK COLLEGE
M.S., RUTGERS UNIVERSITY
Ph.D., UNIVERSITY OF MASSACHUSETTS
Directed by: Professor Daniel Hillel

An analysis is presented of the responses of simulated wheat and corn growth in the Great Plains to a doubling of atmospheric carbon dioxide (CO_2). Findings are based on predictions of two global climate models (GISS and GFDL GCMs) and the CERES crop models. Modifications in the crop models reflect changes in photosynthesis and stomatal resistance caused by doubled CO_2.

Climate change alone reduced mean simulated dryland wheat yields by about one third in both scenarios; dryland corn yields were reduced by 18 and 47%. Higher temperature was the major cause of yield reductions because shorter life cycles occurred with corresponding decreases in grain-fill. Precipitation changes produced a relatively minor effect on wheat, but did diminish corn yields in some locations.

Physiological effects of increased CO_2 on simulated grain growth often compensated for negative impacts of

climate change, except when hot, dry conditions of the GFDL scenario resulted in severe yield decreases.

Simulations of climate change effects at Northern Great Plains sites indicated that winter wheat may replace spring wheat. Greater warming at high latitudes caused wheat yield decreases to be greater than or equal to those in the Southern Great Plains.

Comparison of simulated wheat and corn responses to doubled-CO_2 climate change and to observed climate of the 1930s indicated that future climate may be even more detrimental to crops than that of the past.

Irrigated yields under climate change scenarios were better maintained and less variable than dryland yields. Change in planting dates had little effect on simulated wheat and corn yields, but changing cultivars did compensate for negative climate change effects at some sites.

If higher temperatures predicted by GCMs occur, wheat and corn production as practiced in the Great Plains is likely to become more difficult to sustain.

TABLE OF CONTENTS

LIST OF TABLES

LIST OF FIGURES

CHAPTER 1

INTRODUCTION

1.1 Background

Human activity is causing the release into the atmosphere of several radiatively active gases which absorb terrestrial infrared radiation (Ramanathan, 1988). By blocking the escape of heat emitted from the earth's surface, these gases can cause a shift in the planetary energy balance, leading to higher prevailing temperatures and to changed hydrological regimes (Hansen et al., 1984). The action of these gases has been named the greenhouse effect, as it is analogous (though not completely) to the action of the glass shielding of a greenhouse.

Among the gases causing the greenhouse effect are water vapor (H_2O), and the trace gases (so-called because they are present in small, or trace, concentrations): carbon dioxide (CO_2), methane (CH_4), nitrous oxide (N_2O), tropospheric ozone (O_3), and various chlorofluorocarbons (CFCs) (Ramanathan, 1988). The latter are synthetic gases used in refrigeration, aerosol sprays, and as foaming agents.

Chief among the culprit gases is carbon dioxide. Burning of fossil fuels and eradication of forests have contributed to an increase of about 25% in CO_2 concentration (from about 275 to about 350 parts per million by volume (ppm) since the beginning of the Industrial Revolution (1750-1800) (Lashof and Tirpak, 1989; Boden et al., 1990).

Carbon dioxide concentration is continuing to increase at a rate of about 0.5% per year, with the annual increment now exceeding 1 ppm. The other trace gases are present in much smaller concentrations than CO_2, but most are increasing at even faster relative rates. Moreover, their ability to absorb longwave radiation is mostly greater than that of CO_2 (Ramanathan et al., 1985), so their combined influence has recently become quantitatively comparable to that of carbon dioxide (Hansen et al., 1989; Lashof and Tirpak, 1989).

Global climate models predict that the mean temperature rise resulting from the greenhouse effect will be in the range of 2.5 to 5.5°C for a doubling in the concentration of carbon dioxide. The Intergovernmental Panel on Climate Change, a group of international scientists convened by the World Meteorological Organization and the United Nations Environment Programme to report on climate change to policymakers, endorses a range of 1.5 to 4.5°C for CO_2 doubling, with a "best estimate" of 2.5°C (IPCC, 1990). While the exact character, magnitude, and regional distribution of the potential climate change are not yet known, some regions might be affected severely. Not only are mean temperatures likely to rise, but the incidence of extreme events, such as heat spells and droughts, may increase significantly (Hansen et al., 1989; Rind et al., 1990). Global average precipitation is also predicted to increase (IPCC, 1990).

Detecting climate change is difficult because of the natural variability of the climate system and because of the human phenomenon of urbanization. The instrumental record shows that there has been an irregular increase in global surface temperature in the last century of 0.45 +/- 0.15°C; less than 0.05°C of this increase is attributable to the urban heat island effect (IPCC, 1990; see also Hansen and Lebedeff, 1987 and 1988; Wigley et al., 1985). While reasonably consistent with the amount of trace gas accumulation, the global warming observed thus far does not yet prove that an enhanced greenhouse effect is occurring (IPCC, 1990). While large-scale analyses of observed precipitation have shown that precipitation has been increasing in the Northern Hemisphere mid-latitudes and in the Southern Hemisphere (Bradley et al., 1987; Diaz et al., 1989), it is even harder to detect evidence of the greenhouse effect in precipitation records than in temperature records, because precipitation is more variable in both temporal and spatial dimensions.

1.2 Statement of Problem

Future changes in climate are likely to have an impact on ecosystems because light, water, and temperature regimes are governing factors in the growth and reproduction of plants (Fitter and Hay, 1987). If the predictions and indications regarding the greenhouse effect are even partly correct, these consequences could be profound, leading to major environmental problems in the coming decades (Smith and Tirpak, 1989).

A drastic modification of pre-existing climatic patterns may disrupt managed vegetation, such as agriculture, as well as natural ecosystems (Hillel and Rosenzweig, 1989). Crop production and patterns may be significantly affected (Parry et al., 1988). At the same time, higher levels of atmospheric CO_2 may stimulate crop growth and improve water use because CO_2 is a necessary component of photosynthesis and also affects stomatal opening (Acock and Allen, 1985). The combined effects of climate change and increased levels of atmospheric CO_2 on crops in any one location may therefore be either positive or negative, depending upon the current climate conditions, the potential changes, and the characteristics of the crops grown (Smit et al., 1988). Current climate conditions are important because they determine, for example, if crops are at present temperature or moisture limited, or if they are growing under conditions close to their environmental optima.

This study examines the separate and combined effects that climatic and physiological factors might have upon two specific crops in a specific region. Scenarios of climate change were developed for the study using results from global climate model (GCM) simulations and the scenarios were subsequently used as inputs to crop production models. The crops chosen are wheat (Triticum aestivum L.) and corn (Zea mays L.), both major grain crops that differ in their photosynthetic pathways and consequently their response to increased CO_2.

The region chosen is the Great Plains of the United States, first because its production of wheat and corn accounts for approximately 45% and 15% of total U.S. production respectively (U.S. Dept. of Commerce, 1984), and second because the region has been sensitive to climate fluctuations in the past. Most notably, the Southern Great Plains states of Nebraska, Kansas, Oklahoma, and Texas were the hardest hit during the Dust Bowl years of the 1930s (Worster, 1979; Hurt, 1981). Some analysts argue that the region remains susceptible to climate-induced reductions in crop yields and that it will be one of the first U.S. agricultural regions to exhibit impacts of climate change (e.g., Lockeretz, 1978; Warrick, 1984).

The analysis focuses primarily on the potential impacts of CO_2 and climate change on agriculture in the Southern Great Plains, and then compares these potential impacts to how climate change may affect wheat production in the Northern Great Plains (comprised of North and South Dakota). The two sub-regions both have fertile soils and dominantly smooth topography favorable for agriculture (USDA, 1981), but they differ in present temperature and water regimes:

The Northern Great Plains has lower precipitation (250-550 mm/year) and a shorter growing season (100-155 days), while the Southern Great Plains has higher annual precipitation (500-750 mm/year) and longer growing seasons (170-180 days). These differences in current climatic conditions may cause crops in the sub-regions to differ in their responses to the greenhouse effect.

The study further compares these future impacts of climate change to occurrences in the past during the drought years of the 1930s, in order to put the magnitude of the projected yield changes in historical perspective. Finally, because farmers will not react passively to climate change, the study considers possible adaptations such as modification of irrigation systems, changes in planting date, and adoption of climatically appropriate cultivars.

This research integrates climate change predictions from the discipline of atmospheric science and experimental results from the discipline of agronomy in order to begin to project actual biophysical effects on crop production. Since both projections of future climate change and understanding of the physiological responses of crops to higher levels of atmospheric CO_2 should improve over time, the results should be regarded as preliminary. However, the study does contribute to the development of a methodology for analyzing such combined effects.

CHAPTER 2

LITERATURE REVIEW

2.1 The Greenhouse Effect

Solar radiation received on the earth's surface provides the energy that drives almost all processes in the biosphere. Nearly all of the solar radiation is in the shortwave range of 0.15 to 4.0 micrometers (μm) (Sellers, 1965). In passage through the atmosphere, solar radiation diminishes in intensity through reflection, scattering, and absorption caused by water vapor and other gases, aerosols, and suspended particles (Chandrasekhar, 1960).

The earth itself also emits radiation, but its radiation is longwave (infrared or thermal), i.e., 4 to 50 μm (Kondratyev, 1972). The atmosphere absorbs about 90% of the longwave radiation coming from the earth's surface and reradiates some of the absorbed terrestrial longwave radiation back to the planetary surface and some of it to space (Sellers, 1965). Over long periods of time, solar radiation absorbed by the earth must be balanced by thermal radiation leaving the earth and thus the earth's surface is maintained at a more or less constant mean temperature (Budyko, 1974).

If the atmosphere were transparent to the outgoing longwave radiation emitted by the earth, the equilibrium mean temperature of the earth's surface would be -18°C (Gedzelman, 1980). In reality, however, the absorption of the outgoing radiation by some of the atmospheric gases raises the mean surface temperature to 15°C (Gedzelman, 1980), a much more hospitable environment for human beings and other plant and animal species of the biosphere. This additional warming caused by the trapping of longwave radiation is known as the natural greenhouse effect and the trace gases responsible are known as the greenhouse gases.

2.1.1 Evidence

The atmospheres and surface temperatures of other planets provide evidence for the existence of the greenhouse effect. Venus is much warmer than Earth, and only part of the difference can be ascribed to its closer proximity to the sun. Venus is calculated to be 450°C warmer than if it were devoid of its atmosphere, which is rich in CO_2 (Hansen et al., 1988a). In contrast, Mars, at -53°C, is much cooler than Earth (though not proportionately farther from the sun) because of its extremely thin atmosphere (Hansen et al., 1988a).

Paleoclimatic records of glacial-interglacial CO_2 changes in the air trapped in ancient ice also suggest the validity of the greenhouse effect because they show positive correlations between atmospheric CO_2 level and temperature (Delmas et al., 1980; Neftel et al., 1982; Barnola et al., 1987). Significantly high levels of CO_2 occurred during warmer interglacial periods and low levels of CO_2 occurred during glacial periods over the last 160,000 years in Antarctica (Barnola et al., 1987). However, determination of the physical mechanisms of cause and effect between CO_2 and temperature in the past is difficult, in part because changes in both records appear almost simultaneously in the data when proceeding from glacial to interglacial conditions, while the temperature signal decreases before the CO_2 signal during transitions from warm to cold periods (Barnola et al., 1987).

2.1.2 Increases in Trace Gases

Increases in the major radiatively active trace gases (CO_2, CH_4, N_2O, O_3 and CFCs), have been measured (see Lashof and Tirpak, 1989, for a summary of measurements and characteristics). The anthropogenic increases in these trace gases are likely to augment the existing natural greenhouse effect and cause significant warming of the earth's atmosphere (IPCC, 1990; National Research Council, 1983).

The contribution of a gas to the greenhouse effect is known as its radiative, climate, or greenhouse forcing. Radiative forcing depends on the wavelength at which the gas absorbs radiation, the concentration of the gas, the strength of absorption per molecule, and whether or not other gases absorb strongly at the same wavelengths (Mitchell, 1989). Carbon dioxide is the most important and most abundant of the affected trace gases, accounting for about two-thirds of the radiative forcing from 1880 to 1980, and about one-half during the 1980s (Ramanathan et al., 1985; Hansen et al., 1988a). The increases in CO_2 since the Industrial Revolution are attributed primarily to burning of fossil fuels for industry, electricity, and transportation, and, to a lesser extent, to conversion of forests to agricultural land (Lashof and Tirpak, 1989). Tropical deforestation accounts for approximately 10-30% of the annual anthropogenic CO_2 emissions to the atmosphere (Houghton et al., 1987).

The other trace gases, especially the CFCs, are more radiatively absorptive than CO_2, but they are present in the atmosphere in smaller amounts (Lashof and Tirpak, 1989). Methane is a product of anaerobic decomposition in wetlands, rice paddies and other biological systems, and of enteric fermentation in domestic animals. Methane makes up 90% of natural gas, is present in the gas trapped in coal, and is released in the processing of most fossil fuels (Lashof and Tirpak, 1989). The steady growth of methane and its absorption strength (it absorbs infrared radiation 20 times more effectively than CO_2) has made it next to CO_2 in importance as a greenhouse gas contributor to global warming (Ramanathan et al., 1985; Hansen et al., 1988; Blake and Rowland, 1988). Methane increases were 0.0016 +/- 0.001 ppm per year over the period 1978-1987 (Blake and Rowland, 1988).

The chlorofluorocarbons, industrial chemicals used in blowing plastic foams, aerosol cans, and refrigeration, are both greenhouse gases and stratospheric ozone scavengers (Lashof and Tirpak, 1989). The CFCs destroy stratospheric ozone which selectively filters ultraviolet radiation, thereby preventing skin cancer and genetic mutations of plants and animals at the earth's surface (Watson, 1986; Emmett, 1986). As greenhouse gases, their radiative forcing is on the order of 10^4 stronger than that of CO_2 (Ramanathan, 1985). The CFCs are still increasing at about 5% per year (Lashof and Tirpak, 1989), notwithstanding recent efforts to curtail their production (Montreal Protocol, 1987). Increases in other radiatively important halocarbons range from 1.3 to 20% per year (Prinn, 1988).

Nitrous oxide is another greenhouse gas which is a stronger infrared absorber than CO_2. N_2O is emitted mainly from nitrogen metabolism of soil microorganisms, through the processes of denitrification, nitrification, nitrate dissimilation, and nitrate assimilation (Sahrawat and Keeney, 1986). Additions of nitrogen fertilizers enhance soil emissions of N_2O; other sources are the oceans, contaminated aquifers, and combustion (Lashof and Tirpak, 1989).

2.2 Global Climate Models (GCMs)

While even an elementary understanding of the earth's energy balance is sufficient to predict that progressive increases in the concentration of the greenhouse gases should eventually lead to global warming, more sophisticated tools are needed to quantify the predictable effect in terms of the many variables composing the overall climate. Global climate models (GCMs) are such tools. GCMs calculate the temporal and spatial transports and exchanges of heat and moisture throughout the earth's surface and atmosphere. Some of the interactions involved in these processes may reinforce a greenhouse warming and can therefore be termed positive feedbacks, whereas some may lessen the warming and can be referred to as negative feedbacks.

2.2.1 Description

Global climate models (GCMs) are mathematical formulations of the atmospheric, oceanic, ice, and land-surface processes which enter into the prediction of climate change (Henderson-Sellers and McGuffie, 1987). GCMs simulate climate by solving the fundamental equations for conservation of mass, momentum, energy, and water for the boundary conditions relevant to earth's principal features. With the relevant parameters, those equations constitute numerical representations of radiation, turbulent transfers at the ground-atmosphere boundary, cloud formations, condensation and precipitation of moisture, transport of heat by ocean currents, and other physical processes.

2.2.2 Equilibrium Climate Change

At least ten GCMs have been developed by various research groups in the U.S. and other countries. Of these, about six have been used to simulate the effects of greenhouse gas increases (MacCracken and Luther, 1985; Grotch, 1988; IPCC, 1990). Typically, calculations are made with a doubling of CO_2 concentration, which is then taken to represent the combined radiative forcing of all the greenhouse gases (e.g., CO_2, CH_4, N_2O, CFCs, etc.) equivalent to that of doubled CO_2. Results from these numerical simulations show a mean global warming in the range of 1.3°C to 5.2°C. The GCM doubled-CO_2 simulations also result in an increase in global precipitation (precipitation increases range from 2.7 to 15.8%). This result is reasonable because the saturated vapor pressure of water increases with temperature, allowing warmer air to hold more water vapor. Thus, at higher temperatures, equal downward temperature fluctuations result in more condensation.

The GCMs further predict that:

(1) The high latitudes will experience greater warming than the equatorial regions (Hansen et al., 1981). High latitudes are subject to greater-than-average warming in the GCM simulations because the melting of snow and ice should

reduce the albedo (thus allowing more of the incoming solar radiation to warm the earth) and also because the stable polar air (with less vertical mixing) is likely to keep the warmed air near the surface.

(2) The mid-latitude mid-continental land areas are likely to undergo a drying trend, because of earlier snowmelt, increased runoff, and increases in potential and actual evaporation (Manabe and Wetherald, 1987; Kellogg and Zhao, 1988).

(3) Ice on sea and land will tend to melt and the transfer of snow and ice from land to sea by melting or deglaciation may result in a rise in sea level (as long as these effects are not offset by additional accumulation of snowfall on land) (Hoffman et al., 1983). Thermal expansion of ocean water would also contribute to sea-level rise, because warming will decrease the density of the top layers of the ocean, thus increasing its volume (Hoffman et al., 1983).

2.2.3 Transient Climate Change

GCM scenarios representing an abrupt doubling of CO_2 concentration constitute a synthetic climate, since in reality the changes in atmospheric composition are gradual. A few simulations with the Goddard Institute for Space Studies (GISS) GCM have been made with more realistic trace gas forcings, e.g., continued exponential growth of emissions, fixed annual growth of greenhouse forcing, and a leveling of emissions after the year 2000 (Hansen et al., 1988b). The GISS GCM transient simulations with the three different growth rates of trace gas emissions all produced global warming equivalent to the warmest periods in the current and previous interglacial period. Furthermore, the authors conclude that the predicted warming should be discernible in observed records in the coming decades, because simulated temperatures for the near future were at least three standard deviations above the climatology of the 1950s. Ocean areas both near Antarctica and the North Pole warm, relative to interannual variability, rapidly in the GISS GCM transient runs.

Simulations with the Geophysical Fluid Dynamics Laboratory (GFDL) and National Center for Atmospheric Research (NCAR) GCMs with explicit heat transport by ocean currents have also been performed to analyze the transient response of climate to gradually increasing atmospheric CO_2 (Washington and Meehl, 1989; Stouffer et al., 1989). The transient simulation with the NCAR GCM produced patterns of regional climate anomalies that differed from those produced by an instantaneous CO_2 doubling case, particularly in the North Atlantic and northern European regions (Washington and Meehl, 1989). These results led the authors to conclude that instantaneous doubled-CO_2 simulations may not be analogous to those done with slowly increasing CO_2.

In contrast to the GISS GCM transient runs, the GFDL GCM simulation exhibited interhemispheric asymmetry in that the increase of surface air temperature was less in the Southern Hemisphere, while the Northern Hemisphere warmed more at higher latitudes (Stouffer et al., 1989). The North Atlantic warmed slowly because weakened thermohaline circulation (due to increased runoff and precipitation over evaporation) in the ocean reduced northward advection of warm and saline subtropical surface water.

2.2.4 Strengths and Weaknesses

The advantages of GCMs as predictors of climate change are their consistent internal logic, inclusion of simultaneous and interacting processes, and global integration. Their limitations result from incompletely understood ocean circulation patterns, lack of knowledge concerning the formation and feedback effects of clouds (whether positive or negative), simplistically formulated hydrological processes, and coarse spatial resolution. Consequently, existing GCMs often fail to give accurate simulations of current regional climates, raising uncertainties about the predictions of future regional climates needed for impact assessment studies (see, for example, Grotch, 1988). Mitchell et al. (1987) showed that differences in current climate representation affect the regional response of climate models to perturbations such as doubled CO_2 and sea surface temperature increases. This result again emphasizes the need for accurate simulations of present day climate as a basis for the estimation of future climate.

2.3 Dynamic Crop Models

Dynamic plant growth simulation models describe the state of the crop quantitatively and progressively in terms of defined state variables (Rimmington and Charles-Edwards, 1987). In a dynamic model, the present state of a system depends on the initial conditions and on the influence of all the inputs up to the present. Dynamic plant growth models formulate the principal physiological, morphological, and physical processes involving the transfers of energy and mass within the crop and between the crop and its environment. There exists a continuum of empirical and functional relationships in the structure of these models. From these relationships, the models derive predictions of integrated crop performance under various conditions (Loomis et al., 1979). Such models have been developed for most of the major grain crops, with the aim of predicting their responses to specified climatic, edaphic, and management factors governing production (Joyce and Kickert, 1987). Crop growth models capable of simulating the response of agricultural plants to climatic variables may be used in conjunction with GCM climate change scenarios to explore the consequences of increased atmospheric CO_2 and climate change on yields.

2.4 Physiological Effects of Increased CO_2

A large body of literature on the physiological effects of increased atmospheric CO_2 on crops is available (Lemon, 1983; Acock and Allen, 1985; Cure, 1985; and Rose, 1988). Plants growing in greater atmospheric CO_2 concentrations exhibit increased rates of photosynthesis and net photosynthesis (defined as total photosynthesis minus respiration), and associated increases in accumulated biomass and yield. Another physiological effect of CO_2 enrichment is the partial closure of stomates, the small openings in leaf surfaces through which the CO_2 used in photosynthesis is absorbed and the water vapor of transpiration is released.

2.4.1 Photosynthetic Responses

As the concentration of carbon dioxide in the air rises, the diffusion gradient increases between the outside and inside of the leaf, thus enriching the substomatal cavity with CO_2. In C3 plants, CO_2 enrichment has been shown to decrease photorespiration, the rapid oxidation of sugars recently formed by photosynthesis in the light, a process which inhibits photosynthesis. Photorespiration occurs because the chief photosynthetic enzyme, ribulose-

1,5-bisphosphate (RuBP or rubisco) functions both as an oxygenase or a carboxylase. Under current ambient CO_2 concentrations the photorespiratory oxygenase reaction is favored; under higher CO_2 concentrations more carboxylation occurs, resulting in higher rates of photosynthesis (Tolbert and Zelitch, 1983).

C4 plants are a priori more efficient photosynthetically under current CO_2 levels than C3 plants, because they fix CO_2 into malate in their mesophyll cells before delivering it to the RuBP enzyme in the bundle-sheath cells. Probably because of this CO_2-concentrating and photorespiration-avoiding mechanism, experimental data show that C4 plants are less responsive to CO_2 enrichment (Tolbert and Zelitch, 1983).

Some crop plants reduce their response to higher CO_2 levels over time, with photosynthetic rates declining to levels only slightly higher than those observed for presently ambient atmospheric concentrations of CO_2 (Azcon-Bieto, 1983). A possible explanation is that an increased level of leaf sucrose (the major end product of photosynthesis in most leaves) tends to inhibit further sucrose production in the Calvin cycle and to promote the synthesis of starch which is less readily exported from the chloroplast (Huber et al., 1984). Apart from that process, the plant itself may be unable to utilize increased assimilates due to its genetically limited carbohydrate sinks (e.g., small grain size or quantity), and may therefore fail to sustain a positive response to increased CO_2 over a period of time (Acock and Allen, 1985).

The above limitations notwithstanding, it appears that increased CO_2 does produce more biomass and yield for many crops at moderate temperatures (less than 30°C). Kimball (1983) reviewed 70 research reports and calculated an average yield increase for C3 crops of 33% with a doubling of atmospheric CO_2. Leaf areas of soybeans, wheat, and cotton increased (Jones et al., 1984; Schönfeld et al., 1989; and Kimball et al., 1984), as did leaf thicknesses (Thomas and Harvey, 1983). Corn, which has the C4 photosynthetic pathway, also showed higher total dry matter production and yields at doubled CO_2 concentrations (King and Greer, 1986).

2.4.2 Transpiration Responses

The stomatal conductances of 18 agricultural species have been observed to decrease markedly (by 36%, on average) in an atmosphere enriched by doubled CO_2 (Morison and Gifford, 1984). Although the stomates of C4 plants were previously thought to close more in response to CO_2 than the those of C3 plants, Morison and Gifford (1983) reported that the stomates of C3 and C4 species are equally sensitive to CO_2 levels.

Stomatal closure reduces transpiration per unit leaf area (Larcher, 1980). However, transpiration per plant or per ground area may not exhibit a commensurate reduction with higher atmospheric CO_2 levels, and may even rise, as plants growing in higher CO_2 levels almost always develop a greater leaf area over which to transpire (Allen et al., 1985). This may be the reason why data from recent studies indicate little or no change in overall transpiration or evapotranspiration with higher CO_2 levels, as decreases in individual leaf conductance tend to be offset by increases in crop leaf area (Allen et al., 1985). In any case, the crop water-use efficiency (a measure of the yield per unit amount of water transpired) tends to rise with increased CO_2 (Acock and Allen, 1985).

Another consequence of stomatal closure and the concomitant reduction in transpiration (and hence also of latent heat loss) is a rise in the sensible heat absorbed by the leaves. Leaf and/or canopy temperatures have risen from 1° to 3°C when plants were exposed to elevated concentrations of CO_2 in controlled-environment chambers (Chaudhuri et al., 1986; and Idso et al., 1987a). This rise in leaf temperature induces greater transpiration and respiration, thus tending to offset in part the improvement in water use efficiency (Allen et al., 1985).

2.4.3 Interaction with Thermal Regimes

A few experiments have been conducted with both high CO_2 concentrations and high temperatures. In several cases, high CO_2 contributed to upward shifts in temperature optima for photosynthesis (Jurik et al., 1984) and to enhanced growth with higher temperatures (Idso et al., 1987b). Results of other experiments suggest that higher air temperatures combined with high CO_2 concentrations may not enhance plant development and yield in crops such as spring wheat (Wall and Baker, 1987) and soybeans (Jones et al., 1985; Baker et al., 1989). Growth and development responses and yields of soybeans grown at high day/night temperatures (31/24°C and 36/29°C) and high CO_2 concentrations (660 ppm) were relatively lower than the responses of soybeans grown at lower temperatures (26/19°C) and high CO_2 (Baker et al., 1989).

Higher temperatures in general hasten plant maturity in annual species, thus shortening the growth stages during which pods, seeds, grains or bolls can absorb photosynthetic products. Because crop yield depends on both the rate of carbohydrate accumulation and the duration of the filling periods, the economic yields of some crops grown in a warmer and CO_2-enriched environment may not rise substantially above present levels, despite increases in net photosynthesis (Rose, 1989).

Yields of determinate plants (i.e., those with finite growth potential) may be more negatively affected by increased temperatures than yields of indeterminate plants, which can continue to reproduce indefinitely. For example, indeterminate soybean varieties were observed to be more responsive to CO_2 enrichment than determinate varieties (Ackerson et al., 1984). Moreover, some of the highest yield responses to CO_2 enrichment (an overall average increase of 70%) have been reported for the indeterminate crop cotton (Kimball et al., 1986).

2.5 Linking GCMs and Dynamic Crop Models

The combination of GCMs and dynamic crop growth models provides a means to evaluate the relative contributions of the climatic and the physiological effects that the rise in greenhouse gases may have on agricultural crops (WMO, 1985).

2.5.1 Requirements for Linkage

To accomplish such an evaluation, the crop growth models must account for the primary responses for CO_2 enrichment, which have been defined as photosynthesis, photorespiration, dark CO_2 fixation, and stomatal aperture (Strain, 1985), and their interactions with temperature. Dark respiration is not included as a primary response because little is known about the effects of elevated CO_2 concentration on respiration rates (Bazzaz, 1990).

The crop models can then be run with baseline and changed atmosphere scenarios to investigate potential changes in yield, evapotranspiration, crop growing season, and irrigation requirements. Owing to climate model limitations, however, the representation of current climate simulated by GCMs may not be accurate enough for direct use in crop models on a daily basis for either current or changed climates (Bach, 1988). Therefore, most climate change scenarios devised are hybrids of GCM simulation results and observed climate data (Parry et al., 1988; Smith and Tirpak, 1989).

2.5.2 Previous Studies

Previous climate change agricultural impact studies have typically considered climate change effects alone, without accounting for the physiological effects of CO_2 on crop growth. Thus, results from GCMs have been used to study impacts of CO_2-induced climate change on West European agriculture (Santer, 1985), potential shifts in the U.S. corn belt (Blasing and Solomon, 1984), potential impacts on North American wheat-producing regions (Rosenzweig, 1985), yields of spring wheat in Saskatchewan, Canada (Stewart, 1986), and implications for Ontario's agriculture sector (Smit et al., 1989). An international study combined agronomic and economic effects of GCM climate change scenarios in high-latitude regions (Parry et al., 1988).

Relatively few studies have specifically addressed both climatic and physiological effects of CO_2. Stewart (1986) and Robertson et al. (1987) have reported on the potential combined effects in various locations in the Great Plains. Peart et al. (1989) and Ritchie et al. (1989) have simulated the combined effects in the Southeast and Great Lakes regions of the U.S., respectively.

2.6 Climate Change in the Great Plains

The Great Plains region has been sensitive to climate fluctuations in the past, most notably during the Dust Bowl years of the 1930s (Worster, 1979; Hurt, 1981). This sensitivity to past climate makes the region a candidate for analysis of the potential impacts of future climate change (Smith and Tirpak, 1989).

2.6.1 Description of Region

The Great Plains region in the U.S. is a predominantly treeless expanse of relatively flat topography stretching from the Rocky Mountains in the west to the Corn Belt of Iowa and Missouri in the east, and from the Texas panhandle in the south to the Canadian prairie in the north. The natural vegetation, now mostly plowed under, is primarily short-grass prairie, because there is not enough soil moisture to sustain either tall-grass species or tree roots (Frazier, 1989). Nearly 100,000 farms in the Southern Great

Plains (Nebraska, Kansas, Oklahoma, and Texas), occupying over 111 million acres, produce about 33% of the nation's wheat and about 14% of the nation's corn (U.S. Department of Commerce, 1984). The Northern Great Plains (North Dakota and South Dakota) produce an additional 12% of the total wheat grown in the United States.

2.6.2 Dryland Agriculture in the Region

Although irrigation is important in certain areas, agriculture in the Great Plains region is primarily dryland farming, and therefore is vulnerable to climatic stresses, such as the severe droughts that occurred in the 1930s (Worster, 1979; Hurt, 1981). Even with the adoption of conservation tillage techniques, drought-resistance cultivars, and risk management programs, some analysts argue that this region is likely to be one of the first agricultural regions in the U.S. to suffer the impacts of the enhanced greenhouse effect (Riebsame, 1990).

The danger of renewed episodes of serious land degradation and economic losses have been made more likely by the rapid acreage increases in the 1970s, accompanied by the elimination of windbreaks aimed at forming larger fields so as to accommodate bigger machinery. The dangers will be exacerbated if the predicted climate change brings about an increased frequency and severity of heat waves and droughts in the region. Some climate models predict a general drying trend in the Great Plains, along with the warming trend (Manabe and Wetherald, 1987), a dual effect which points to especially negative impacts on dryland farming and an increased demand on the already depleted groundwater supplies for irrigation.

2.6.3 Irrigated Agriculture in the Region

Farmers who practice irrigation are less vulnerable to climate change than dryland farmers, provided, of course, that the former are assured of a continuing supply of water. In 1982, 19 million acres, or 12% of the cropland in the Great Plains, mostly in the southern Plains, were irrigated. Groundwater supplies most of the water for irrigation: 61 to 86% of the water used in Nebraska, Oklahoma, and Kansas, compared with only 20% nationally. The improvement and application of well drilling and pumping technology after World War II permitted the use of water from the immense Ogallala Aquifer. In 1982, the aquifer supplied irrigation for approximately 14 million acres in the Great Plains States of Colorado, Nebraska, Kansas, Oklahoma, New Mexico, and Texas (High Plains Associates, 1982). The aquifer allows the irrigation of terrain too far from surface supplies, and provides water for municipal and industrial purposes as well. The southern section of this aquifer, however, is already seriously depleted.

The Ogallala aquifer varies spatially in the depth of the water table, in the rate of natural recharge, and in the saturated thickness of the water-bearing strata (Frederick and Hanson, 1982). In Texas and its neighboring areas of Oklahoma and New Mexico, where the Ogallala has long been tapped chiefly for cotton (and to a lesser extent for corn, wheat, and sugarbeets), the depletion has been most serious. Here, the high withdrawal and low recharge rates have resulted in "mining" of the resource and have recently forced the abandonment of thousands of formerly irrigated acres (Wilhite, 1988). In Nebraska, where the aquifer has a higher recharge rate than in the southern areas, significant drawdown problems have not yet occurred. Farmers in Nebraska recently began to use the aquifer to irrigate corn, which is grown mostly for livestock feed. Glantz and Ausubel (1984) have argued, in any case, that projections of the region's future must include consideration of its diminishing water resources as well as of its susceptibility to future droughts such as are projected by GCM simulations, since both factors are critical to the future of agriculture in the area.

2.6.4 Drought Years of the 1930s

The Great Plains states of Nebraska, Kansas, Oklahoma, and Texas were the hardest hit during the drought years of the 1930s (Worster, 1979; Hurt, 1981). During this disastrous decade, wheat yields fell as much as 26% below normal (Warrick, 1984) and corn yields dropped as much as 50% below normal. Low crop yields, year after year, led to the failure of about 200,000 farms and migration of more than 300,000 people from the region. In Oklahoma, the net migration was about 18% of the state's population in 1930 (Warrick and Bowden, 1981).

2.6.5 Prior Studies

Several systematic modeling studies exist of climate change impacts on agriculture in the Great Plains. Warrick (1984) reported that a recurrence of 1930s conditions would reduce wheat yields by over 50%, based on a study with a statistical model for dryland crop yield combining 1975 technology together with 1934 and 1936 temperature conditions. Terjung et al. (1984), using a crop water demand and yield model, concluded that evapotranspiration and total water applied for irrigation are still very sensitive to climate variations in the Central Great Plains. Liverman et al. (1986), in a another study with the same model, observed that the lowest simulated yields from both irrigated and dryland cropping occurred under hot and dry climatic conditions.

As mentioned above, several studies have combined the potential effects of climate change with the physiological effects of CO_2 for sites in the Great Plains. Stewart

(1986) projected negative yields for spring wheat in Saskatchewan; the simulations of Robertson et al. (1987) resulted in increase in winter wheat and corn yields in North Dakota, and a decrease in winter wheat yields and an increase in corn in Texas.

CHAPTER 3

METHODS

3.1 CERES Crop Models

The CERES crop models were chosen for this study because they simulate physiological crop responses to the major factors of climate, soils, and management. They have been validated with independent field experiment data over a wide range of environments, making them suitable for projecting the potential yield changes in the Great Plains, in which climate ranges from semitropical in southern Texas to midcontinental in the Dakotas. Predictive capability for climate change is also enhanced by robust validation.

3.1.1 Description

The CERES models (Ritchie and Otter, 1985; Jones and Kiniry, 1986) employ simplified functions to predict the growth and yield of wheat and corn as influenced by plant genetics, weather, soil, and management factors. Modeled processes include phenological development (Hodges, 1991), vegetative and reproductive plant development stages, partitioning of photosynthates, growth of leaves and stems, senescence, biomass accumulation, and root system dynamics. The CERES models also simulate the effects of soil-water deficits and nitrogen deficiencies on photosynthesis and the pathways of carbohydrate movement in the plant.

The CERES models have been validated with numerous independent test plot data (Figure 3.1) (Otter-Nacke et al., 1986; Jones and Kiniry, 1986); for these validation comparisons between observed and simulated yields, the Fisher Z transformation is 13.5 and 6.3 standard deviations away from 0 correlation for wheat and corn, respectively.

In the CERES models, the input variables are the daily solar radiation (MJ m^{-2} day^{-1}), maximum and minimum air temperatures (°C), and precipitation (mm day^{-1}). Windspeed and direction are not included because data are not readily available; therefore the explicit effects of wind on evapotranspiration and of wind damage on the wheat crop are not considered. Starting day of year, plant population (plants m^{-2}), row spacing (cm), depth of sowing (cm), and irrigation regime are specified at the beginning of a simulation, as well as the latitude of the site, soil characteristics and initial conditions of the soil profile, and genetic coefficients of the crop variety.

The soil characteristics that are entered into the model are: soil albedo, upper limit of Stage 1 soil evaporation (mm), soil-water drainage constant, and the USDA Soil Conservation Service curve number which is used to calculate runoff. For each soil layer, there are parameters describing the lower limit of plant extractable soil water, the drained upper limit water content, the saturated water

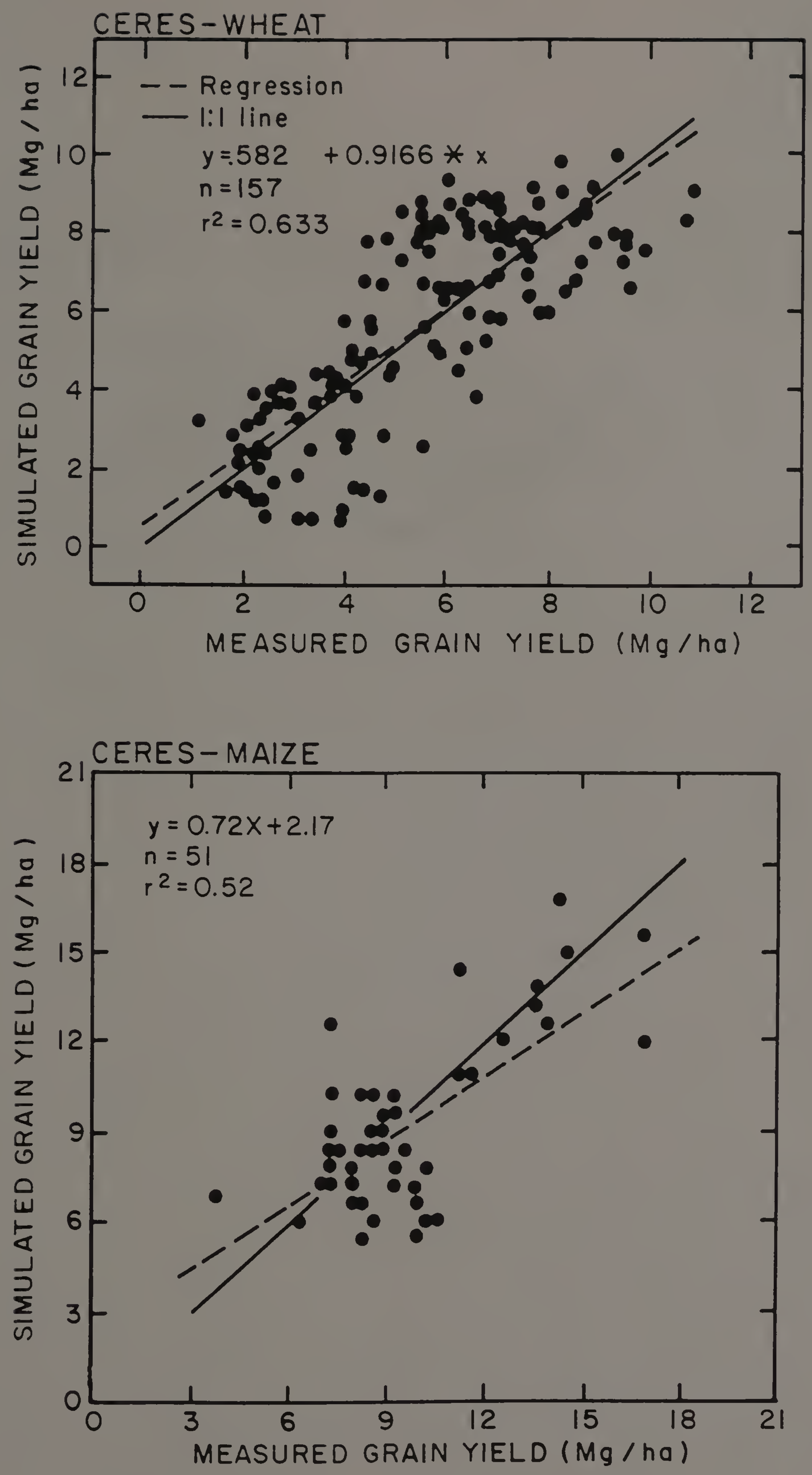

Figure 3.1 Simulated versus measured yields for CERES-Wheat and CERES-Maize. Sources: Otter-Nacke et al. (1986); Jones and Kiniry (1986).

content, and the initial soil water content (all as volume fraction). In addition, the model requires values for the soil bulk density and a weighting factor for the distribution and extent of root growth.

The genetic coefficients for CERES-Wheat relate to photoperiod sensitivity, duration of grain filling, conversion of biomass to grain number and grain filling, vernalization, stem size, tillering habit, and cold hardiness. For CERES-Maize, the genetic coefficients are the thermal time required from emergence to end of juvenile stage, photoperiod sensitivity coefficient, thermal time required for grain filling, potential kernel number, and maximum daily rate of kernel fill.

3.1.2 Limitations

The major limitation of the CERES models for use in climate change impact analysis is that the empirical relationships used in these models were derived under current climate conditions and may not be valid for a changed climate. Most of the data used to derive the models were obtained at temperatures below 35°C, whereas the projected doubled-CO_2 temperatures often exceed 35° and may even exceed 40°C during parts of the growing season (See Appendix D).

Some other assumptions of these models, as used in this study, are that nutrients are non-limiting; that weeds, diseases, and insect pests do not constrain yields; and that there are no deleterious soil conditions or catastrophic weather events. These assumptions all tend to bias simulated yields upwards. Finally, agronomic practices and technology, as well as the climatic tolerances of crop cultivars, are held constant, even though these management variables are likely to be adapted to changing climate.

3.2 Modifications for CO_2 Enrichment

A method was developed to approximate the changes in photosynthesis and evapotranspiration caused by a doubling of CO_2 from 330 to 660 ppm (Peart et al., 1989). The method was designed to be applicable under both current and changed climate conditions. Ratios were calculated between measured daily photosynthesis and evapotranspiration rates for a canopy exposed to 660 ppm CO_2 and those rates of the same canopy exposed to 330 CO_2, from published reports of controlled environment experiments. These ratios based on empirical data were then applied to the rates of photosynthesis and evapotranspiration computed by the model for current CO_2 concentrations (Table 3.1).

3.2.1 Photosynthesis

Published experimental results for crops grown in doubled-CO_2 atmospheres were reviewed to obtain estimates of increases in canopy photosynthesis for both corn and wheat.

Table 3.1 Photosynthesis ratio and leaf stomatal resistance (seconds/meter) used in CERES modifications for CO_2 enrichment.

PHOTOSYNTHESIS RATIO

Wheat	1.25	(based on Cure, 1985)
Corn	1.10	

LEAF STOMATAL RESISTANCE (s/m)

	330ppm	660ppm	
Wheat			
dryland	78	75	(Chaudhuri *et al*., 1986)
irrigated	48	63	
Corn	56	106	(Rogers *et al*., 1983)

Instantaneous corn canopy photosynthesis in midday was observed to increase by 15% (Peart et al., 1989). Consequently, the daily integrated increase was set at 10% in CERES-Maize, to allow for lower light intensities in morning and evening. This value is consistent with data regarding plant light-use efficiency at normal and high CO_2 concentrations given by Charles-Edwards (1982).

The photosynthetic response of wheat to a doubling of CO_2 appears to lie between that of soybeans (with a reported increase of 35%, according to Peart et al., 1989) and that of corn (10%, as above; see also Cure, 1985). Therefore an intermediate value of 25% increase to daily canopy photosynthesis was simulated in the CERES-Wheat model.

Although the CERES models include the effects of water stress and temperature on growth and yield, there are no explicit formulations for the relation of these factors to level of CO_2 per se. Changes in respiration, likewise, are not taken into account explicitly.

3.2.2 Evapotranspiration

To account for the effect of elevated carbon dioxide on stomatal closure and increased leaf area index, and hence on potential transpiration (see Hillel, 1990, for a discussion of potential evapotranspiration), the evapotranspiration formulation of the CERES models was changed to include a ratio of transpiration under elevated CO_2 conditions to that under ambient conditions. This was developed from the Penman-Monteith formula (as written in France and Thornley, 1984):

$$\lambda E = \frac{s\ R_n + c_p\ \rho\ (p_s(T_a) - p_a)\ g_a}{s + \gamma(1 + g_a/g_c)} \qquad (3.1)$$

where λE is evapotranspiration rate in energy units, s is the slope of the saturated vapor pressure - temperature curve, γ is the psychrometric constant, R_n is net radiation, c_p is specific heat of the air at constant pressure, ρ is the density of air, $(p_s(T_a) - p_a)$ is the vapor pressure deficit of the air, g_a is the boundary layer conductance between the canopy and the bulk air, and g_c is the canopy conductance to water vapor.

To derive the ratio, Peart et al. (1989) applied the Penman-Monteith equation to the same canopy and environment, except for differing CO_2 concentrations. The only variable which is changed thereby is the canopy conductance to vapor transport. Thus, a ratio of evapotranspiration rates under elevated and ambient CO_2 concentrations is obtained:

$$\text{RATIO} = \frac{\lambda E^c}{\lambda E} = \frac{s + \gamma\ (1+g_a/g_c)}{s + \gamma\ (1+g_a/g_c^c)} \qquad (3.2)$$

where g_c^c is the canopy conductance to water vapor under elevated CO_2 conditions.

The canopy resistance is computed by

$$R_c = (r_L + r_b)/LAI \tag{3.3}$$

where r_L is the leaf stomatal resistance (s m^{-1}), LAI is the leaf area index, and r_b is the leaf boundary layer resistance.

Then, the canopy conductances for ambient and elevated CO_2 (g_c and g_c^c) were computed by:

$$g_c = 1/R_c$$

$$g_c^c = 1/R_c^c \tag{3.4}$$

In CERES-Wheat, stomatal resistance values for well-watered (0.48 and 0.63 s cm^{-1}) and drought-stressed (0.78 and 0.75 s cm^{-1}) winter wheat under 330 and 660 ppm were specified from Chaudhuri et al. (1986) for irrigated and dryland runs, respectively. These experimental results show that elevated CO_2 increased stomatal resistance of well-watered wheat plants, but decreased it slightly for drought-stressed plants.

For corn, leaf resistance was calculated as a function of CO_2 concentration using the equation developed by Rogers et al. (1983).

$$r_s = 1/(3.28 \times 10^{-2} - 5.49 \times 10^{-5} [CO_2] + 2.96 \times 10^{-8} [CO_2]^2) \quad (3.5)$$

Temperature, wind speed, LAI and CO_2 concentration are needed to calculate RATIO (Equation 3.2). Average daily temperature was computed from maximum and minimum temperatures, which are inputs to the CERES models; windspeed was set at 2.0 m s^{-1}. LAI was specified directly as calculated in the models. The ratio procedure results in a lower transpiration rate for higher CO_2 levels on a daily basis. Seasonal evapotranspiration, however, may not change proportionately, and may even increase, because of the greater leaf area grown under elevated CO_2 conditions.

3.2.3 Limitations

The simulated physiological effects of CO_2 in this study, although based on experimental results, are arbitrary and may be overestimated for two reasons. First, experimental results from controlled environments used as inputs to the model may not represent variable, windy, and pest-infested field conditions (Rose, 1989). Second, the simulations attribute the entire greenhouse effect to a concentration of 660 ppm CO_2, ignoring the actual increase in other radiatively active gases which are likely to raise temperature without enhancing photosynthesis. A warming equivalent to doubled-CO_2 may occur when atmospheric concentration is only about 550 ppm, given current emissions growth rates (Hansen et al., 1988b). Other limitations of the model modifications are that differences in canopy temperature, canopy height, and leaf vapor pressure with increased CO_2 were not taken into account; neither were changes in photosynthesis versus light intensity relationships under the higher CO_2 concentration.

3.3 Study Sites and Baseline Data

The CERES-Wheat and CERES-Maize models were run with climate, soil, and management inputs specified for twelve and fourteen locations, respectively, in Nebraska, Kansas, Oklahoma, and Texas. The sites were chosen because observed climatic variables (daily maximum and minimum temperatures and total daily precipitation from 1951-1980) were available for model inputs and because the sites were geographically distributed around the region. Mean monthly maximum and minimum temperature and precipitation for the fourteen sites are shown in Figure 3.2. The climate records are from the National Climate Data Center, Asheville, NC, provided by Dr. Roy Jenne of the National Center for Atmospheric Research. The missing data, calculated by Dr. Amos Eddy of the Oklahoma Climatological Survey, were derived from interpolations of data from neighboring stations.

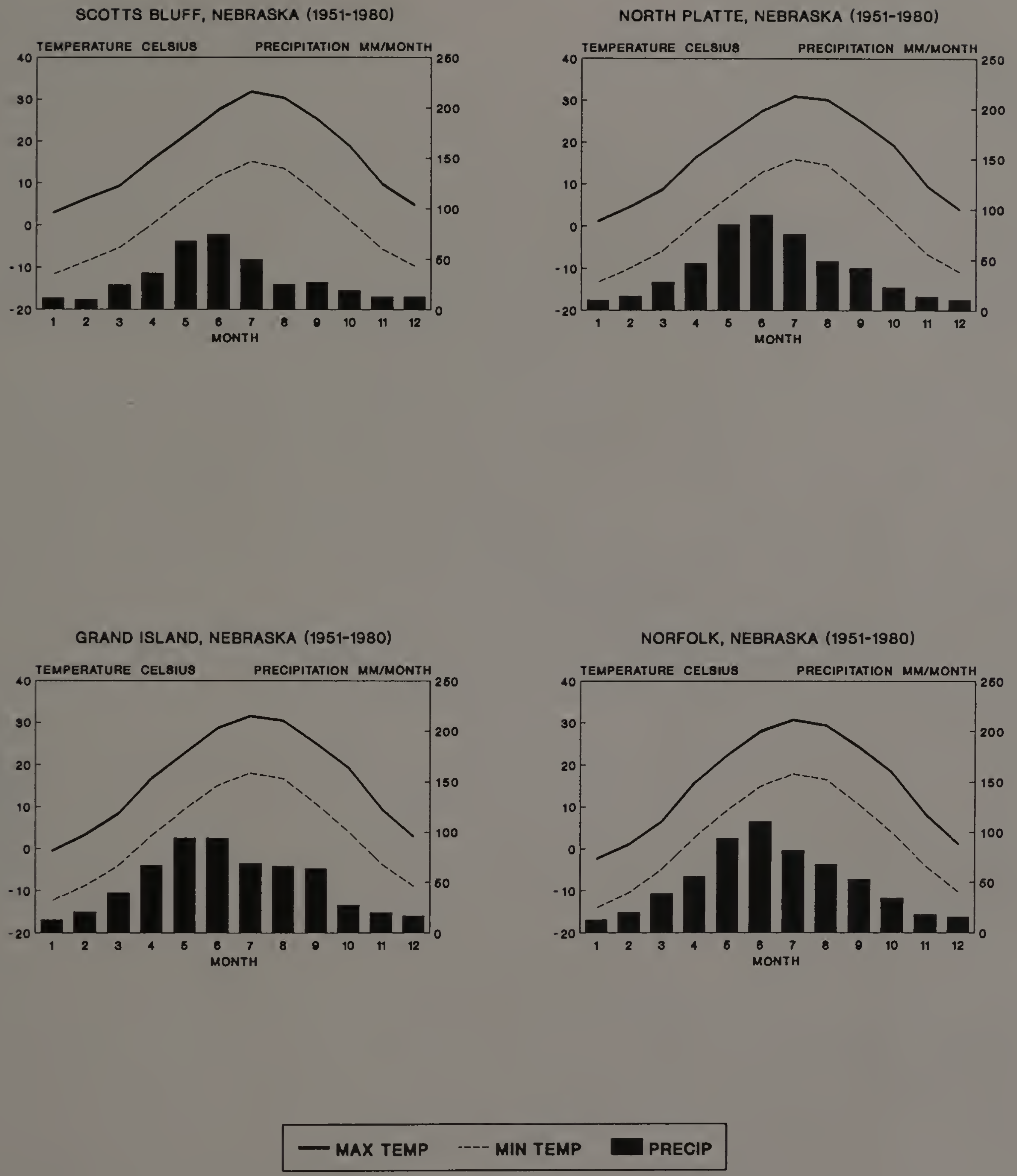

Continued, next page

Figure 3.2 Mean monthly maximum and minimum temperature and precipitation for Southern Great Plains study sites.

Figure 3.2 Continued

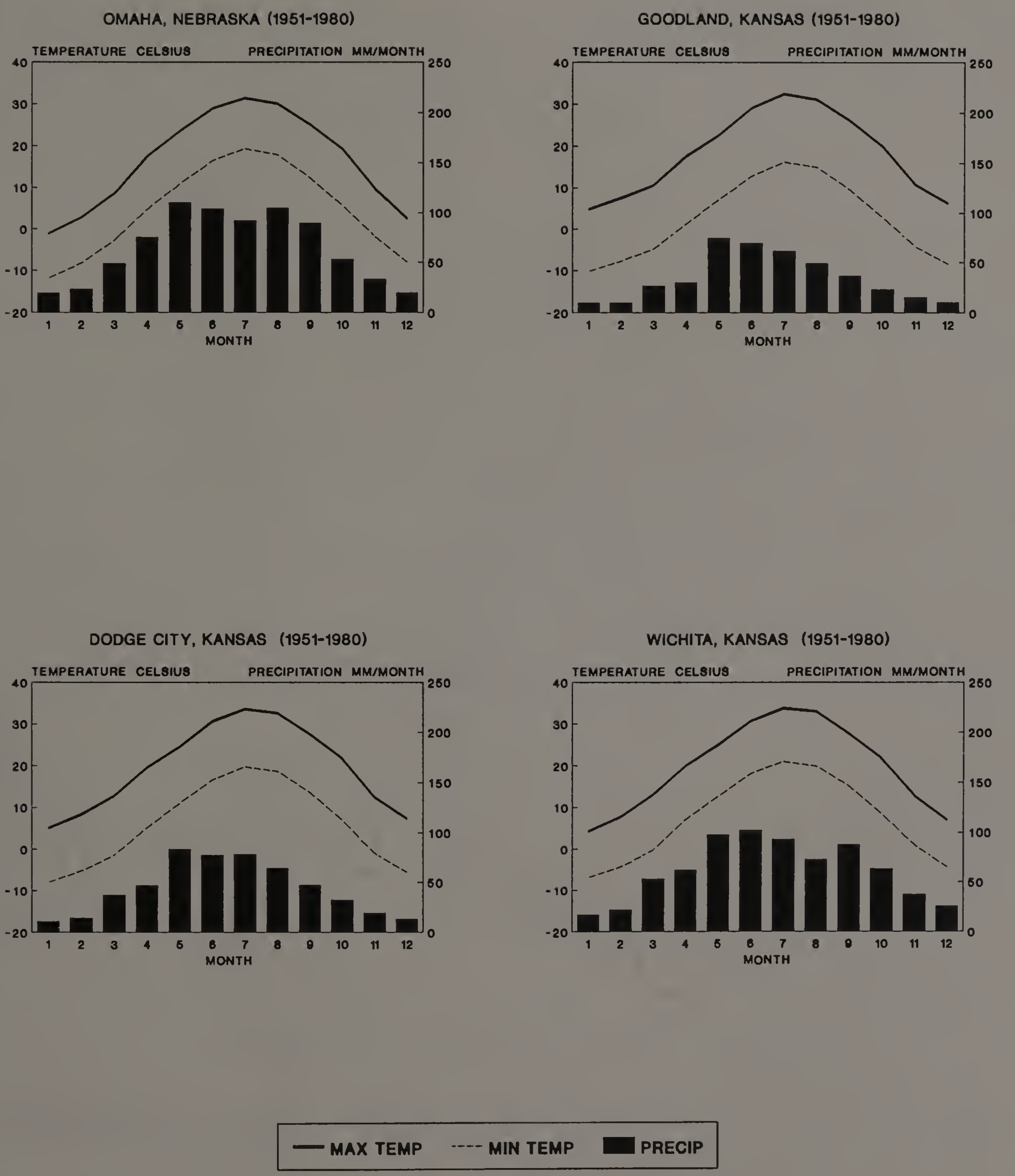

Continued, next page

Figure 3.2 Continued

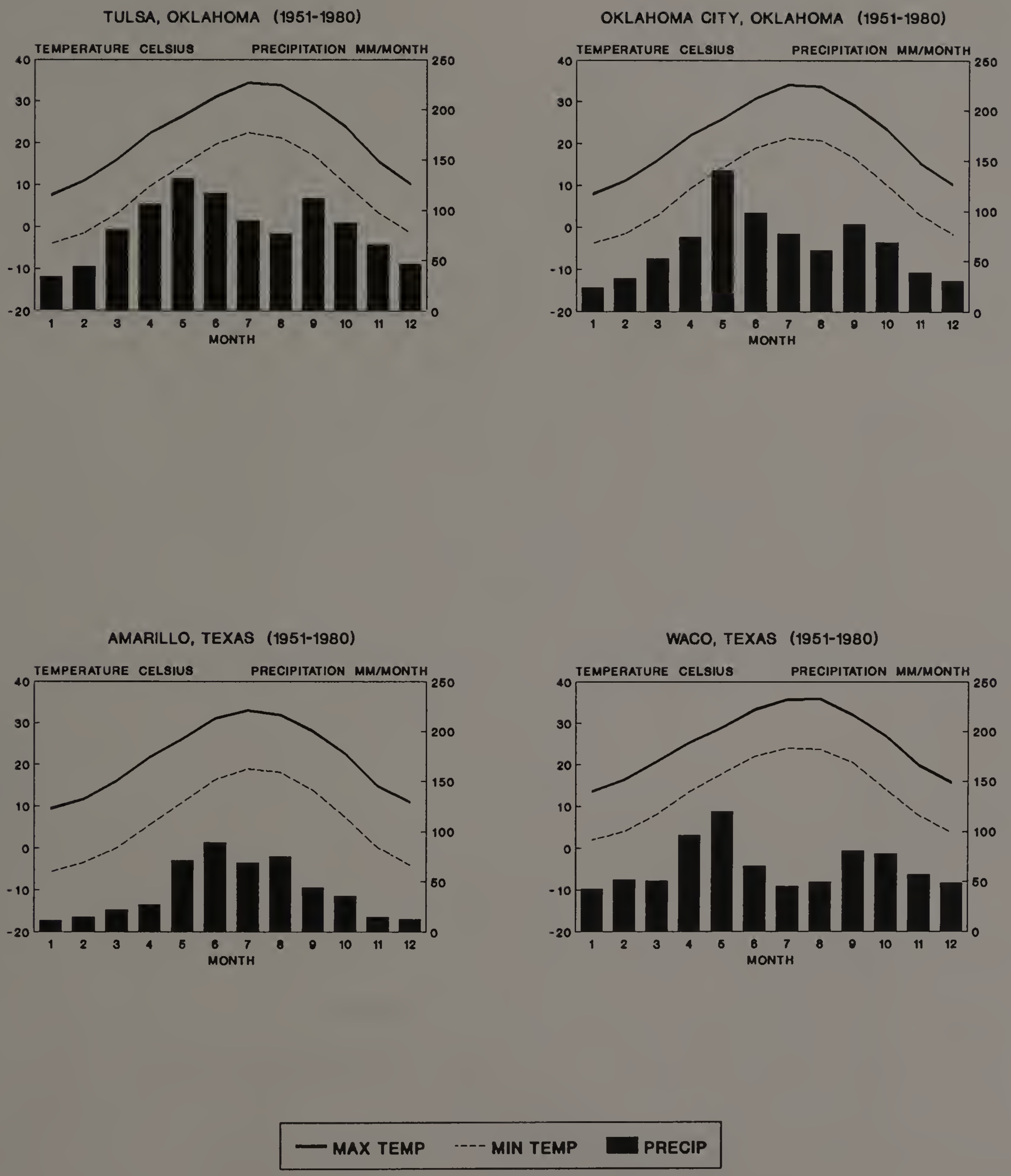

Continued, next page

Figure 3.2 Continued

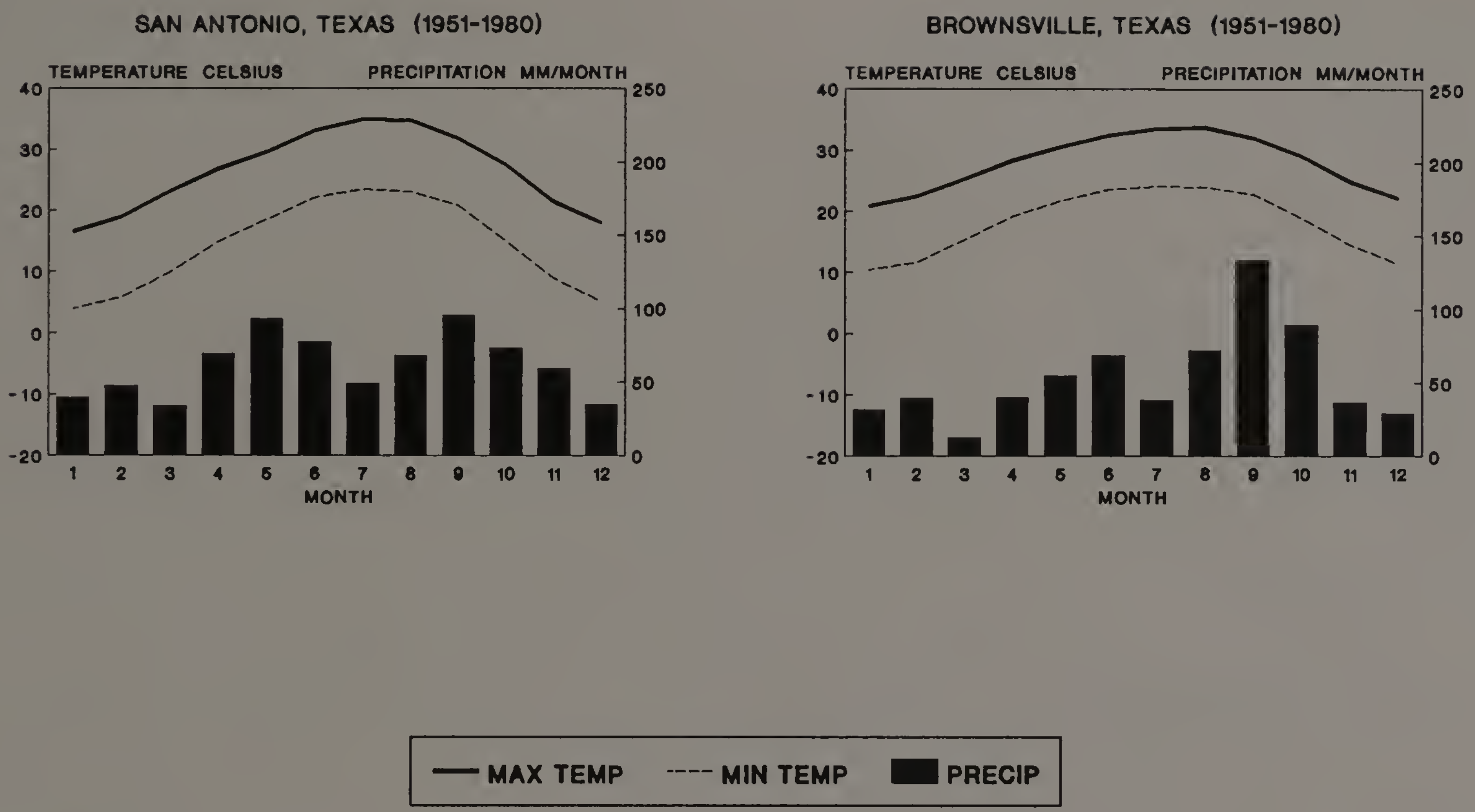

Records of daily solar radiation vary in duration and calibration method among the study sites. Therefore, daily solar radiation was simulated for each site according to the method of Richardson and Wright (1984) as modified by Hodges et al. (1985), with an accuracy of predicted mean annual radiation within 1% of observed. In this method, daily solar radiation is estimated based on correlations between departures of observed daily solar radiation from long-term daily means and departures of daily maximum and minimum temperatures from long-term daily means stratified according to wet and dry days. The correlations at sites for which long-term daily means are available have been computed by Richardson and Wright (1984); these were interpolated spatially to estimate daily solar radiation for the study sites.

3.4 Climate Change Scenarios

Climate change scenarios were devised using a monthly modification factor applied to observed baseline daily data. This factor was calculated from the ratio of climatic variables, mean monthly temperature, precipitation, and incident solar radiation, predicted by two GCMs (GISS and GFDL, described respectively by Hansen et al., 1983 and Manabe and Wetherald, 1987) for doubled CO_2 relative to the current climate simulation. The appropriate monthly factor was then applied to the daily data for each month of the 1951 to 1980 time series.

The GCMs compute climatic variables for distinct latitude by longitude gridboxes, which are shown in Figure 3.3 for the GISS and the GFDL GCMs, along with the Southern Great Plains sites used in the crop modeling simulations. Climate variables at individual locations were multiplied by the ratios of climate change from the appropriate GCM gridbox. No interpolations were made between or within gridboxes, because GCM calculations are for the entire area and do not account for variations at sub-gridbox scales.

A comparison of the mean monthly observed climate (1951-1980) at the study sites and the GCM-simulated current climate for the appropriate gridbox indicates that GCMs do not represent the current climate of the Southern Great Plains realistically. Data comparing observed and simulated climate for the central portion of the study region are shown in Figure 3.4. Simulated mean daily precipitation was multiplied by 30 to approximate the simulated mean monthly precipitation. The GISS modeled temperatures for the gridboxes are consistently too low when compared to the observed climate of sites within the gridboxes, and the modeled precipitation too high, especially in the growing season. In contrast, the GFDL modeled temperatures are consistently too high in the growing season, while the simulation of precipitation is either too high or too low

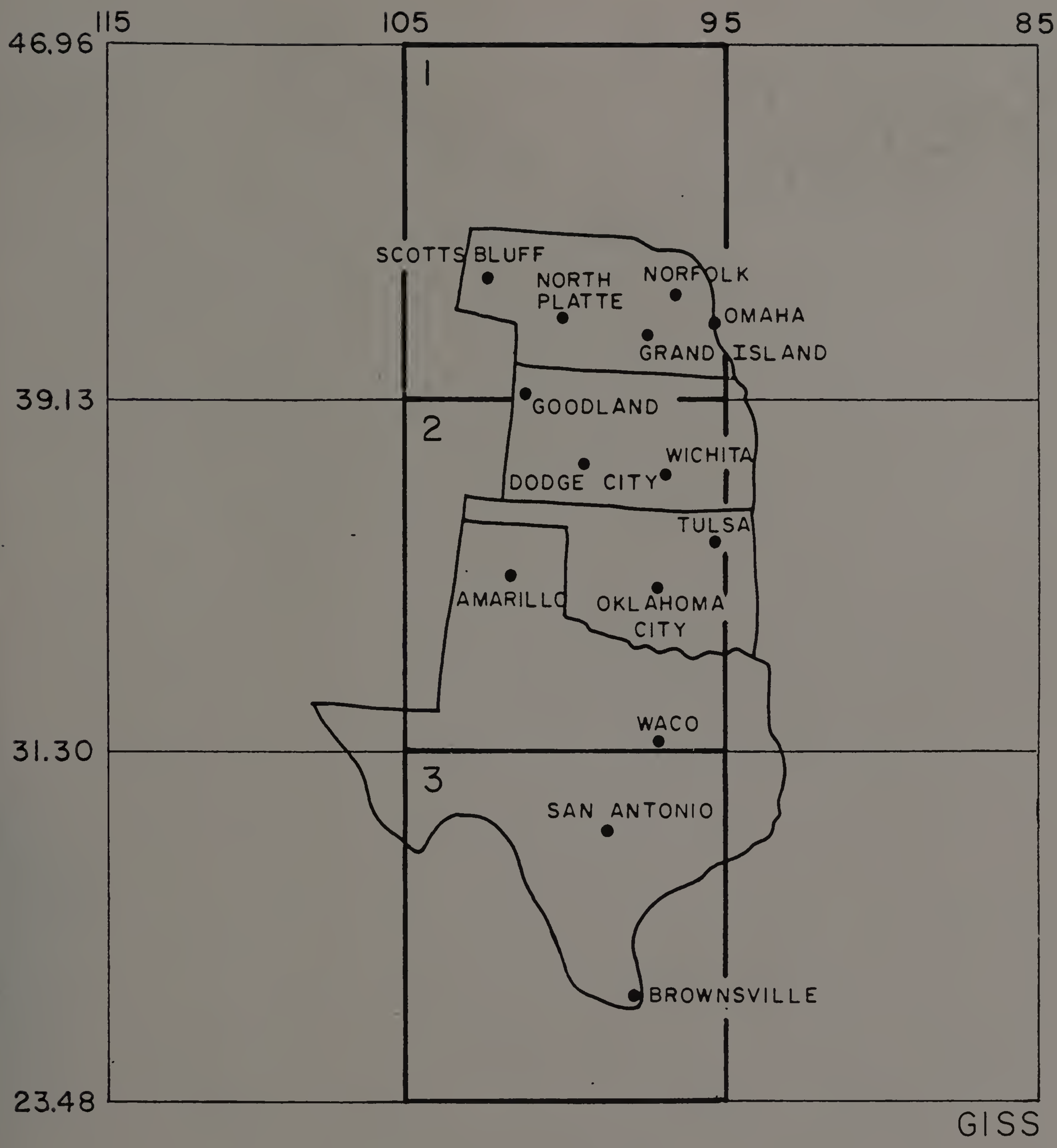

Continued, next page

Figure 3.3 Climate stations and gridboxes for GISS and GFDL GCMs in the Southern Great Plains.

Figure 3.3 Continued

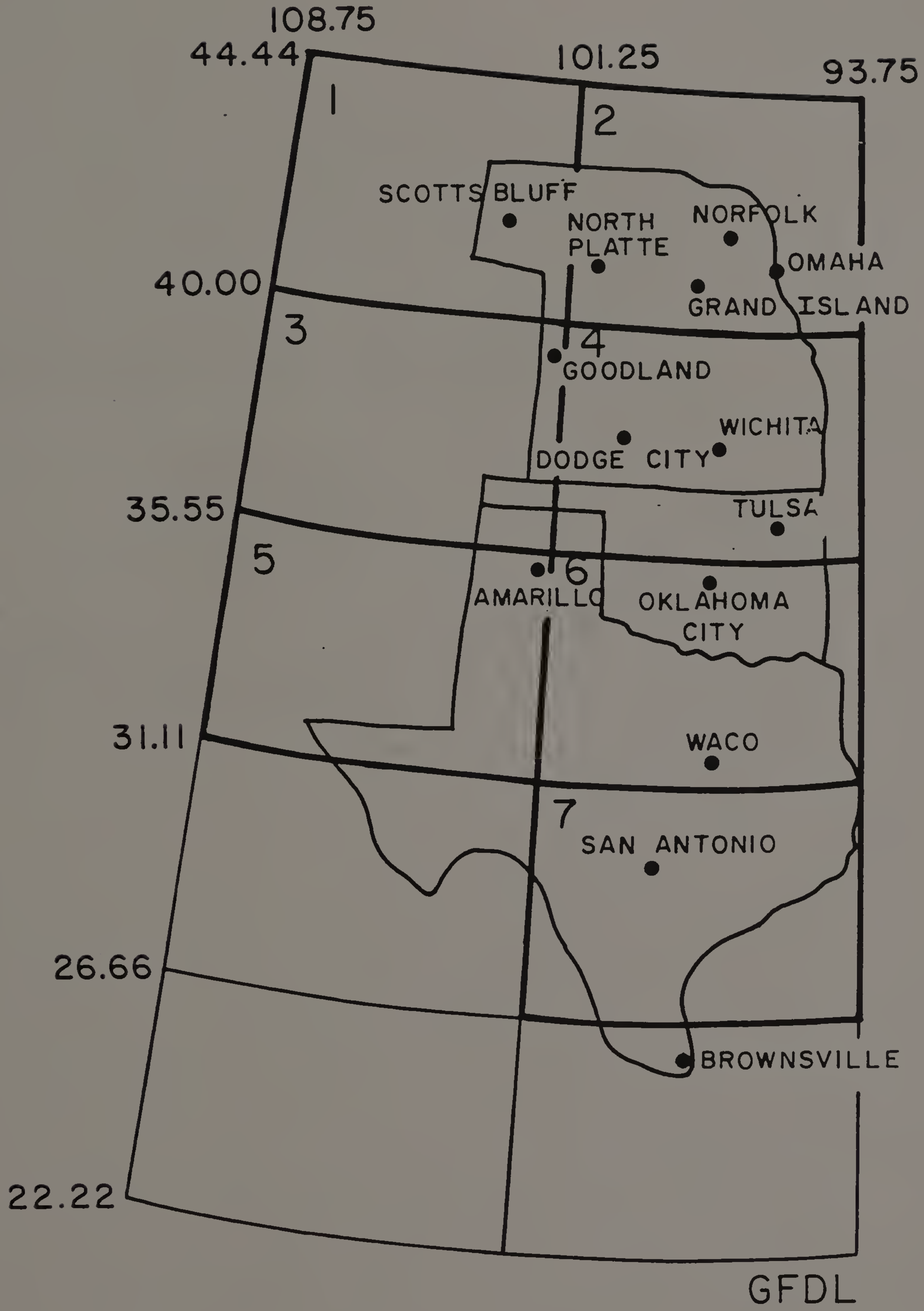

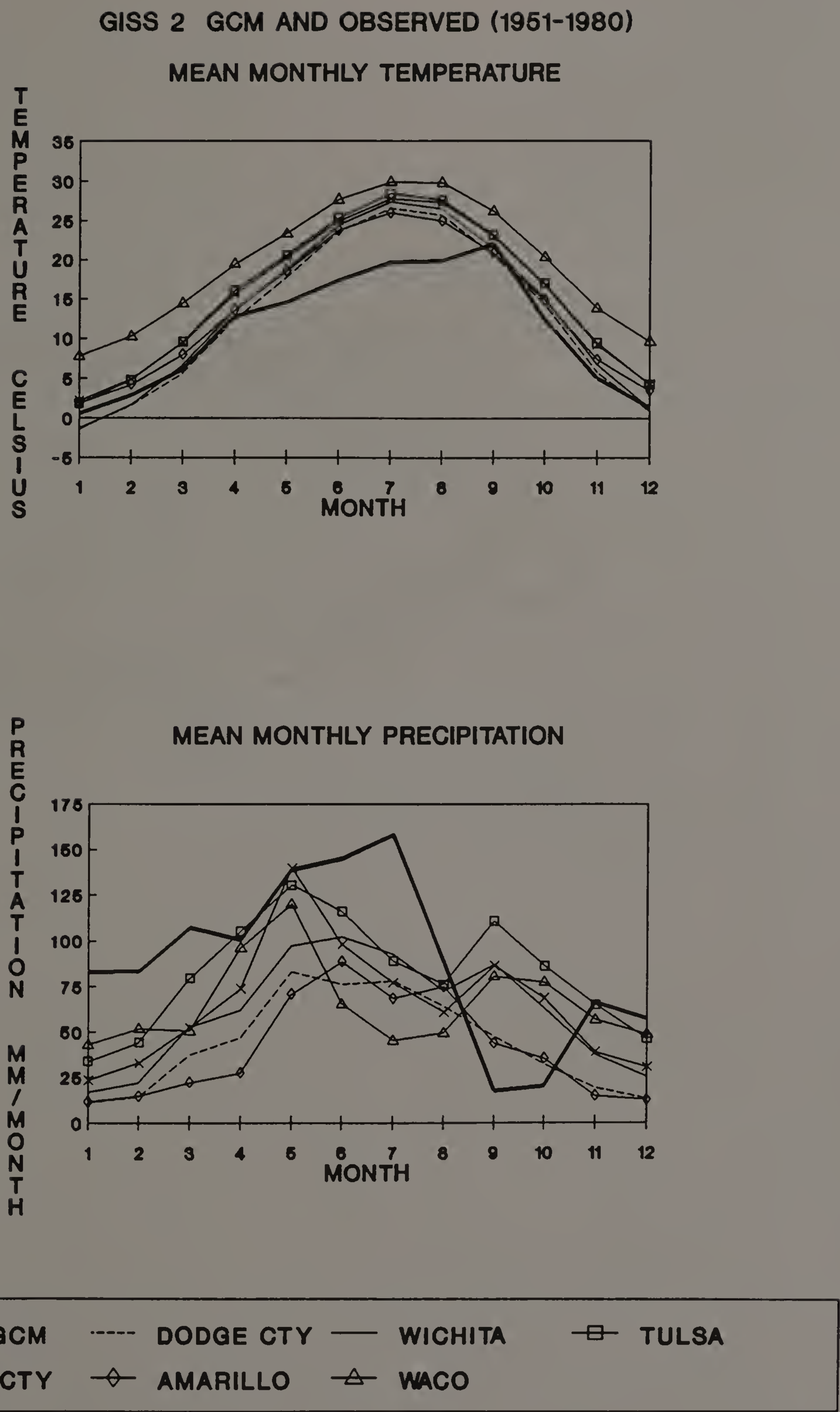

Continued, next page

Figure 3.4 Observed and $1XCO_2$ GCM mean monthly temperature and precipitation for selected gridboxes in the Southern Great Plains.

Figure 3.4 Continued

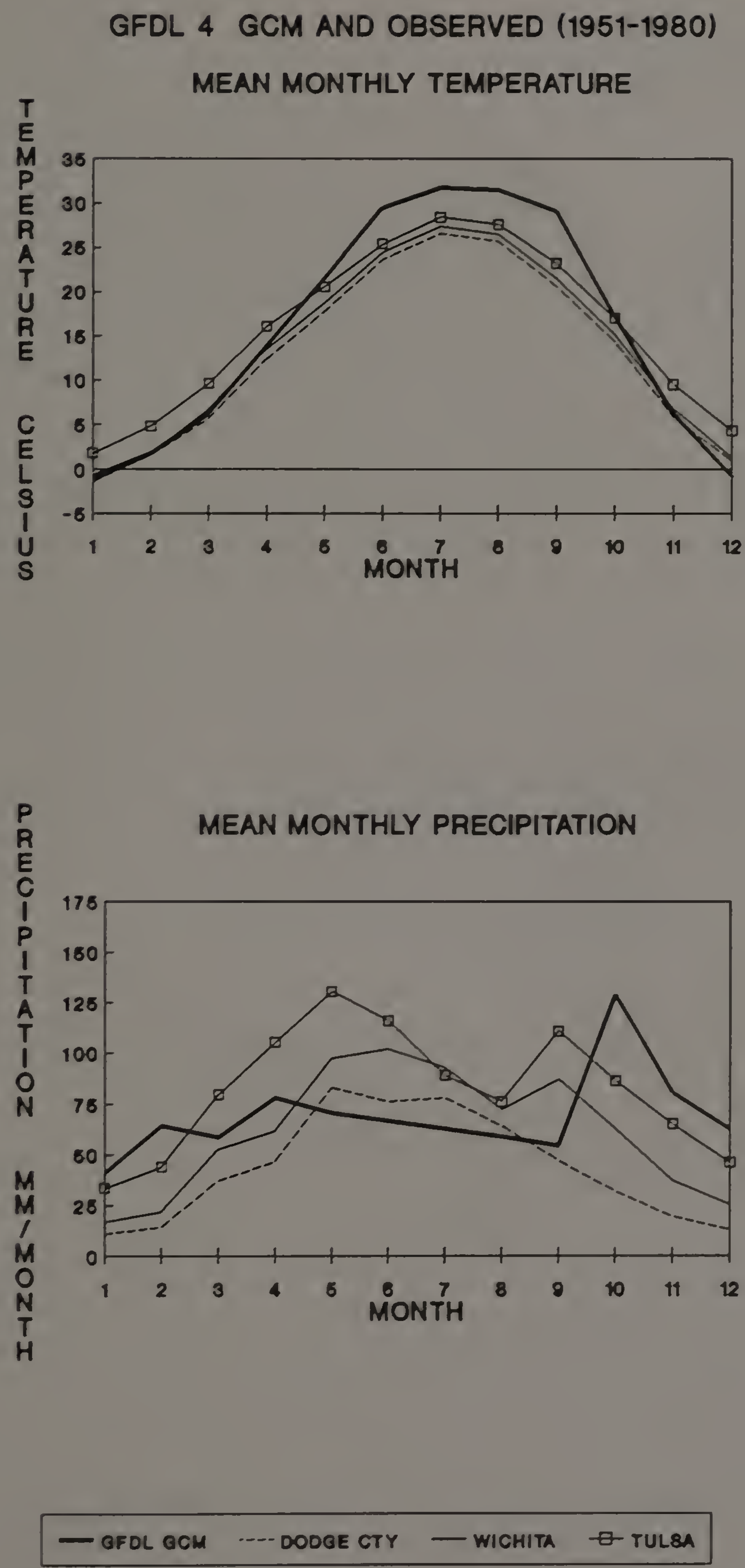

depending on season and gridbox. This lack of realism in current climate GCM simulations makes the direct use of GCM simulated climate variables in crop models difficult on even a monthly basis and explains the use of the climate change ratios from the GCMs and observed climate to create climate change scenarios for use in this study.

Temperature and precipitation changes from the GISS and GFDL climate change scenarios averaged by gridbox are presented in Figure 3.5. The changes shown in the figure were calculated by applying the ratios of climate change to the observed weather data at each site within a gridbox and then averaging the resulting changes in climate variables by season and gridbox.

For the GFDL climate change scenario, Brownsville was included in the gridbox directly north (i.e., GFDL 7) because it is specified as totally ocean in the GFDL GCM. The GFDL climate change scenario has higher temperatures and greater decreases in summer precipitation than the GISS scenario at most sites except in the southern portion of the study region.

Because a historical base period is used without interpolation of ratios within gridboxes, the variation from station to station within each gridbox is the same as in the base period, and interannual and daily variability remains the same. For example, the number of days with precipitation remains the same in the climate change

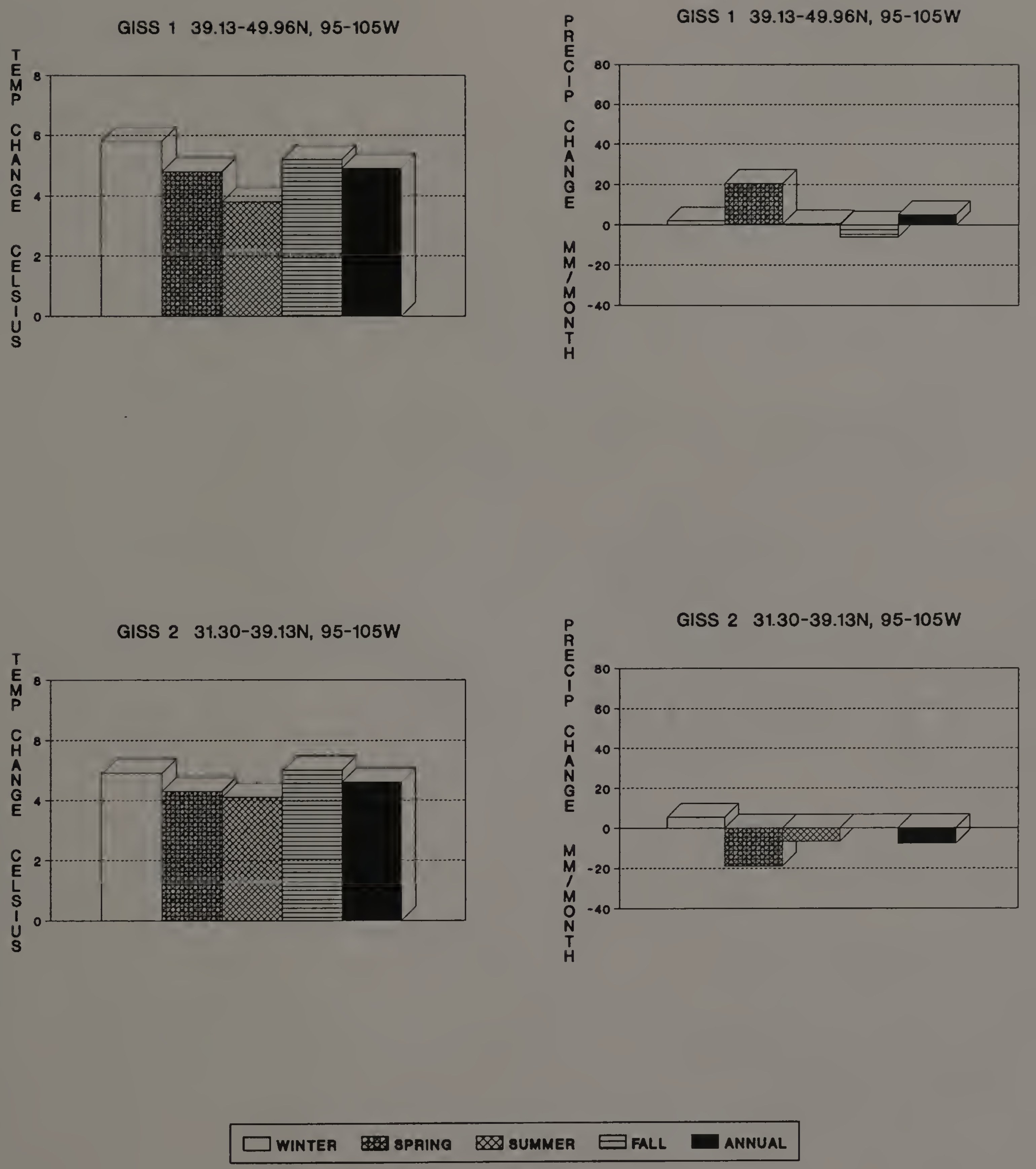

Continued, next page

Figure 3.5 Seasonally averaged change in temperature and precipitation in GISS and GFDL $2XCO_2$ climate change scenarios.

Figure 3.5 Continued

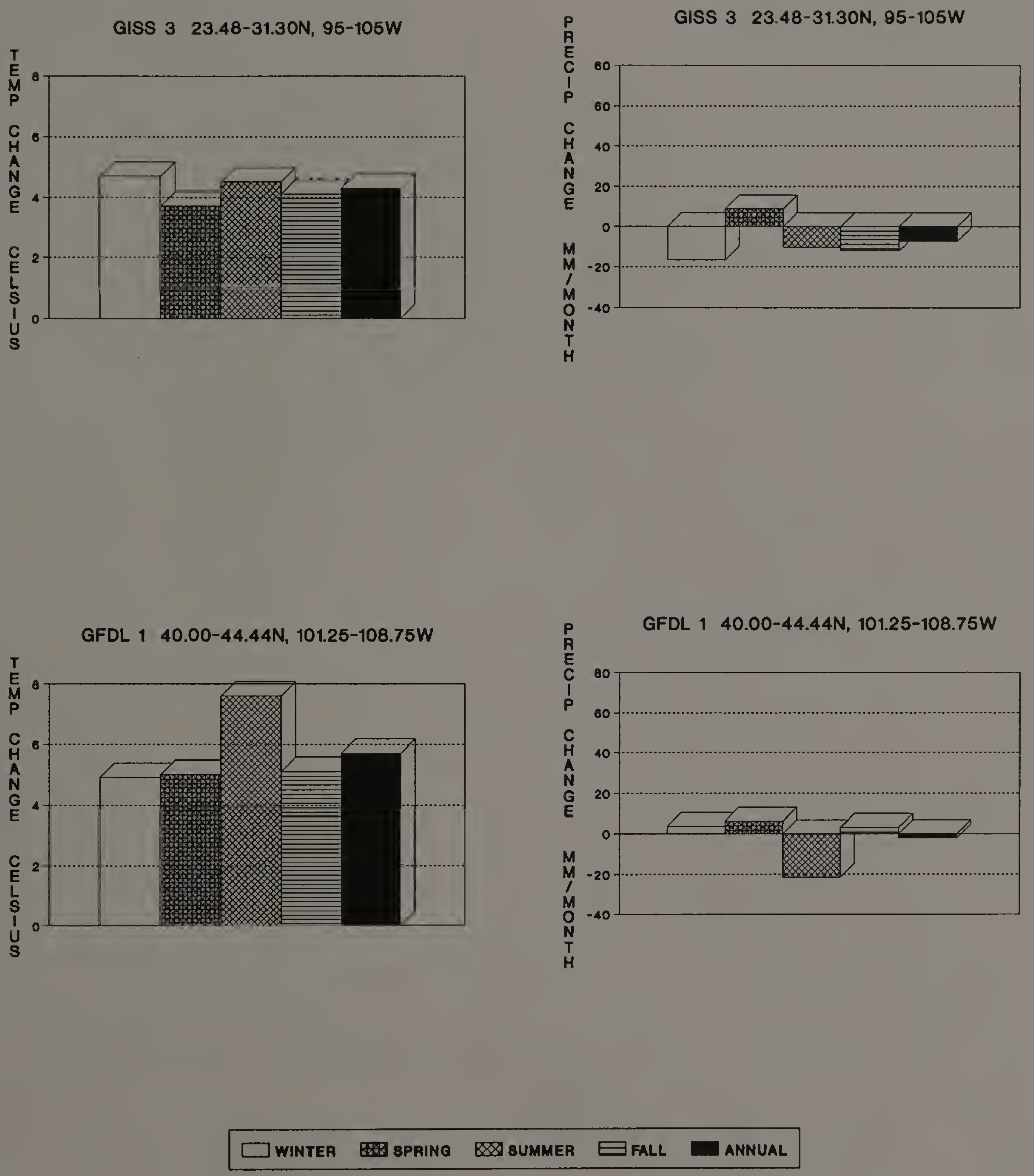

Continued, next page

Figure 3.5 Continued

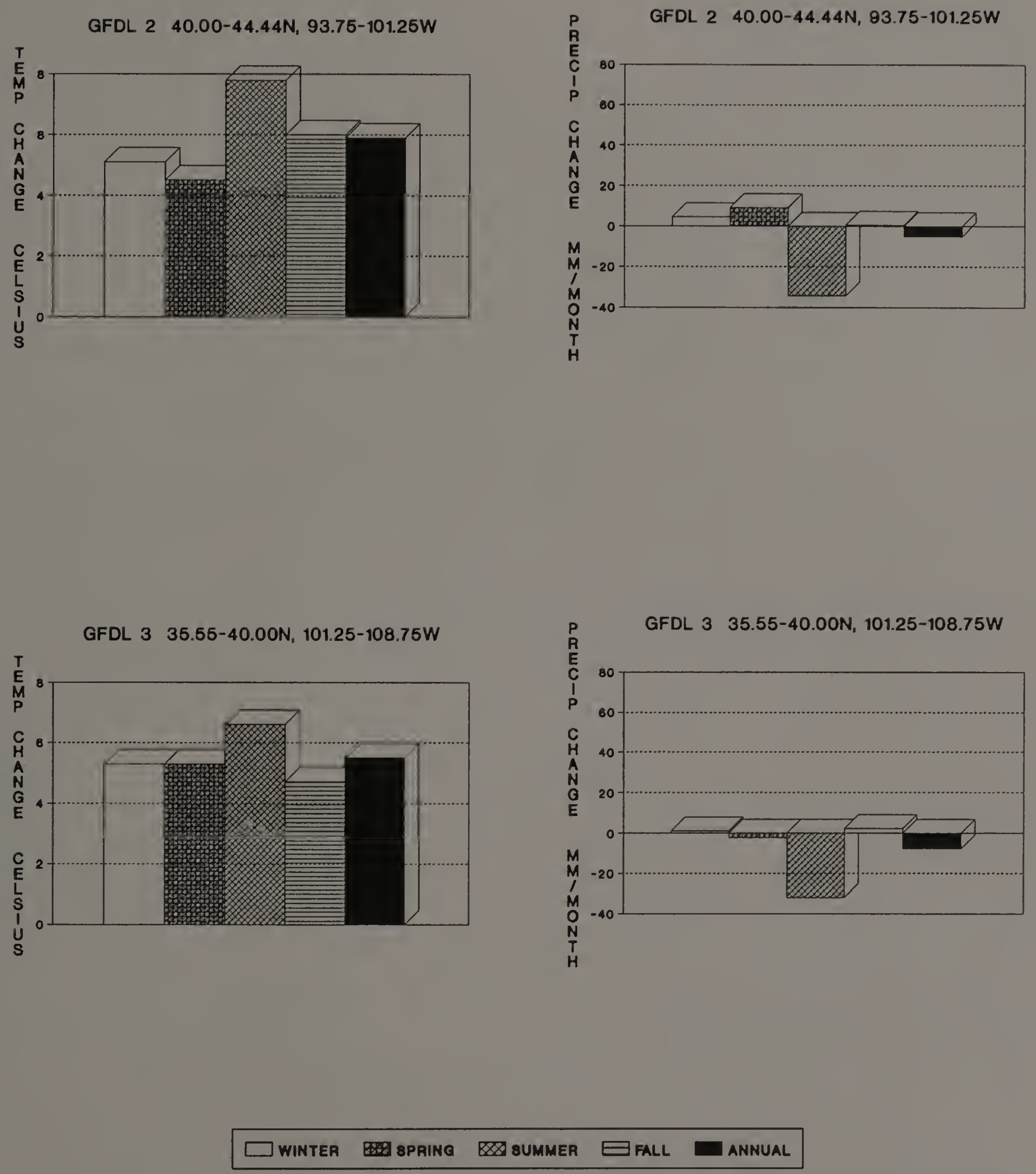

Continued, next page

Figure 3.5 Continued

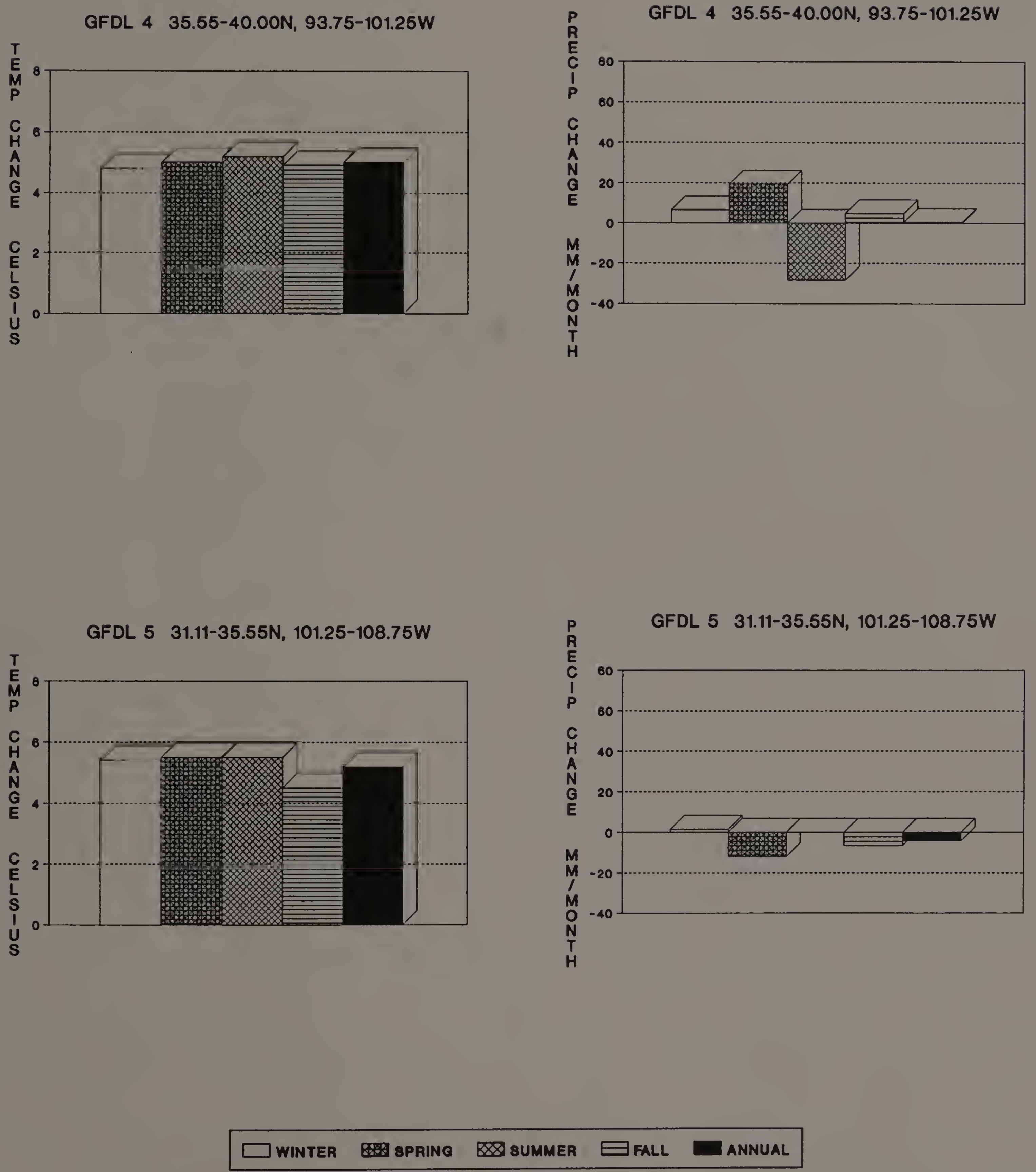

Continued, next page

Figure 3.5 Continued

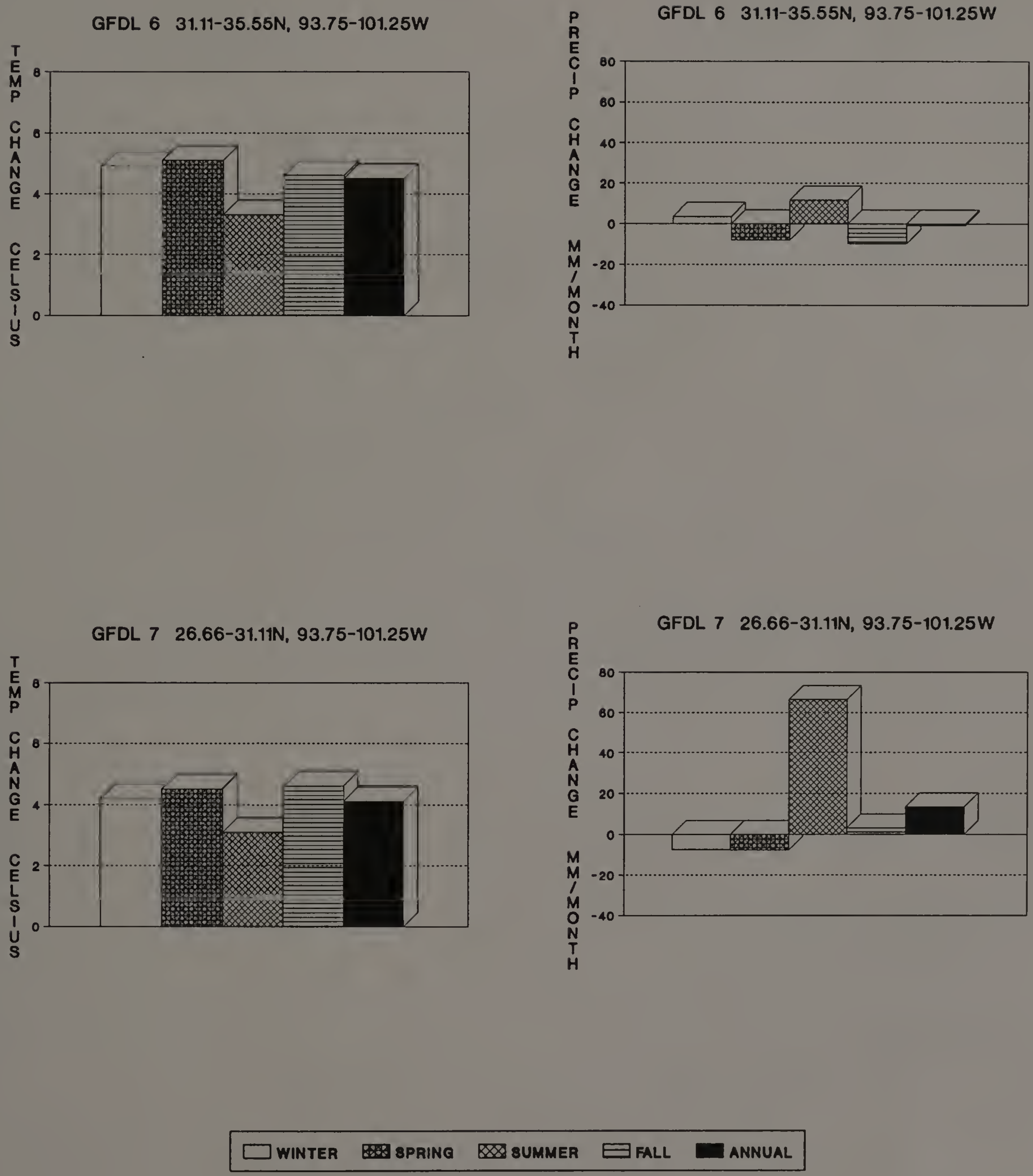

scenarios as in the historical base period; only the amount of rainfall is adjusted by the global climate model ratio. The frequency of extremes of daily maximum temperature changes in the climate change scenarios, but the patterns of the extreme episodes are determined by the observed climate.

This method of climate simulation may result in underestimation of impacts of climate change on agriculture, because in a changed climate dry years, as well as wet years, are likely to differ in intensity, frequency, and duration of rainfall events or heat spells (Parry and Carter, 1985). Mearns et al. (1984) noted that the relationship between changes in mean temperature and changes in the probability of daily extremes is highly non-linear, and that small changes in the mean can sometimes produce relatively large changes in the probabilities of consecutive days of high temperatures. These kinds of variations can have significant effects on agriculture and other activities important to society (Wigley, 1985).

3.5 Soil and Agronomic Parameters

Of the agricultural soils at each study site, three were chosen as described for the Major Land Resource Areas (USDA, 1981) to represent low, medium, and high soil productivity levels (Appendix A). The characteristics of these representative soils were specified for twelve generic soil types: shallow, medium, and deep profiles of silty clay, silt loam, sandy loam, and sand (Ritchie et al., 1989) (Appendix B).

Agronomic parameters (cultivars, planting densities, and planting dates) for CERES-Wheat were specified for each location according to information on current practices provided by local county extension agents. For CERES-Maize, cultivars were specified according to Jones and Kiniry (1986). Other variables were specified as suggested by county agents for Nebraska sites.

For irrigated crop production, each irrigation event was simulated by setting the soil moisture profile to the drained upper limit whenever the water content in the top meter fell below 80% of that content. Irrigation efficiency was assumed to be 100%, that is, all water applied was available for crop use. These irrigated simulations are admittedly unrealistic, since few farmers fully irrigate wheat or corn. They were performed, however, to estimate relative changes in water requirements under changed climate.

3.6 Simulation Runs Conducted

CERES-Wheat and CERES-Maize were run for 30 years of baseline climate and with the GISS and GFDL climate change scenarios under dryland and irrigated conditions at the study sites in the Southern Great Plains. Percent change and standard deviation of percent change were calculated for crop yields, total crop evapotranspiration, and water requirements for each climate change scenario (Appendix C). Changes in maturity date were also computed. Another set of simulations was executed with the crop models modified for the physiological effects of CO_2 with baseline climate only. Simulations were then done with the combined climate change scenarios and the physiological effects of CO_2. The results of these simulations are reported in Section 4.

In order to evaluate the results of the simulations run for the Southern Great Plains, the CERES models were further applied in three different ways. Comparisons between the results of these model runs and the Southern Great Plains simulations are described in Section 5. The first model application was designed to test whether climate change would be more favorable for crop production in the Northern Great Plains than in the Southern Great Plains, due to lower temperatures in the current climate. If this were the case, wheat production might shift northward in response to climate change. These runs were done for both spring and winter wheat at three sites in the Northern Great Plains. Only one soil was used at each site.

The second model application was designed to compare the projected future climate with the "Dust Bowl" climate of the 1930s. The CERES crop models were run with observed climate data from the decade of the 1930s at 9 of the study sites for wheat and at 11 of the study sites for corn. In the 1930s simulations, cultivars and management were specified as for current dryland conditions. The changes from the baseline yields generated with the 1930s data were then compared to the changes generated with both the GISS and GFDL climate change scenarios.

Finally, three possible adaptations to climate change – modifications in irrigation, planting date, and cultivar – were tested with the CERES models:

First, the effect of climate change on irrigated yields and the amount of water applied for irrigation over an entire season were calculated in runs with climate change alone and with the combined climatic and physiological effects of CO_2. This was done for both the GISS and the GFDL scenarios.

Second, planting dates of both wheat and corn were altered in response to the changes in the length of the growing season in the GISS scenario.

Third, to test whether different cultivars are more adapted to the predicted climate, new cultivars were used in CERES-Wheat simulations with the GISS climate change scenario selected on the basis of vernalization requirement and photoperiod sensitivity and new cultivars were selected for CERES-Maize simulations on the basis of growing degree day requirements.

CHAPTER 4

SIMULATION RESULTS

4.1 Current Climate

A comparison was made between actual and simulated dryland wheat yields on a year-to-year basis for Goodland, Kansas (Figure 4.1). Wheat yields were simulated both with and without fallowing, i.e., the practice of planting a crop every other year so that the soil profile contains antecedent moisture accumulated over the previous year. This moisture source is not taken into account in the "no-fallow" simulations, which assume that the crop relies on each season's precipitation alone. The actual yield data are from the USDA Crop Reporting District for Sherman County provided by Dr. Linda Mearns of the National Center for Atmospheric Research.

The coefficient of correlation (R) between actual and simulated "no-fallow" wheat yields is 0.55, and between actual and simulated fallow yields is 0.68. The higher correlation of actual yields with fallow simulations is to be expected because fallowing is a frequently applied practice in the region. While the year-to-year fluctuations of the actual and both sets of simulated yields show generally similar trends, the no-fallow simulations underestimated the actual yields in most years, while the fallow simulations often overestimated yields.

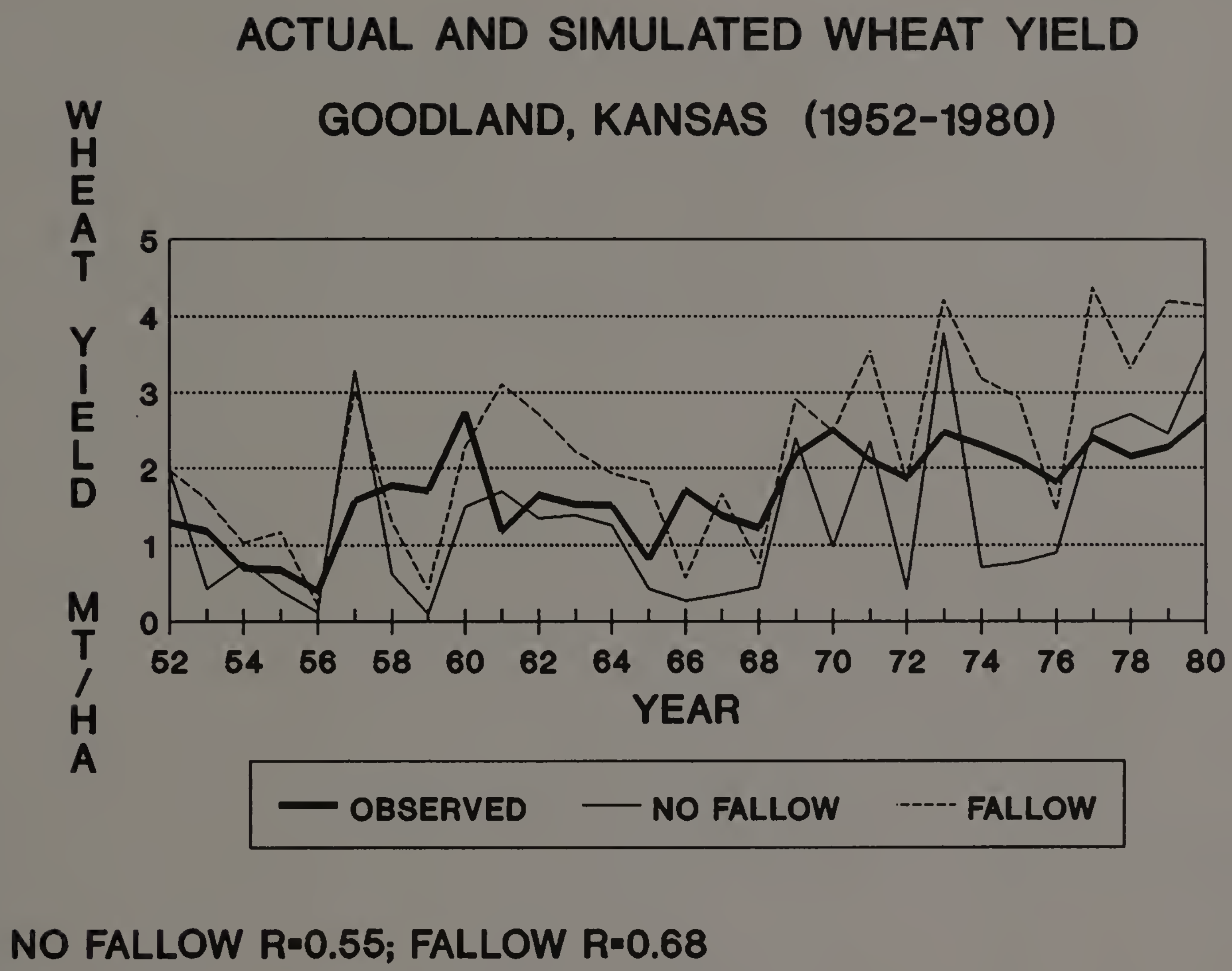

Figure 4.1 Actual and simulated wheat yield Goodland, Kansas (1952-1980).

4.2 Modified Climate

The following section compares the results of CERES-Wheat and CERES-Maize simulations made with the climate change scenarios to crop model results from the baseline (1951-1980) climate. The physiological effects of CO_2 were not included in these runs.

4.2.1 Wheat

CERES-Wheat simulations produced results of changes in yield, thermal units, evapotranspiration, days to maturity, and water use efficiency for dryland and irrigated conditions.

4.2.1.1 Dryland Yields

When CERES-Wheat was run with the GISS climate change scenario without taking account of the physiological effects of CO_2, simulated dryland wheat yields were lower than the yields from the baseline period in every location (Table 4.1). These yield decrements ranged from 10 to 55%, with an average of about 30%. Results were not weighted spatially to account for differences in cropped areas surrounding the different study sites, a procedure which can produce unrealistic estimates of mean changes in regional production.

Table 4.1 Change in CERES-Wheat yield with GISS and GFDL 2XCO2 climate change scenarios.

a) CERES-WHEAT $2XCO_2$ DRYLAND

Site	GISS Yield (%Δ)	GISS sd (%Δ)	GFDL Yield (%Δ)	GFDL sd (%Δ)
NEBRASKA				
Norfolk	-10.5	6.0	-30.1*	5.6
Grand Island	-17.1*	6.0	-26.0*	5.9
Scottsbluff	-25.9*	9.6	-45.3*	9.1
Omaha	-13.9*	4.3	-20.1*	4.1
North Platte	-27.7*	8.4	-40.4*	8.3
KANSAS				
Goodland	-10.5	16.1	-46.9*	11.7
Dodge City	-38.7*	11.7	-12.3	13.2
Wichita	-33.6*	6.9	-18.8*	6.8
OKLAHOMA				
Tulsa	-33.9*	3.3	-20.4*	3.3
Oklahoma City	-45.3*	4.1	-40.4*	3.9
TEXAS				
Amarillo	-55.4*	12.3	-55.1*	13.0
Brownsville	-45.3*	4.1	-40.4*	3.9
Mean	-29.8		-33.0	

b) CERES-WHEAT $2XCO_2$ IRRIGATED

Site	GISS Yield (%Δ)	GISS sd (%Δ)	GFDL Yield (%Δ)	GFDL sd (%Δ)
NEBRASKA				
Norfolk	-3.2	2.4	-9.9*	2.3
Grand Island	-3.7	2.0	-9.2*	1.9
Scottsbluff	6.1*	1.8	-2.2	1.9
Omaha	-11.6*	2.4	-16.3*	2.3
North Platte	6.5	2.8	0.2	2.8
KANSAS				
Goodland	0.8	1.9	-14.8*	3.1
Dodge City	-6.9*	2.0	-15.6*	1.9
Wichita	-10.7*	2.0	-17.9*	2.0
OKLAHOMA				
Tulsa	-21.5*	2.0	-19.4*	2.4
Oklahoma City	-19.6	2.1	-20.8*	2.1
TEXAS				
Amarillo	-18.3*	1.8	-17.3*	1.9
Brownsville	-48.3*	3.3	-42.7*	3.1
Mean	-10.9		-15.5	

*Greater than two times the st. dev. of percent change.

The lower simulated wheat yields were primarily due to the increased temperatures of the climate change scenario, which caused the rapid accumulation of degree days, shortened the duration of crop growth, and hastened occurrence of phenological stages (Figure 4.2). The total length of the crop's growing season (from germination to maturation) was shorter by about three weeks (Table 4.2). In particular, an earlier and shorter grain-filling period reduces the amount of solar radiation received by the crop and hence the carbohydrates available for grain production.

The wheat yield decrements indicated by the simulations were more pronounced in lower latitudes (Oklahoma and Texas) than in higher latitudes (Kansas and Nebraska). Under current climate conditions in the southern latitudes, wheat growth is already close to its temperature limit of 25°C for grain development (Tandon, 1985) and the higher temperatures of the climate change scenario often exceed that limit (See Appendix D), producing more negative yield effects.

The above results were obtained using the GISS global climate model. For comparison, parallel simulations were done with an alternative climate model, namely the GFDL climate model. Results of the two sets of simulations were similar for wheat yields. For the GFDL climate change scenario, dryland CERES-Wheat yields decreased everywhere, with reductions ranging from 12 to 55%. The mean decrease was about 33%. In contrast to the GISS results, large

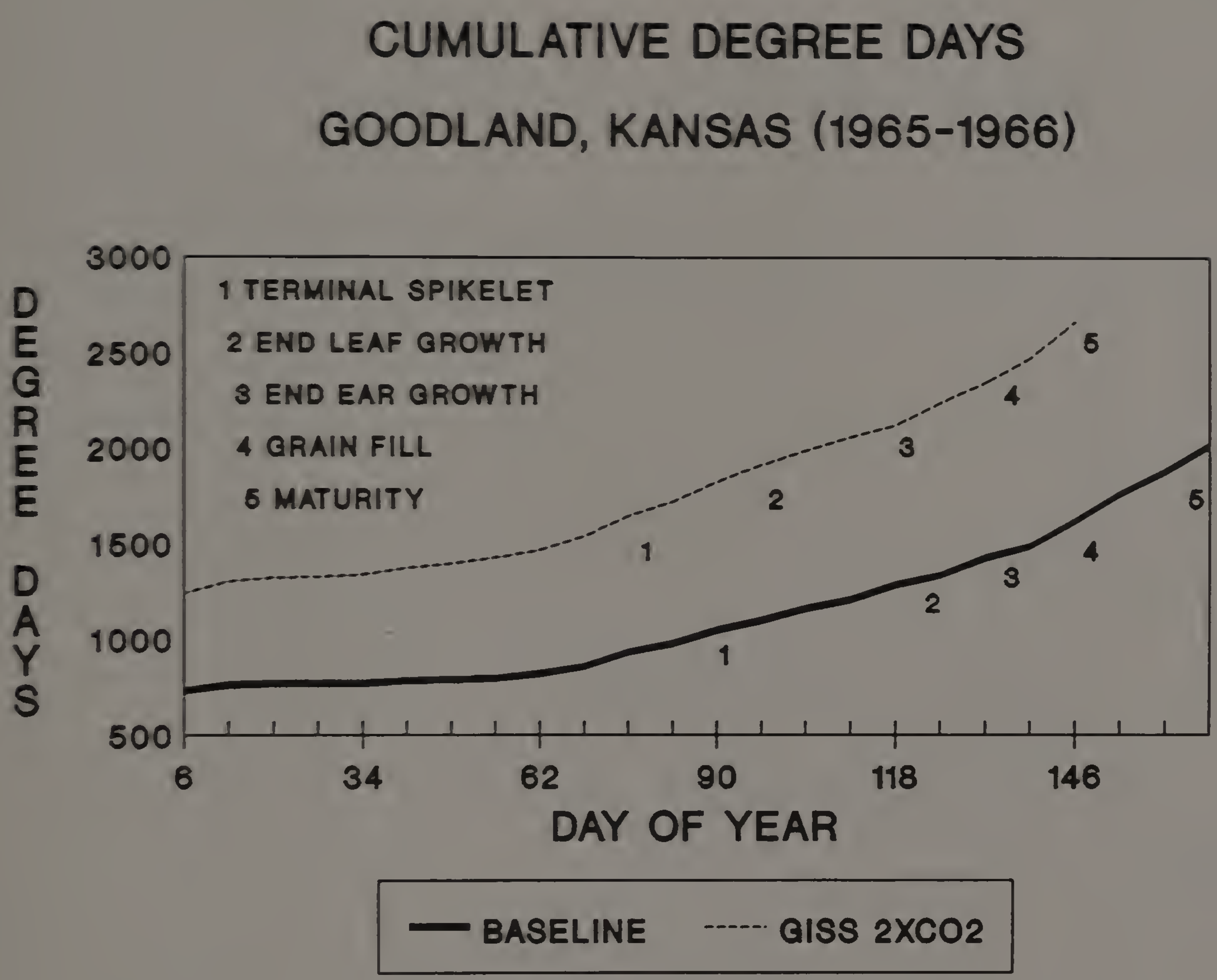

Figure 4.2 CERES-Wheat cumulative degree days and growth stages in baseline and GISS $2XCO_2$ climate change simulations, Goodland, KS (1965-1966).

Table 4.2 Change in CERES-Wheat days to maturity with GISS and GFDL 2XCO_2 climate change scenarios.

a) CERES-WHEAT 2XCO_2 DRYLAND

Site	GISS Days	GISS sd	GFDL Days	GFDL sd
NEBRASKA				
Norfolk	-25*	0.9	-22*	0.9
Grand Island	-25*	1.0	-22*	0.9
Scottsbluff	-30*	0.9	-29*	0.9
Omaha	-24*	0.9	-21*	0.8
North Platte	-27*	0.9	-24*	0.8
KANSAS				
Goodland	-27*	0.9	-27*	0.8
Dodge City	-20*	0.9	-22*	0.9
Wichita	-20*	0.8	-21*	0.8
OKLAHOMA				
Tulsa	-8*	0.9	-27*	0.8
Oklahoma City	-17*	0.9	-18*	0.9
TEXAS				
Amarillo	-18*	0.9	-23*	0.9
Brownsville	-11*	1.6	-15*	1.6
Mean	-21		-23	

b) CERES-WHEAT 2XCO_2 IRRIGATED

Site	GISS Days	GISS sd	GFDL Days	GFDL sd
NEBRASKA				
Norfolk	-24*	0.9	-21*	0.9
Grand Island	-25*	0.9	-21*	0.9
Scottsbluff	-29*	0.9	-28*	0.8
Omaha	-24*	0.9	-21*	0.8
North Platte	-27*	0.9	-24*	0.8
KANSAS				
Goodland	-28*	0.9	-28*	0.8
Dodge City	-21*	1.0	-22*	1.0
Wichita	-20*	0.8	-21*	0.8
OKLAHOMA				
Tulsa	-8*	0.9	-27*	0.9
Oklahoma City	-16*	0.9	-18*	0.9
TEXAS				
Amarillo	-17*	1.0	-23*	1.0
Brownsville	-11*	1.4	-13*	1.5
Mean	-20		-22	

*Greater than two times the st. dev. of change.

decreases in yields occurred at both higher and lower latitudes, a phenomenon attributable to the combination of high temperatures and low precipitation in the GFDL climate predictions for several sites in Nebraska and Kansas. Maturity dates of simulated dryland wheat advanced by up to four weeks in the GFDL scenario, relative to the baseline simulations (Table 4.2).

To test which of the climatic factors are dominant, CERES-Wheat was run with the GFDL scenario with only one climate variable changed at a time. Thus, in these simulations, either temperature, precipitation, or radiation was changed as forecast by the GFDL GCM doubled-CO_2 experiment; the other climate variables were held at their observed baseline values. The yield changes resulting from these runs with isolated climate change variables are compared with the yield changes resulting from the full GCM scenario simulations in Figure 4.3. At all locations, temperature changes forecast by the GFDL GCM had the single largest negative effect on simulated wheat yields.

4.2.1.2 Irrigated Yields

In the climate change simulations with automatically applied irrigation, wheat yields were generally lower than their baseline levels, but not as much as in the dryland case (Table 4.1). The mean change in the yield of irrigated wheat was about -10% in the GISS scenario, and about -15% in

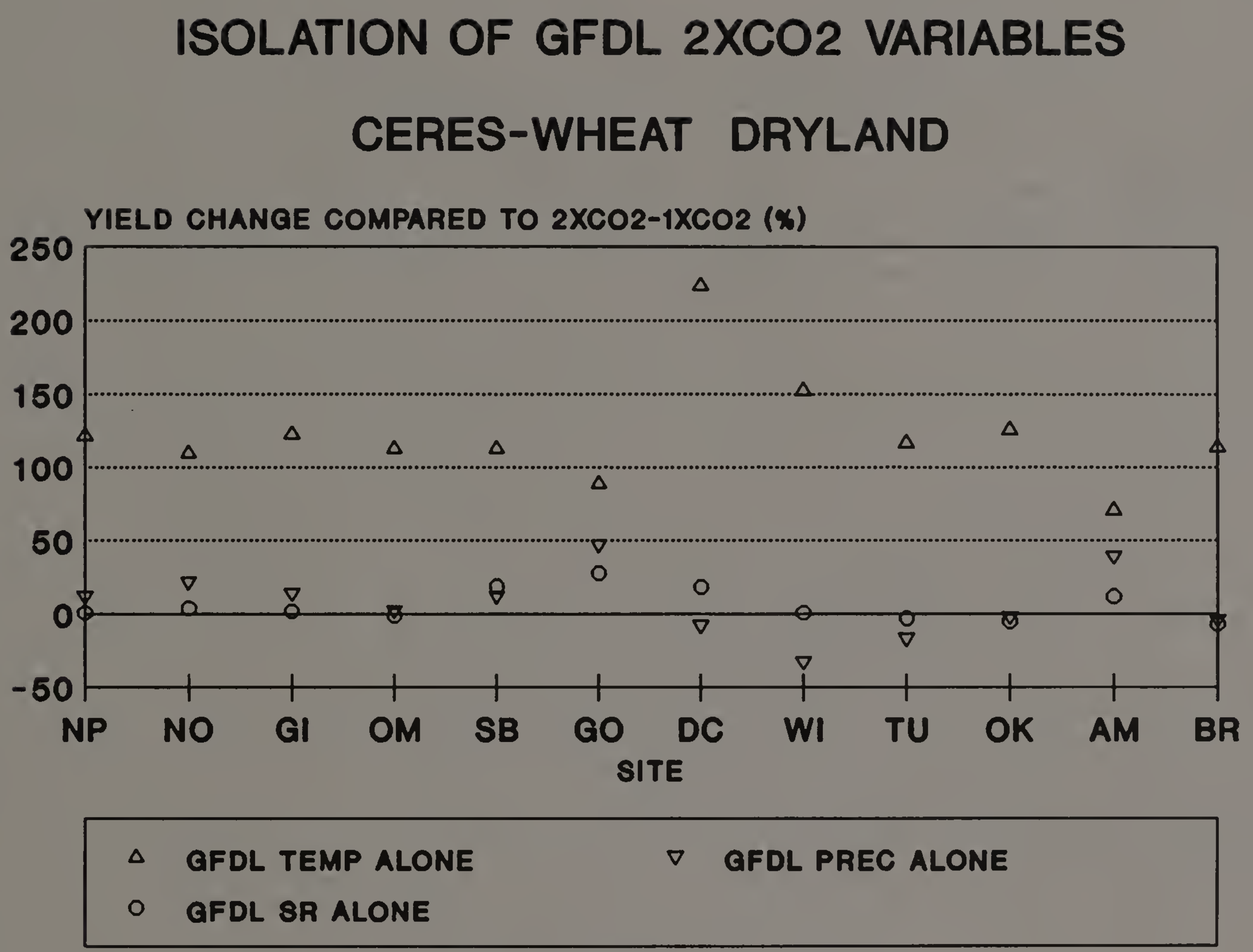

Figure 4.3 CERES-Wheat yield changes with climate variables changed alone as percent of yield changes with full GFDL $2XCO_2$ scenario.

the GFDL scenario, in which temperature changes were greater. These results suggest that the high temperatures of the climate change scenarios had a negative impact on simulated crop growth even under fully irrigated conditions. The shortening of phenological stages due to rapidly accumulating degree-days obtained in the dryland simulations was also evident in the irrigated ones. Maturity dates occurred about three weeks earlier in the irrigated as well as the dryland simulations for both the GISS and GFDL climate change scenarios.

A measure of the relative dispersion about the mean yield of the 29 years of simulation at each site can be estimated using the coefficient of variation. In all but one location, simulated irrigated yields had consistently lower coefficients of variation than dryland yields, under both current and changed climate conditions (Table 4.3). This was most likely due to the removal of the effects of year-to-year variability in precipitation in the fully irrigated simulations. While the coefficients of variation of both dryland and irrigated crop yields were higher in the changed climate simulations than in the current climate simulations, the irrigated yields tended to be much less variable. This result suggests that farmers may be able to moderate the higher year-to-year variability in dryland crop yields likely to result from a warmer climate by adopting irrigation.

Table 4.3 Coefficients of variation of CERES-Wheat yields for baseline (1951-1980), GISS and GFDL $2XCO_2$ climate change scenarios.

a)	CERES-WHEAT DRYLAND		
Site	Base	GISS	GFDL
NEBRASKA			
Norfolk	20.7	27.3	32.7
Grand Island	20.4	30.2	32.7
Scottsbluff	37.8	45.4	32.3
Omaha	16.6	18.9	17.6
North Platte	32.9	40.8	47.5
KANSAS			
Goodland	47.0	76.6	74.0
Dodge City	44.1	63.9	54.7
Wichita	26.7	38.5	30.2
OKLAHOMA			
Tulsa	11.2	21.7	12.6
Oklahoma City	24.3	37.4	30.5
TEXAS			
Amarillo	55.3	64.6	18.6
Brownsville	17.8	22.8	82.2
b)	CERES-WHEAT IRRIGATED		
NEBRASKA			
Norfolk	8.2	10.2	10.4
Grand Island	7.3	8.6	8.1
Scottsbluff	7.0	6.4	7.5
Omaha	9.4	10.4	9.7
North Platte	13.0	7.3	8.0
KANSAS			
Goodland	6.1	8.2	18.0
Dodge City	7.2	8.6	8.9
Wichita	7.6	8.7	9.2
OKLAHOMA			
Tulsa	8.4	8.9	8.7
Oklahoma City	7.7	10.3	10.3
TEXAS			
Amarillo	6.3	9.4	17.3
Brownsville	13.8	22.0	9.7

4.2.1.3 Water Regime

Evapotranspiration was summed over the entire period of crop growth for the current and climate change simulations. Total ET over this period decreased at every site when CERES-Wheat was run with the GISS and GFDL climate change scenarios for dryland conditions (Table 4.4). Even though the warmer climate caused the daily rate of ET to increase for most of the growing season, the significant shortening of the crop growing season reduced the overall seasonal ET (Figure 4.4). Under dryland conditions in the crop model, soil moisture deficits caused by periods of drought further reduced total crop evapotranspiration. When the simulated crops were fully irrigated, total crop evapotranspiration also decreased at most locations, but not as much as in the dryland simulations.

Water use efficiency is a measure of crop productivity that combines carbohydrate production and evapotranspiration. In this study, water use efficiency is defined as simulated crop yield per unit area divided by total evapotranspiration over the period of crop growth (kg/ha/mm). Thus calculated, simulated water use efficiency for dryland wheat declined at four locations in both the GISS and GFDL climate change scenarios (Figure 4.5). These declines occurred because the yield reductions in the climate change simulations were relatively greater than the reductions in evapotranspiration.

Table 4.4 Change in CERES-Wheat evapotranspiration with GISS and GFDL $2XCO_2$ climate change scenarios.

a) CERES-WHEAT $2XCO_2$ DRYLAND

Site	GISS ET	GISS sd	GFDL ET	GFDL sd
	(%Δ)	(%Δ)	(%Δ)	(%Δ)
NEBRASKA				
Norfolk	-12.7*	2.6	-19.2*	2.7
Grand Island	-13.2*	2.6	-15.7*	2.8
Scottsbluff	-17.7*	2.8	-17.7*	2.9
Omaha	-11.2*	2.3	-11.8*	2.4
North Platte	-14.2*	2.8	-19.2*	3
KANSAS				
Goodland	-15.4*	4.1	-23.5*	3.7
Dodge City	-16.7*	3.6	-10.1*	4
Wichita	-14.3*	3.4	-7.7*	3.4
OKLAHOMA				
Tulsa	-5.8*	1.6	-4.3*	1.4
Oklahoma City	-11.6*	2.4	-8.8*	2.5
TEXAS				
Amarillo	-19.0*	3	-13.3*	2.9
Brownsville	-11.8*	4.3	-27.5*	4.2
Mean	-13.6		-14.9	

b) CERES-WHEAT $2XCO_2$ IRRIGATED

Site	GISS ET	GISS sd	GFDL ET	GFDL sd
NEBRASKA				
Norfolk	-9.9*	1.2	-2.2	1.4
Grand Island	-8.4*	1.5	-1.0	1.6
Scottsbluff	-8.7*	1.3	3.3*	1.3
Omaha	-10.5*	1.3	-3.8*	1.3
North Platte	-3.0*	1.4	1.8	1.2
KANSAS				
Goodland	-8.3*	1.2	1.8	1.2
Dodge City	-0.3	1.2	-1.4	1.3
Wichita	-2.5*	1.2	-4.0*	1.3
OKLAHOMA				
Tulsa	2.7	1.4	-11.6*	1.4
Oklahoma City	3.1*	1.2	-1.5	1.2
TEXAS				
Amarillo	-11.2*	2.3	-8.0*	2.1
Brownsville	3.8*	1.4	-0.9	1.6
Mean	-4.4		-2.0	

*Greater than two times the st. dev. of percent change.

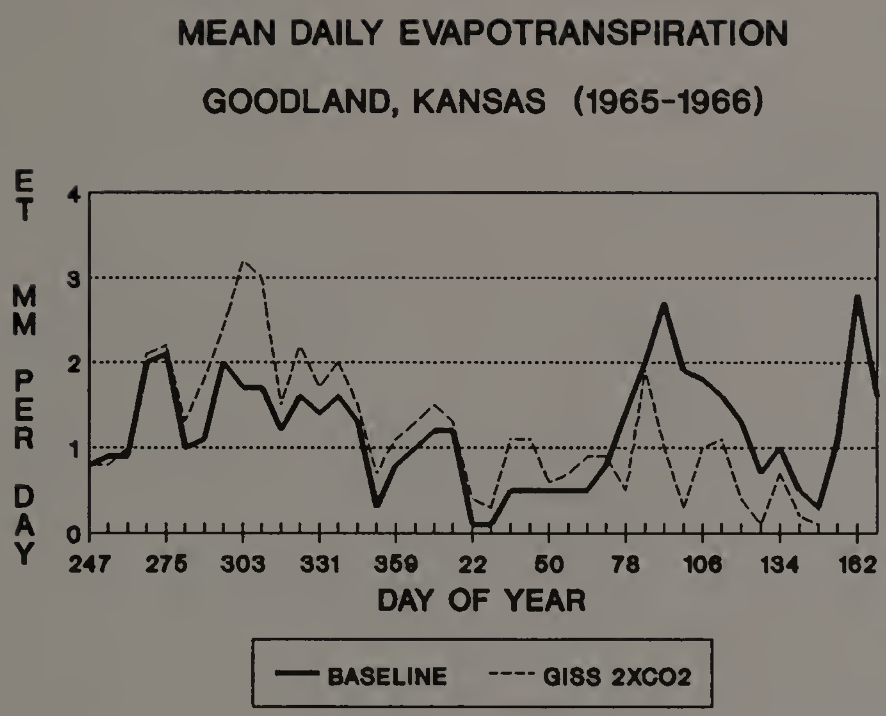

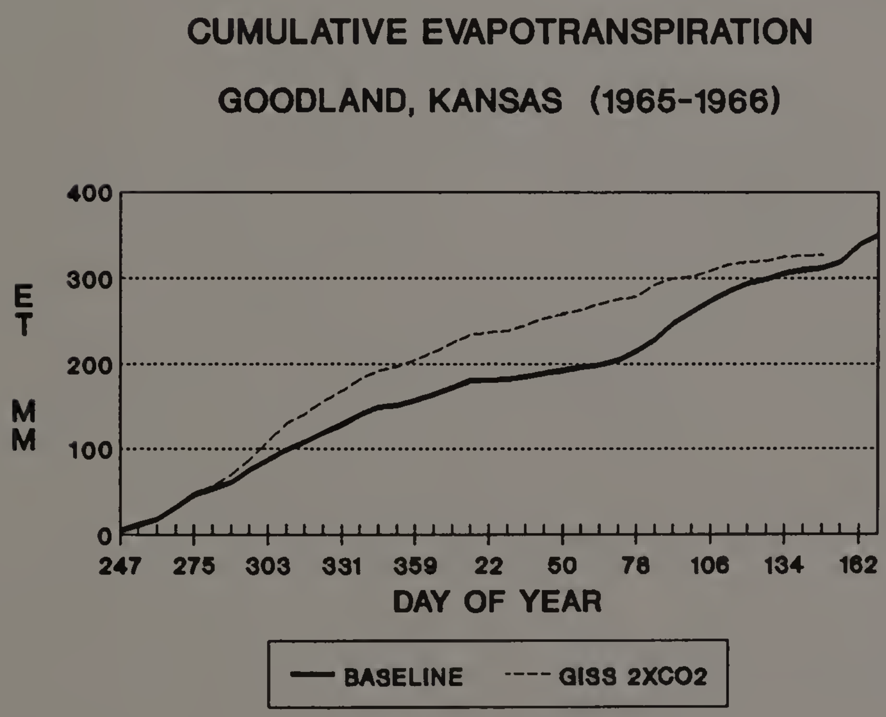

Figure 4.4 Simulated mean daily and cumulative evapotranspiration, Goodland, Kansas (1965-1966).

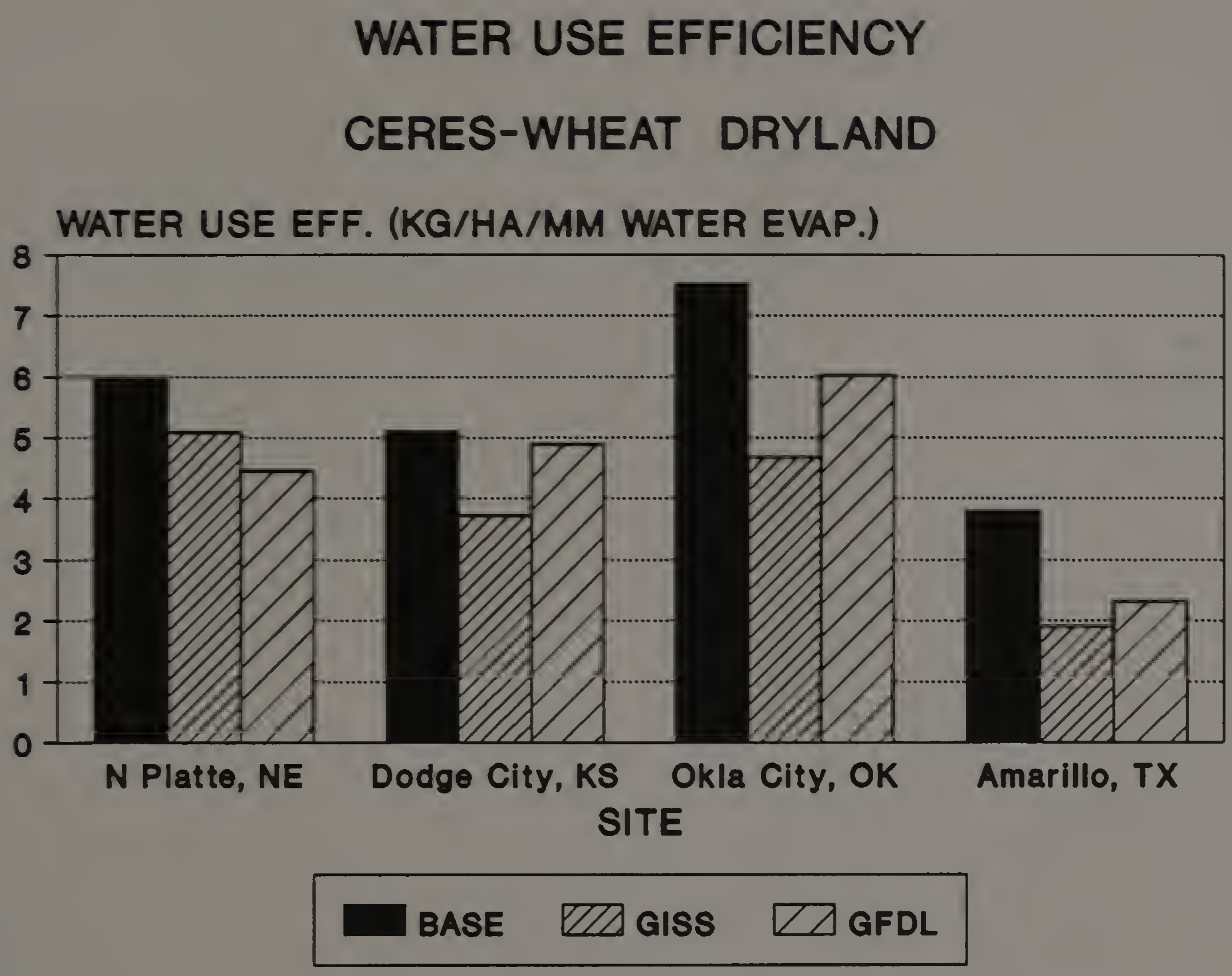

Figure 4.5 CERES-Wheat dryland water use efficiency (yield/total evapotranspiration) for GISS and GFDL $2XCO_2$ climate change scenarios.

4.2.2 Corn

CERES-Maize simulations produced results of changes in yield, thermal units, evapotranspiration, days to maturity, and water use efficiency for dryland and irrigated conditions.

4.2.2.1 Dryland Yields

Simulations similar to the ones described above for wheat were made with the CERES-Maize model to determine the effects of the GISS and GFDL climate change scenarios on corn yield and water use. Overall, the changed climate of the GISS scenario affected corn yields less than it did wheat yields (Table 4.5). The mean decrease in corn yields was 17%, compared to a mean decrease of 30% for CERES-Wheat under the GISS climate change scenario.

Because the difference of the means is approximately normally distributed by the central limit theorem, a difference of means of two standard deviations gives approximately the 95% confidence limits of the null hypothesis that the difference between the means is 0. Using this simple significance criterion of twice the standard deviation, the corn yield reductions were significant in only seven out of the fourteen locations used in the study.

With the GISS scenario, simulated corn yields were more negatively affected by the modified climate than simulated

Table 4.5 Change in CERES-Maize yield with GISS and GFDL climate change scenarios.

a)	CERES-MAIZE 2XCO2 DRYLAND			
	GISS		GFDL	
Site	Yield	sd	Yield	sd
	(%Δ)	(%Δ)	(%Δ)	(%Δ)
NEBRASKA				
Norfolk	-18.6*	7.7	-76.0*	6.4
Grand Island	-19.8*	7.2	-74.5*	5.9
Scottsbluff	-33.2	22.3	-83.4*	19.6
Omaha	-24.5*	3.1	-63.4*	3.2
North Platte	-4.0	12.8	-66.8*	10.9
KANSAS				
Goodland	-26.7	20.6	-90.1*	17.7
Dodge City	-42.9*	14.7	-66.7*	13.7
Wichita	-26.6*	7.4	-42.2*	7.2
OKLAHOMA				
Tulsa	-10.5*	3.7	-23.5*	3.5
Oklahoma City	-12.6*	5.3	-8.2*	5.5
TEXAS				
Amarillo	-12.5	16.4	-38.1*	16.0
Waco	-5.4	5.9	-18.2*	6.0
San Antonio	-3.5	7.4	-12.2	7.7
Brownsville	-7.1	11.5	8.8	10.6
Mean	-17.7		-46.8	
b)	CERES-MAIZE 2XCO2 IRRIGATED			
NEBRASKA				
Norfolk	-20.2*	1.6	-35.0*	1.7
Grand Island	-18.9*	1.6	-33.3*	1.9
Scottsbluff	-12.3*	2.6	-22.7*	2.7
Omaha	-22.6*	1.7	-37.3*	1.7
North Platte	-12.5*	2.6	-26.4*	2.6
KANSAS				
Goodland	-18.7*	1.5	-32.4*	1.6
Dodge City	-21.4*	1.8	-25.3*	1.8
Wichita	-17.5*	2.0	-21.0*	2.1
OKLAHOMA				
Tulsa	-8.7*	* 1.8	-13.3*	2.0
Oklahoma City	-10.5*	2.3	-10.9*	2.3
TEXAS				
Amarillo	-17.1*	1.3	-24.5*	1.5
Waco	-11.5*	1.6	-16.4*	1.7
San Antonio	-18.8*	2.0	-13.3*	2.1
Brownsville	-19.4*	3.1	-22.8*	3.1
Mean	-16.4		-23.9	

*Greater than two times the st. dev. of percent change.

wheat yields at the northern sites and less negatively affected at the southern sites. The cultivars used at the southern study sites in the baseline simulation are those already adapted to high temperatures in the current climate.

The hotter and drier climate of the GFDL scenario had a much greater negative effect on simulated corn yields than did the GISS scenario (Table 4.5). Furthermore, the climate change scenario predicted by GFDL was also much more detrimental to corn yields than it was to wheat yields at most study sites. Simulated decreases in corn yields ranged from 9 to 90% over the fourteen study sites between Norfolk, Nebraska (41.59°N latitude) and Brownsville, Texas (25.54°N latitude). The mean decrease in simulated corn yields with the GFDL climate change scenario over all sites was about 50%, compared to a 33% decrease in CERES-Wheat yields. The largest decreases were seen in Kansas and Nebraska, the northernmost states of the region.

In the case of the GFDL climate change scenario, the corn yield decreases, especially those at higher latitudes, appear to be caused by a combination of the effects of both high temperatures and increased moisture stress, in contrast to the corn yield decreases caused by high temperatures alone in the GISS climate change scenario. When CERES-Maize was tested with GFDL climate change scenarios created with only one climate variable, as was done for CERES-Wheat, both temperature and precipitation factors contributed substantially to yield decreases at most sites (Figure 4.6).

The GFDL climate change model predicts particularly severe effects in Kansas and Nebraska during the summer months (Figure 3.5), and this severity was reflected in the corn yield decreases simulated by the crop model used in conjunction with GFDL. Large increases in summertime temperatures (an average of +7.7°C at the Nebraska sites) contributed to a shortening of the corn crop growing season by about three weeks, a shortening that inhibits the process of grain filling (Table 4.6).

In addition to the extremely high temperature changes predicted for June-July-August, the GFDL scenario also predicts pronounced reductions in summer precipitation. In the two northern gridboxes of the study area, these reductions are about 30 mm per month (see Figure 3.5). Because corn is a summer annual crop that is planted in the spring and harvested in the fall, these decreases in precipitation in the GFDL scenario occur during the critical growth stages of flowering and grain filling (Doorenbos and Kassam, 1979). This crop-climate interaction is in contrast to that of the winter annual wheat which is planted in the fall and harvested in the early part of the following summer, thus avoiding the mid-continental summer dryness of the GFDL scenario.

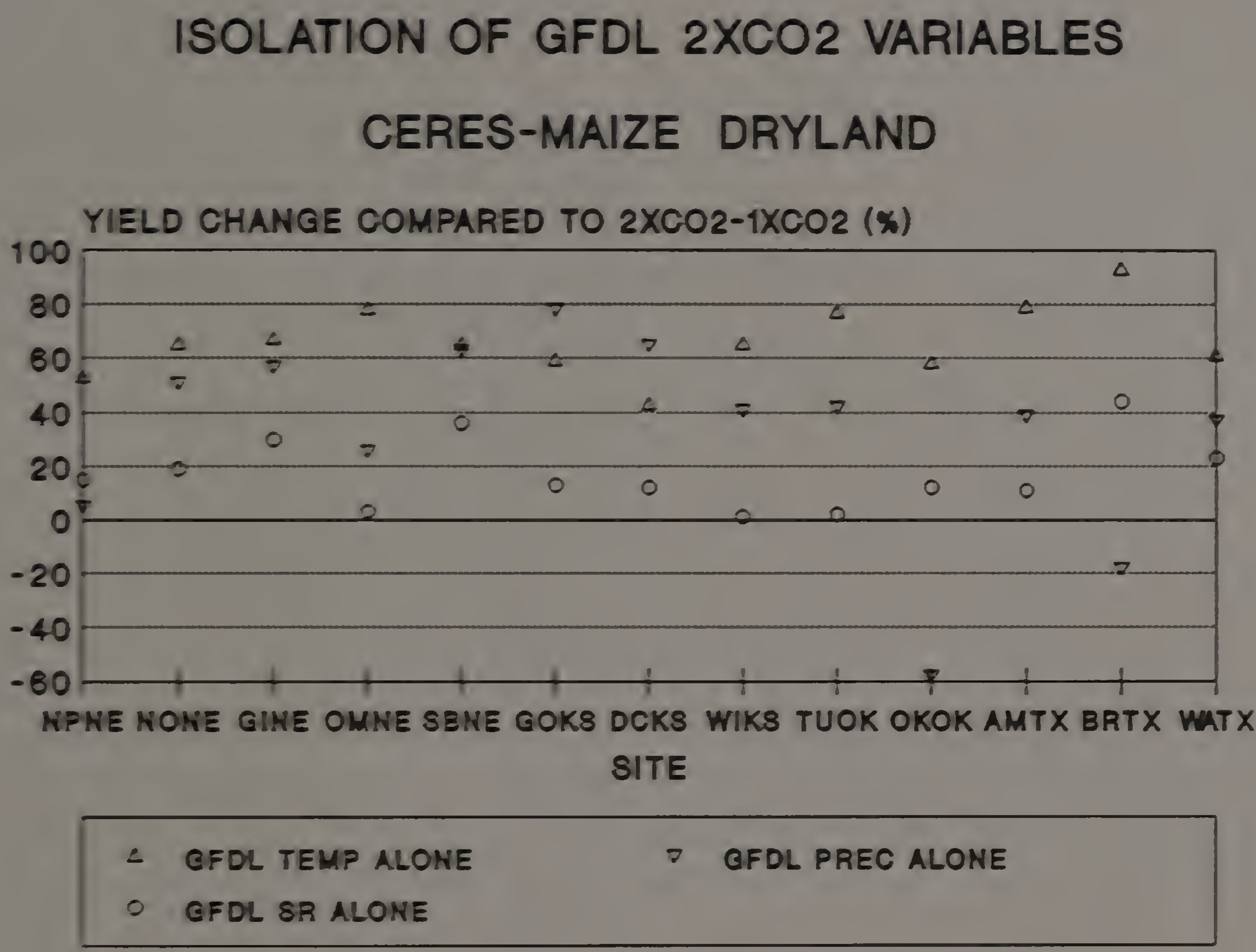

Figure 4.6 CERES-Maize yield changes with climate variables changed alone as percent of yield changes of full GFDL $2XCO_2$ scenario.

Table 4.6 Change in CERES-Maize days to maturity with GFDL climate change scenario.

	CERES-MAIZE GFDL $2XCO_2$ DRYLAND			
	DRYLAND		IRRIGATED	
Site	Days	sd	Days	sd
NEBRASKA				
Norfolk	-24*	1.1	-24*	0.9
Grand Island	-26*	1.2	-23*	1.1
Scottsbluff	-29*	1.3	-30*	1.3
Omaha	-19*	1.0	-18*	0.9
North Platte	-34*	1.6	-33*	1.5
KANSAS				
Goodland	-22*	1.1	-23*	1.0
Dodge City	-15*	1.0	-18*	0.8
Wichita	-17*	1.0	-17*	0.9
OKLAHOMA				
Tulsa	-19*	0.9	-19*	0.9
Oklahoma City	-18*	0.6	-17*	0.7
TEXAS				
Amarillo	-15*	1.3	-19*	0.9
Waco	-18*	0.7	-18*	0.8
San Antonio	-17*	0.6	-16*	0.7
Brownsville	-21	0.8	-21*	0.9
Mean	-21		-21	

*Greater than two times the st. dev. of change.

4.2.2.2 Irrigated Yields

Even with irrigation, simulated corn yields were significantly lower than baseline yields at all locations in both the GISS and GFDL scenarios (Table 4.5). Yield decreases from 9 to 21% occurred in the GISS scenario and from 11 to 37% in the GFDL scenario. These decreases were again most likely caused by early ripening: maturity dates of simulated irrigated corn advanced by 2 1/2 to 3 weeks in both the GISS and GFDL scenarios.

4.2.2.3 Water Regime

Total evapotranspiration for dryland corn decreased, albeit not significantly, with the GISS climate change scenario. This implies that the increased daily rate of evapotranspiration caused by the higher temperatures was more than offset by the shortened growing season (Table 4.7). Greater and more significant decreases in evapotranspiration were observed with the GFDL scenario, reflecting the hotter and drier conditions predicted by it at most locations. Opposite effects were present in the irrigation simulations, where total crop evapotranspiration tended to increase in most locations, as the increased availability of water allowed more evapotranspiration to occur in response to the warmer climate, despite shortening of growing period.

Table 4.7 Change in CERES-Maize evapotranspiration with GISS and GFDL climate change scenarios.

a) CERES-MAIZE $2XCO_2$ DRYLAND

	GISS		GFDL	
Site	ET	sd	ET	sd
	(%Δ)	(%Δ)	(%Δ)	(%Δ)
NEBRASKA				
Norfolk	-3.2	2.6	-24.3*	2.7
Grand Island	-3.1	2.8	-21.1*	2.8
Scottsbluff	-1.6	5.3	-25.6*	4.9
Omaha	-3.6*	1.4	-14.3*	1.8
North Platte	-3.3	3.8	-28.2*	3.9
KANSAS				
Goodland	-1.3	5.2	-38.8*	4.6
Dodge City	-5.5	4.8	-15.8*	4.5
Wichita	-4.5	2.8	-7.7*	2.8
OKLAHOMA				
Tulsa	-2.5	1.7	-4.4*	1.6
Oklahoma City	-3.0	2.1	-3.4	2.1
TEXAS				
Amarillo	-1.2	5.3	-14.7*	5.4
Waco	-4.4	2.3	-7.4*	2.5
San Antonio	-4.1	3.6	-8.3*	3.4
Brownsville	-2.2	5.2	-0.8	4.8
Mean	-3.1		-13.9	

b) CERES-MAIZE 2XCO2 IRRIGATED

	GISS ET	GISS sd	GFDL ET	GFDL sd
NEBRASKA				
Norfolk	0.6	1.1	26.1*	1.6
Grand Island	1.7	1.0	30.6*	1.6
Scottsbluff	3.9*	1.9	36.4*	2.1
Omaha	1.6	1.2	32.4*	1.7
North Platte	1.6	1.5	23.2*	1.9
KANSAS				
Goodland	7.8*	1.1	28.3*	1.6
Dodge City	12.8*	1.3	20.9*	1.6
Wichita	9.4*	1.9	20.9*	1.6
OKLAHOMA				
Tulsa	5.0*	1.3	3.2*	1.5
Oklahoma City	8.0*	1.9	3.7*	1.8
TEXAS				
Amarillo	11.6*	1.2	23.6*	1.5
Waco	-1.9	1.3	-0.6	1.3
San Antonio	-2.4	1.6	-1.6	1.5
Brownsville	-5.4*	2.3	-1.6	2.3
MEAN	3.9		17.5	

*Greater than two times the st. dev. of percent change.

Changes in simulated water use efficiency for corn grown at four sites are shown in Figure 4.7. As in the case of wheat, water use efficiency of corn decreased almost everywhere, especially in the hotter and drier GFDL scenario, where yields were significantly reduced. The decreases in water use efficiency were more pronounced at the northern sites because of the greater severity of the climate changes predicted for those sites.

4.3 Physiological Effects of Increased CO_2

The physiological effects of CO_2 enrichment *per se* are of interest, even without concomitant global warming. Results of small-scale experiments in controlled atmospheres suggest that this can stimulate photosynthesis, while often increasing stomatal resistance, thus culminating in higher yields and more efficient water use (see Acock and Allen, 1985). To consider this, the CERES models were modified to account for the physiological effects of doubled CO_2 (specified as 660 ppm) under the baseline climate conditions (1951-1980).

4.3.1 Wheat

For the CERES-Wheat model, the modifications for doubled CO_2 included a 25% increase in daily photosynthesis, and a changed stomatal resistance (following Chaudhuri *et al.*, 1986) from 0.78 to 0.75 s/cm for dryland conditions and

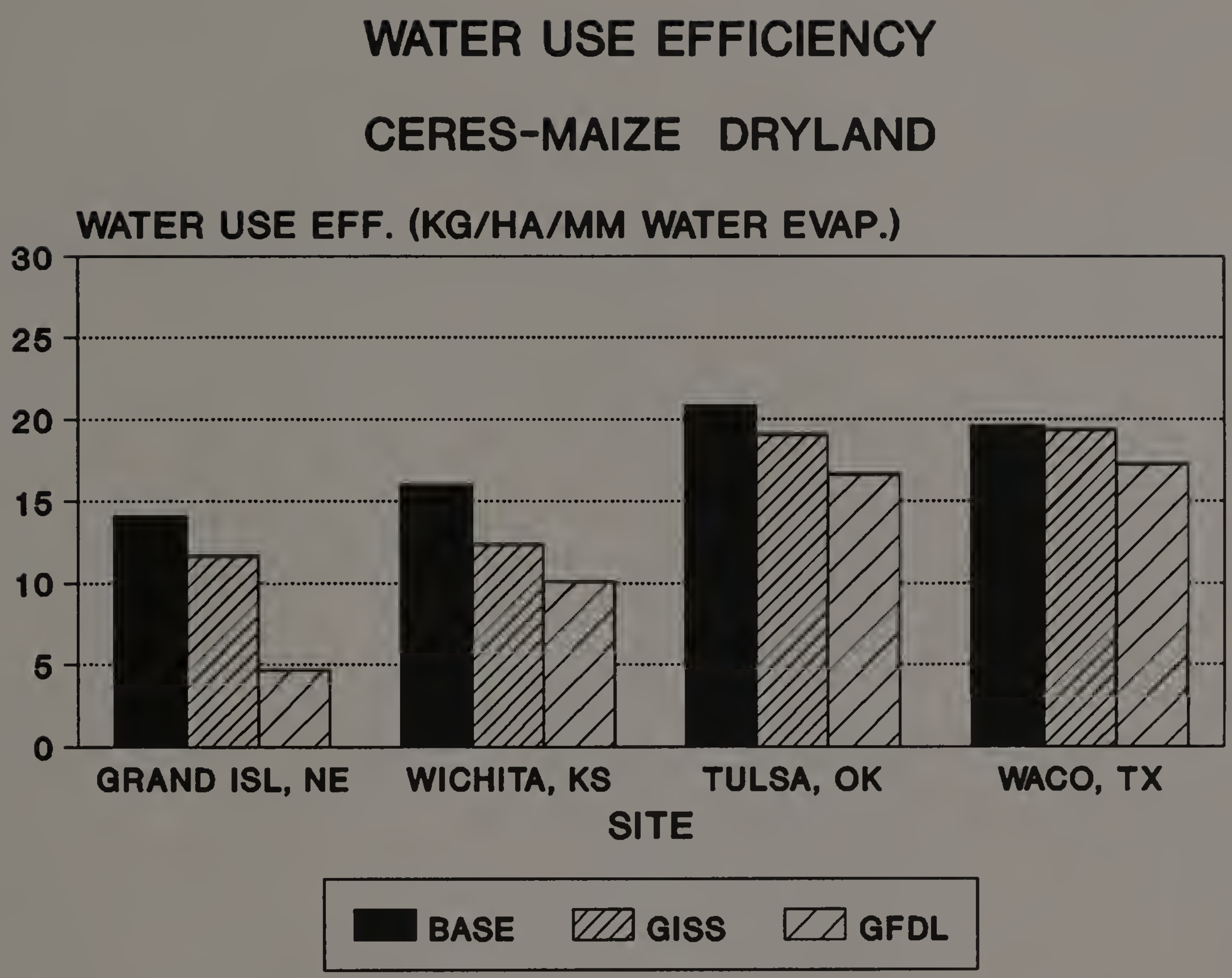

Figure 4.7 CERES-Maize dryland water use efficiency (yield/total evapotranspiration) for GISS and GFDL $2XCO_2$ climate change scenarios.

from 0.48 to 0.63 s/cm for irrigated conditions. Results of these simulations were compared to the results of the baseline simulations run with "current" climate and atmospheric composition (330 ppm CO_2).

The physiological effects of CO_2 increased simulated wheat yields in both dryland and irrigated conditions by an average of about 28% (Table 4.8). This compares with a 45% increase in yield observed in controlled atmosphere (340 ppm to 660 ppm CO_2) experiments by Chaudhuri et al. (1986), and with an average increase in yield of 35 +/-14% from eight studies reported by Cure (1985). Note that the 28% increase in simulated yields is slightly higher than the 25% increase in daily photosynthetic rate used in the modification of the model. The increase in simulated yields over and above the specified increase in photosynthesis was likely caused by a feedback effect, by which the crop leaf area became larger earlier in the season and produced more carbohydrates, thereby enhancing yields.

In the irrigation simulations, there may also have been a beneficial effect on yields from the increment of water saved by the increased stomatal resistance, the other component of the modification for CO_2. This would not have influenced wheat yield in the dryland simulations because wheat plants subject to water stress may not increase their stomatal resistance in response to CO_2 enrichment as do well watered plants (Chaudhuri et al., 1986).

Table 4.6 Change in CERES-Wheat yield with physiological effects of CO_2.

	CERES-WHEAT	PHYSIOL. EFFECTS OF CO_2		
	DRYLAND		IRRIGATED	
Site	Yield	sd	Yield	sd
	(%Δ)	(%Δ)	(%Δ)	(%Δ)
NEBRASKA				
Norfolk	25.4*	6.3	26.0*	2.4
Grand Island	26.4*	6.1	26.4*	2.2
Scottsbluff	32.7*	11.7	28.6*	2.1
Omaha	27.4*	4.9	26.0*	2.8
North Platte	27.9*	10.3	27.5*	3.9
KANSAS				
Goodland	27.8	14.4	27.7*	1.9
Dodge City	32.1*	15.0	26.8*	2.2
Wichita	28.1*	8.2	25.6*	2.2
OKLAHOMA				
Tulsa	27.4*	3.4	27.4*	2.5
Oklahoma City	26.0*	7.3	25.3*	2.3
TEXAS				
Amarillo	22.0	18.9	26.8*	1.8
Brownsville	34.1*	5.9	37.6*	3.9
Mean	28.1		27.6	

*Greater than two times the st. dev. of percent change.

4.3.2 Corn

The CERES-Maize model was modified by increasing the daily photosynthetic rate by 10% and by increasing the stomatal resistance from 0.56 to 1.06 s/cm, following the equation of Rogers et al. (1983). The simulation results from the modified CERES-Maize were compared to results from the original model for the baseline climate.

In general, the modifications led to large increases in corn yields in the dryland simulations and to small increases in the irrigated simulations (Table 4.9). The largest yield increases occurred at sites with low annual precipitation and low yields in the baseline dryland simulation. This result suggests that the increase in stomatal resistance had a strong beneficial effect under simulated dryland conditions, by providing significantly more water for grain production. At some of the study sites, current climatic conditions are too arid for dryland corn production, and simulated yield levels were still low even with the enhanced CO_2 effect. Under simulated irrigated conditions, the stomatal factor had less of an influence and yield increases were mostly below the 10% increase in photosynthetic rate specified in the model.

These simulated corn yield increases with high CO_2 compare to increases in total dry matter of about 7% and no observed yield increase observed in a set of plant growth chamber experiments with three soil-water treatments

Table 4.9 Change in CERES-Maize yield with physiological effects of CO_2.

	CERES-MAIZE PHYSIOL. EFFECTS OF CO_2			
	DRYLAND		IRRIGATED	
Site	Yield	sd	Yield	sd
	(%Δ)	(%Δ)	(%Δ)	(%Δ)
NEBRASKA				
Norfolk	63.1*	7.3	8.6*	1.5
Grand Island	68.4*	7.5	6.3*	1.7
Scottsbluff	142.1*	37.2	7.7*	3.5
Omaha	17.1*	2.8	6.4*	1.7
North Platte	90.5*	14.8	7.4*	3.1
KANSAS				
Goodland	121.8*	34.7	5.4*	1.5
Dodge City	109.0*	23.9	5.6*	1.6
Wichita	42.5*	7.6	7.0*	1.8
OKLAHOMA				
Tulsa	21.4*	3.5	6.4*	2.0
Oklahoma City	46.6*	5.6	6.2*	2.8
TEXAS				
Amarillo	102.0*	22.5	3.3*	1.3
Waco	40.5*	5.5	3.3*	1.3
San Antonio	45.7*	7.9	6.1*	2.3
Brownsville	74.6*	13.7	5.7*	3.7
Mean	70.4		6.3	

*Greater than two times the st. dev. of percent change.

performed by King and Greer (1986). They reported that the effect of CO_2 was greater with limited soil water in their experiments, i.e., increases in dry matter were greater under water-stressed conditions, as was simulated (but at excessive levels) in the model runs. The yield increases in the irrigated simulations seem to be more realistic than those simulated for dryland conditions. Improvement in simulating the effects of CO_2 on corn growth and yield is an objective for further work.

4.4 Combined Climate and Physiological Effects

The next step was to run the CERES models with the combined effects of the climate change scenarios and the modifications for the physiological effects of CO_2. This set of simulations is more realistic, since the two mechanisms are predicted to take place simultaneously. The results of these combined simulations for CERES-Wheat and CERES-Maize are compared to the results of the simulations with climate change effects alone in Figures 4.8 and 4.9.

4.4.1 Wheat

In the dryland simulations of wheat growth, the physiological effects of CO_2 mitigated the detrimental effect of climate change on wheat yields in about half of the locations in both the GISS and GFDL scenarios (Table 4.10). With the GISS scenario, compensation by the

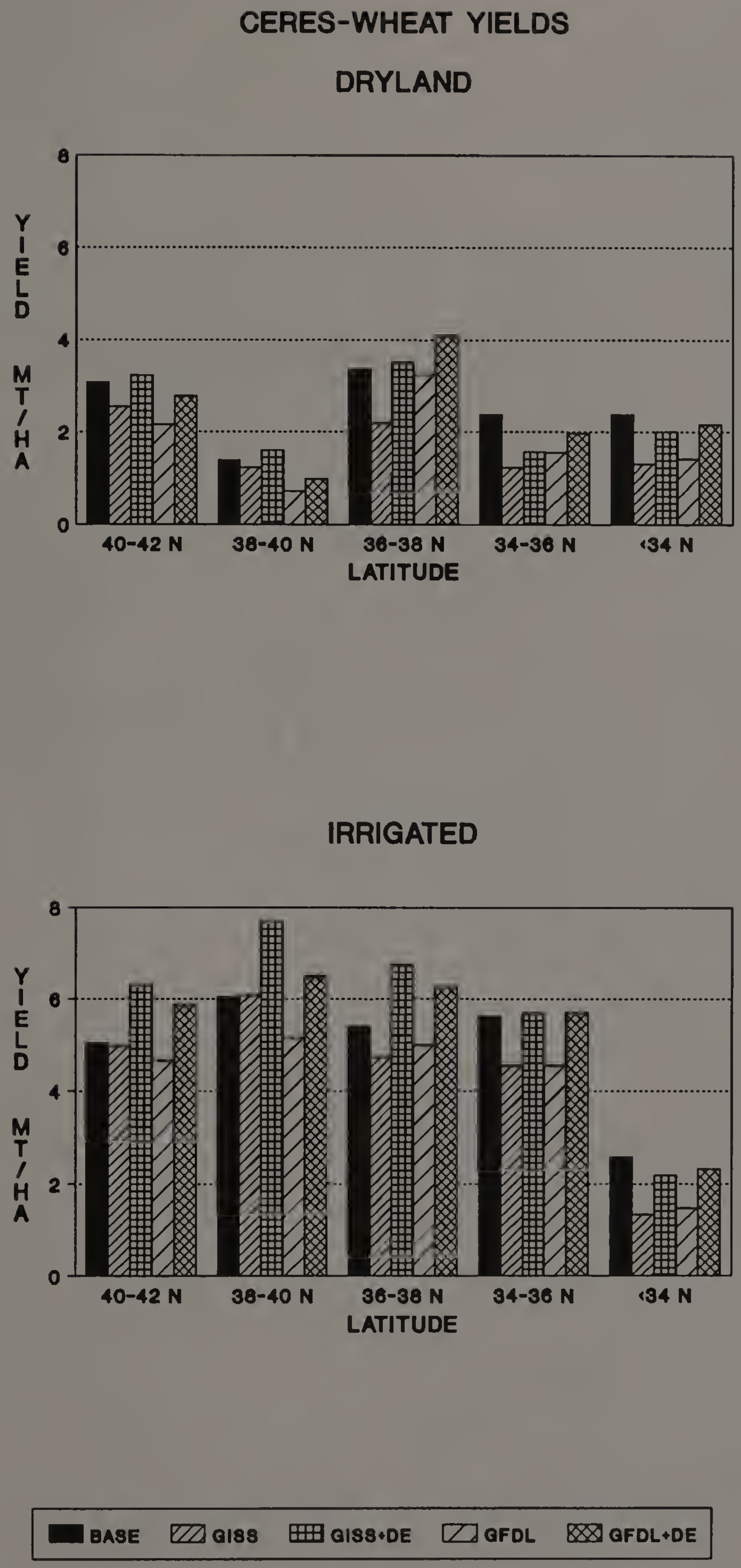

Figure 4.8 CERES-Wheat dryland and irrigated yields with GISS and GFDL $2XCO_2$ climate change scenarios with and without physiological CO_2 effects.

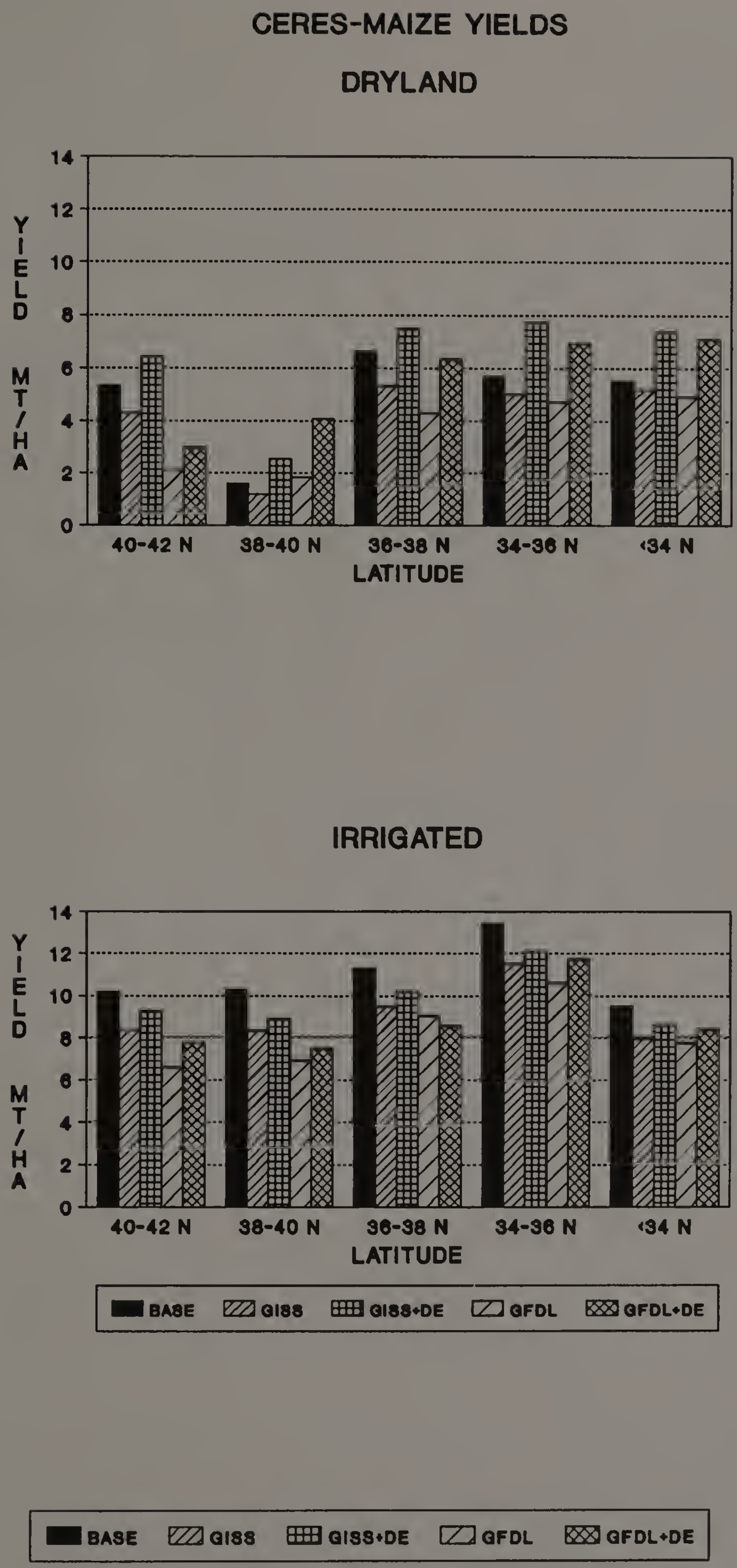

Figure 4.9 CERES-Maize dryland and irrigated yields with GISS and GFDL $2XCO_2$ climate change scenarios with and without physiological CO_2 effects.

Table 4.10 Change in CERES-Wheat yield with GISS and GFDL $2XCO_2$ climate change scenarios and the direct effects of CO_2.

a) CERES-WHEAT $2XCO_2$ PHYS. EFFECTS OF CO_2 DRYLAND

Site	GISS Yield (%Δ)	GISS sd (%Δ)	GFDL Yield (%Δ)	GFDL sd (%Δ)
NEBRASKA				
Norfolk	13.3	7.0	-10.4	6.6
Grand Island	4.9	7.1	-5.0	6.8
Scottsbluff	-1.6	11.1	-27.0*	10.3
Omaha	8.1	5.0	0.8	4.5
North Platte	-8.0	9.6	-22.7*	9.6
KANSAS				
Goodland	17.7	19.4	-27.4*	13.5
Dodge City	-19.4	13.3	13.9	15.3
Wichita	-15.9*	7.8	2.7	7.7
OKLAHOMA				
Tulsa	33.0*	5.1	44.8*	3.9
Oklahoma City	-31.5*	6.6	-8.4	6.9
TEXAS				
Amarillo	-41.4*	13.3	-41.6*	14.4
Brownsville	-15.8*	4.8	-9.4*	4.5
Mean	-5.4		-7.5	

b) CERES-WHEAT $2XCO_2$ PHYS. EFFECTS OF CO_2 IRRIGATED

Site	GISS Yield (%Δ)	GISS sd (%Δ)	GFDL Yield (%Δ)	GFDL sd (%Δ)
NEBRASKA				
Norfolk	22.3*	2.8	13.8*	2.7
Grand Island	21.5*	2.4	14.1*	2.2
Scottsbluff	36.3*	2.0	24.2*	2.1
Omaha	11.5*	2.8	5.3*	2.6
North Platte	34.8*	3.0	26.6*	3.0
KANSAS				
Goodland	27.2*	2.1	7.6*	3.7
Dodge City	14.7*	2.3	5.9*	2.2
Wichita	11.8*	2.3	3.0	2.2
OKLAHOMA				
Tulsa	52.4*	2.9	46.6*	2.8
Oklahoma City	0.6	2.4	-1.0	2.4
TEXAS				
Amarillo	2.1	2.1	3.7	2.2
Brownsville	-15.5*	3.7	-10.4*	3.5
Mean	18.3		11.6	

*Greater than two times the st. dev. of percent change.

beneficial physiological effects on dryland wheat yields appeared to be more effective at the northern sites, where climate change effects on crop yields were predicted to be less severe than at the southern sites. With the GFDL scenario, the compensatory physiological response to CO_2 enrichment was randomly distributed throughout the region.

When automatic irrigation was simulated in the combined climate change and CO_2 enrichment run, wheat yields improved over the baseline in most locations, except in the southernmost latitudes (Table 4.10). This occurred with both the GISS and GFDL climate change scenarios. The 25% increase in wheat photosynthesis evidently overcame the negative impact of the shortened grain filling period. This result implies that wheat farmers in the southern Great Plains may need to irrigate in order to take full advantage of the beneficial effects of CO_2 in the event of climate change similar to that predicted by the global climate models.

4.4.2 Corn

When the CERES-Maize model was run for the combined effects of global climate change and increased CO_2, simulated dryland corn yields increased compared to baseline values under the less severe GISS climate scenario, but decreased significantly in half of the locations with the more severe GFDL scenario (Table 4.11). In the runs with

Table 4.11 Change in CERES-Maize yield with GISS and GFDL $2XCO_2$ climate change scenarios and physiological CO_2 effects.

a) CERES-MAIZE $2XCO_2$ PHYSIOL. CO_2 EFF. DRYLAND

	GISS		GFDL	
Site	Yield	sd	Yield	sd
	%Δ	%Δ	%Δ	%Δ
NEBRASKA				
Norfolk	28.3*	7.1	-44.6*	7.3
Grand Island	30.8*	6.9	-44.7*	6.8
Scotts Bluff	96.3*	30.3	-62.8*	21.1
Omaha	-8.5*	2.8	-40.1*	3.4
North Platte	77.2*	13.7	-28.6*	11.7
KANSAS				
Goodland	63.2*	25.7	-77.6*	18.3
Dodge City	25.9	18.6	-18.9	16.1
Wichita	8.4	7.3	-7.6	7.5
OKLAHOMA				
Tulsa	11.9*	3.2	1.1	3.4
Okla. City	55.1*	5.1	31.1*	5.2
TEXAS				
Amarillo	69.6*	20.1	8.0*	18.4
Waco	29.6*	5.1	17.3*	5.6
San Antonio	24.6*	6.7	22.4*	7.5
Brownsville	55.7*	12.3	64.0*	10.8
Mean	40.6		-12.9	
b) CERES-MAIZE $2XCO_2$ DIR. EFF. CO_2 IRRIGATED				
NEBRASKA				
Norfolk	-13.5*	1.6	-29.5*	1.6
Grand Island	-12.3*	1.5	-28.2*	1.9
Scotts Bluff	-4.6	2.6	-15.8*	2.7
Omaha	-16.3*	1.7	-32.3*	1.7
North Platte	-5.7*	2.6	-19.7*	2.6
KANSAS				
Goodland	-13.2*	1.4	-26.9*	1.7
Dodge City	-15.6*	1.8	-19.2*	1.8
Wichita	-11.6*	1.9	-15.4*	2.0
OKLAHOMA				
Tulsa	-1.4	1.8	-35.2*	1.9
Okla. City	-6.3*	2.2	-3.7*	2.2
TEXAS				
Amarillo	-12.6*	1.2	-19.6*	1.4
Waco	-5.2*	1.5	-9.4*	1.7
San Antonio	-12.3*	2.0	-6.7*	2.0
Brownsville	-11.8*	3.1	-16.2*	3.1
Mean	-10.2		-19.8	

*Greater than two times the st. dev. of percent change.

automatic irrigation, simulated corn yields decreased in comparison with baseline irrigated corn yields almost everywhere, despite the positive effects of increased photosynthesis and stomatal resistance. As simulated in CERES-Maize, this decrease in irrigated yields was primarily caused by the shortening of the grain filling period due to high temperatures, as discussed above. The lower photosynthetic response to CO_2 in corn compared to wheat (10% vs. 25% increase) prevents total compensation of the negative yield effect by increased corn photosynthesis.

4.4.3 Water Use Efficiency

In the simulations of CERES-Wheat and CERES-Maize that combined the climatic and physiological effects of CO_2, water use efficiency was improved at many locations (Figure 4.10). Of the four sites shown, simulated water use efficiency of wheat improved at one site in the GISS scenario and two sites in the GFDL scenario, while water use efficiency of CERES-Maize improved everywhere with the GISS scenario, and at three of the sites with the GFDL scenario.

The greater improvement in water use efficiency for the CERES-Maize simulations was most probably due to the relatively large positive response of corn stomatal resistance to increased atmospheric CO_2 under dryland conditions. In the modified CERES models, as CO_2 level goes

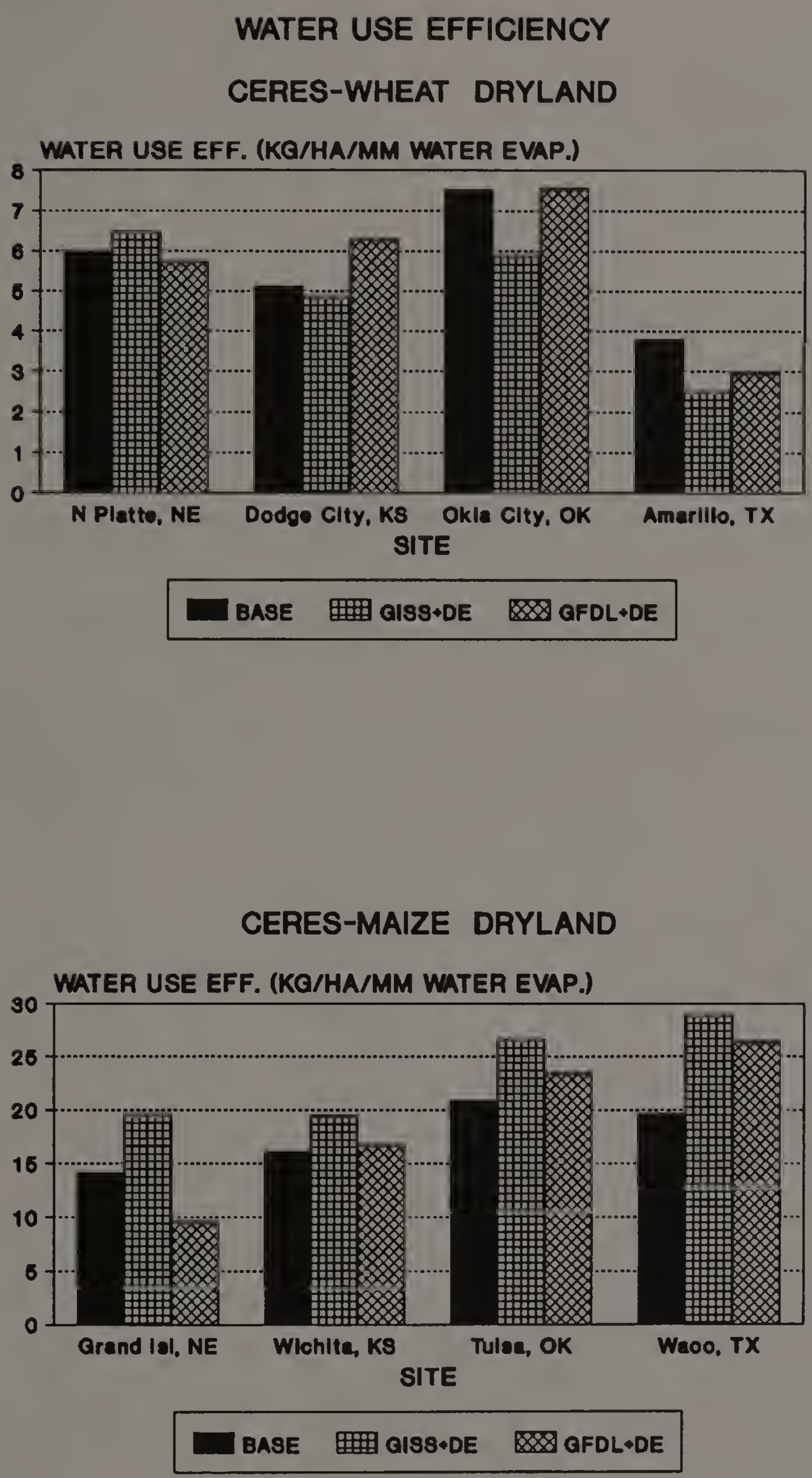

Figure 4.10 CERES-Wheat and CERES-Maize dryland water use efficiencies (yield/total evapotranspiration) with GISS and GFDL 2XCO_2 climate change scenarios and physiological CO_2 effects.

from 330 ppm to 660 ppm, stomatal resistance of corn increases 0.5 s/cm, whereas stomatal resistance of wheat actually decreases by 0.03 s/cm.

Overall, the combination of the increased production of carbohydrates by higher photosynthetic rates and the decrease in crop evapotranspiration appeared to provide significant benefits to crop water use in many locations for both wheat and corn, even with the higher temperatures and changed hydrological regimes of the climate change scenarios.

CHAPTER 5

COMPARISONS AND ADAPTATIONS

5.1 Comparison of Great Plains Subregions

Climate change may cause southern areas of the United States to become less productive relative to northern areas. In southern areas, current temperatures are high and increased temperatures may lead to thermal regimes beyond the optimum for crop growth. In northern areas, crops are currently limited by low temperatures and shorter growing seasons. It has been hypothesized that global warming may actually benefit crop production in these areas (Adams et al., 1989).

5.1.1 Northern Great Plains

To test this hypothesis, baseline and three climate change simulations were made with the CERES-Wheat model at three sites in the northern Great Plains (Figure 5.1) for both winter and spring wheat cultivars. Mean monthly maximum and minimum temperatures and precipitation for the three sites are graphed in Figure 5.2. Because of low winter temperatures which cause damage to winter wheat, spring wheat is currently grown in these locations. Only one representative soil type was used for each Northern Great Plains site.

Besides the GISS and GFDL climate change scenarios used in the Southern Great Plains simulations, the third climate

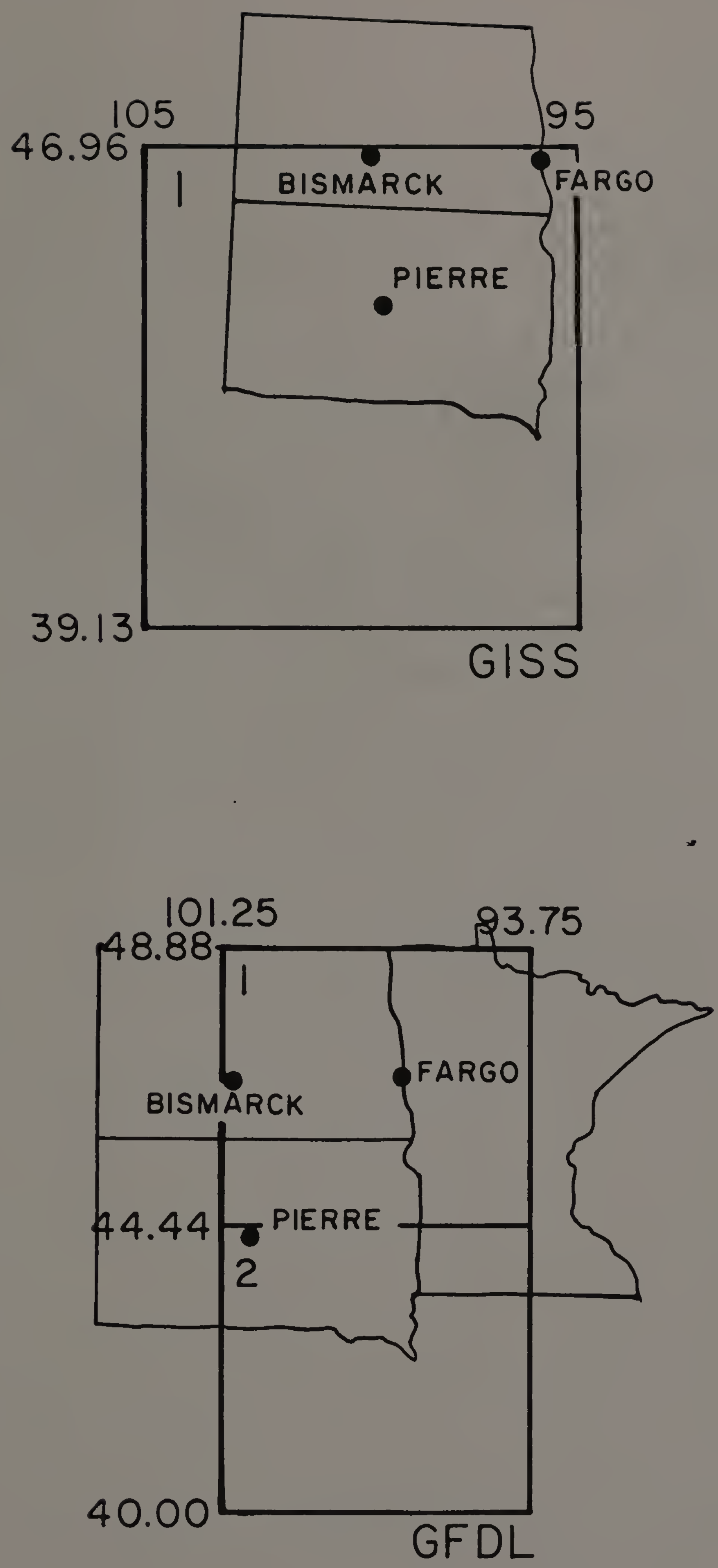

Figure 5.1 Climate stations and GCM gridboxes for GISS and GFDL GCMs in the Northern Great Plains.

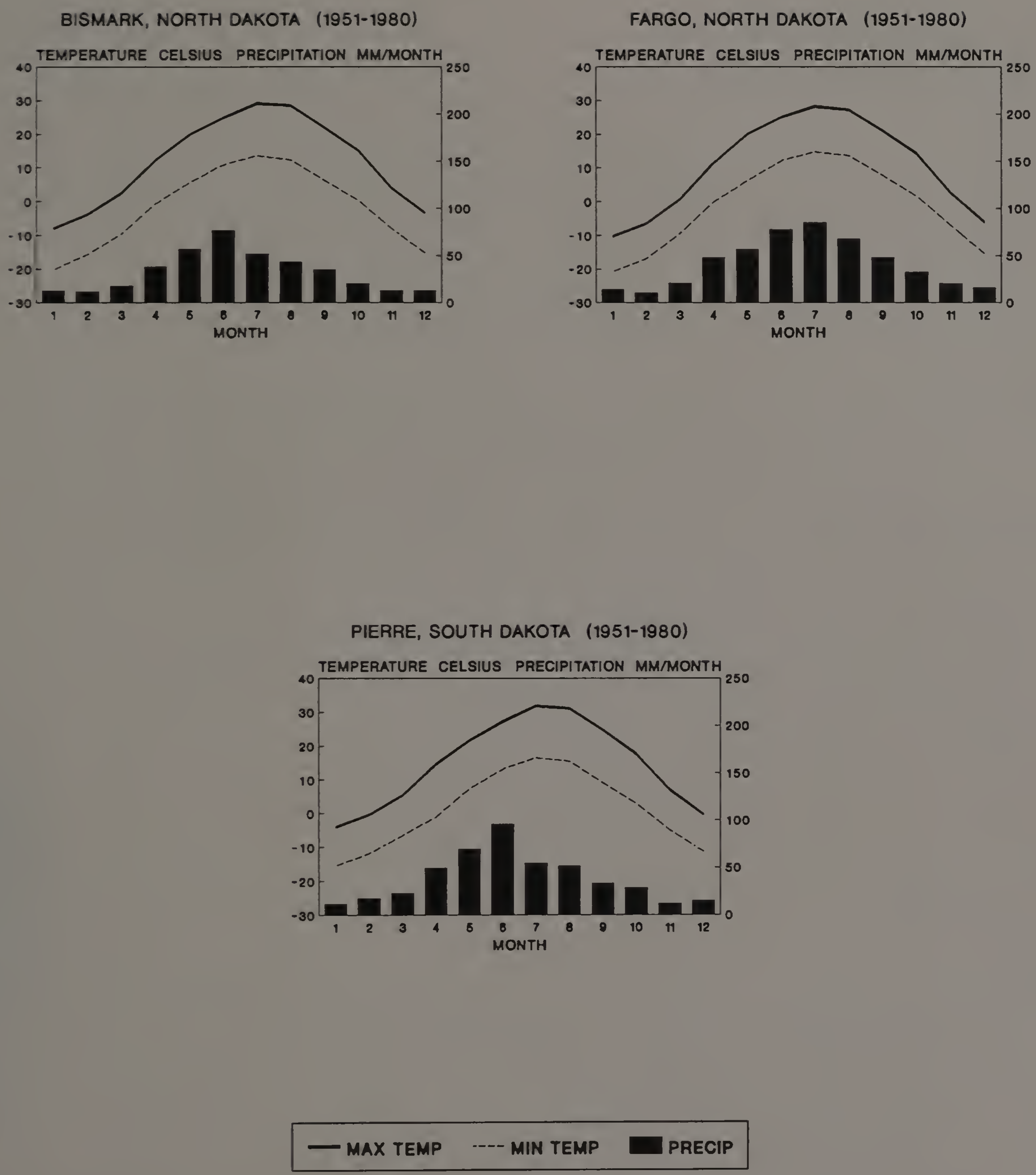

Figure 5.2 Observed mean monthly maximum and minimum temperature and precipitation for Northern Great Plains sites (1951-1980).

change scenario used in the Northern Great Plains simulations is developed from an alternate run of the GFDL GCM which has more realistic sea surface temperatures (Mitchell et al., 1990; R. Wetherald and R. Jenne, pers. com.). This scenario is designated GFDL QFLUX.

Seasonal and annual climate changes for the GISS and GFDL scenarios in the Northern Great Plains are shown in Figure 5.3. The three Northern Great Plains sites are located in the northern part of the GISS 1 gridbox used in the Southern Great Plains study. For these northern sites, the GISS climate change scenario has an annual temperature increase of 5°C and small annual increases in precipitation at the three sites.

The GFDL climate change scenario for the Northern Great Plains sites has large annual temperature increases (5.8° and 6.9°C) and very high increases in the summer (7.8° and 9.2°C). The GFDL scenario has marked decreases in precipitation in the summer of up to 28.6 mm $month^{-1}$. One of the Northern Great Plains sites, Pierre, South Dakota, is located in the GFDL 2 gridbox used in the Southern Great Plains study.

The GFDL QFLUX scenario is the most moderate in temperature increases (4.4°C), and has large increases in precipitation, especially in the summer in Bismark and Fargo, the two sites in North Dakota.

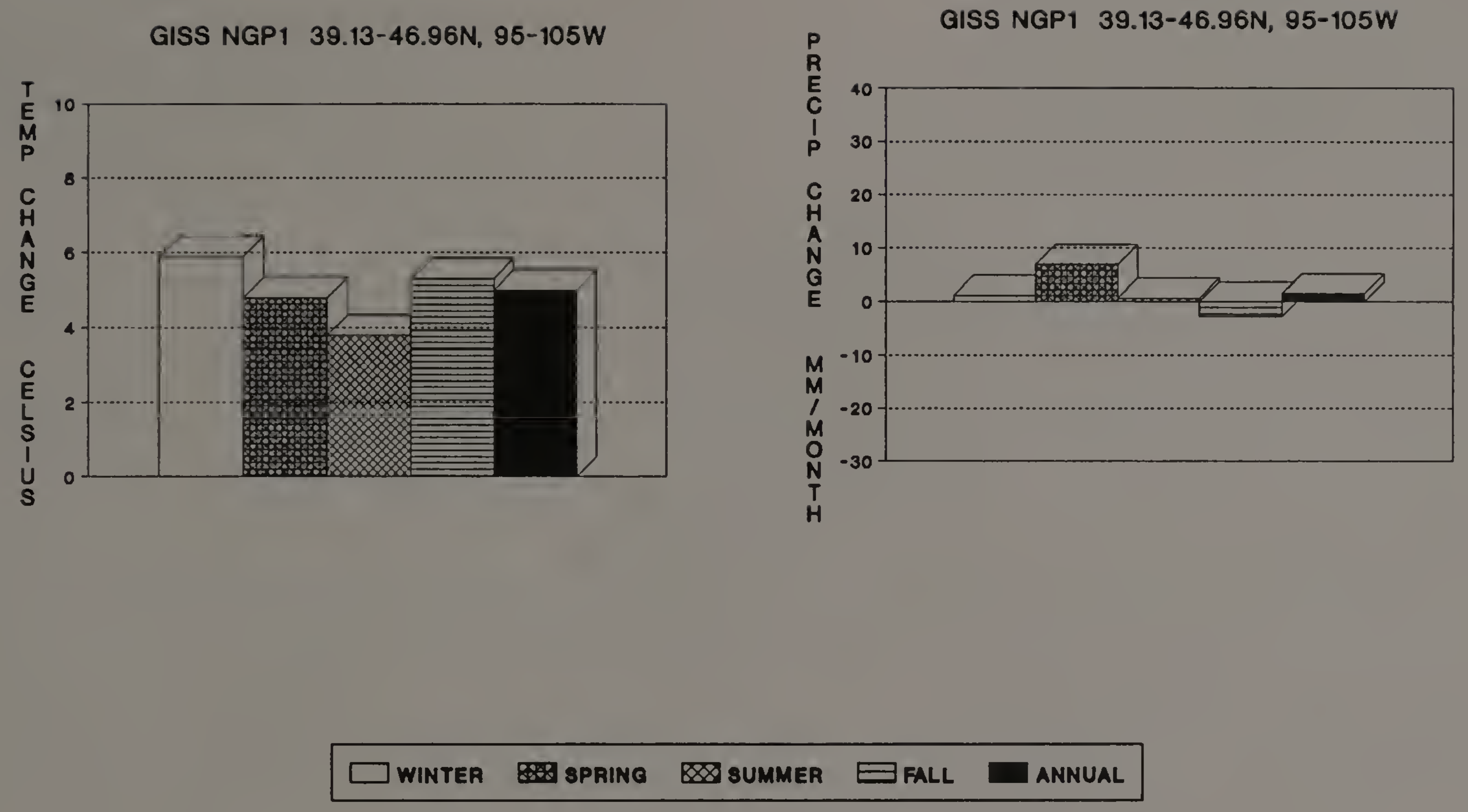

Continued, next page

Figure 5.3 Seasonal and annual temperature and precipitation changes predicted by the GISS and GFDL climate change scenarios for Northern Great Plains sites.

Figure 5.3 Continued

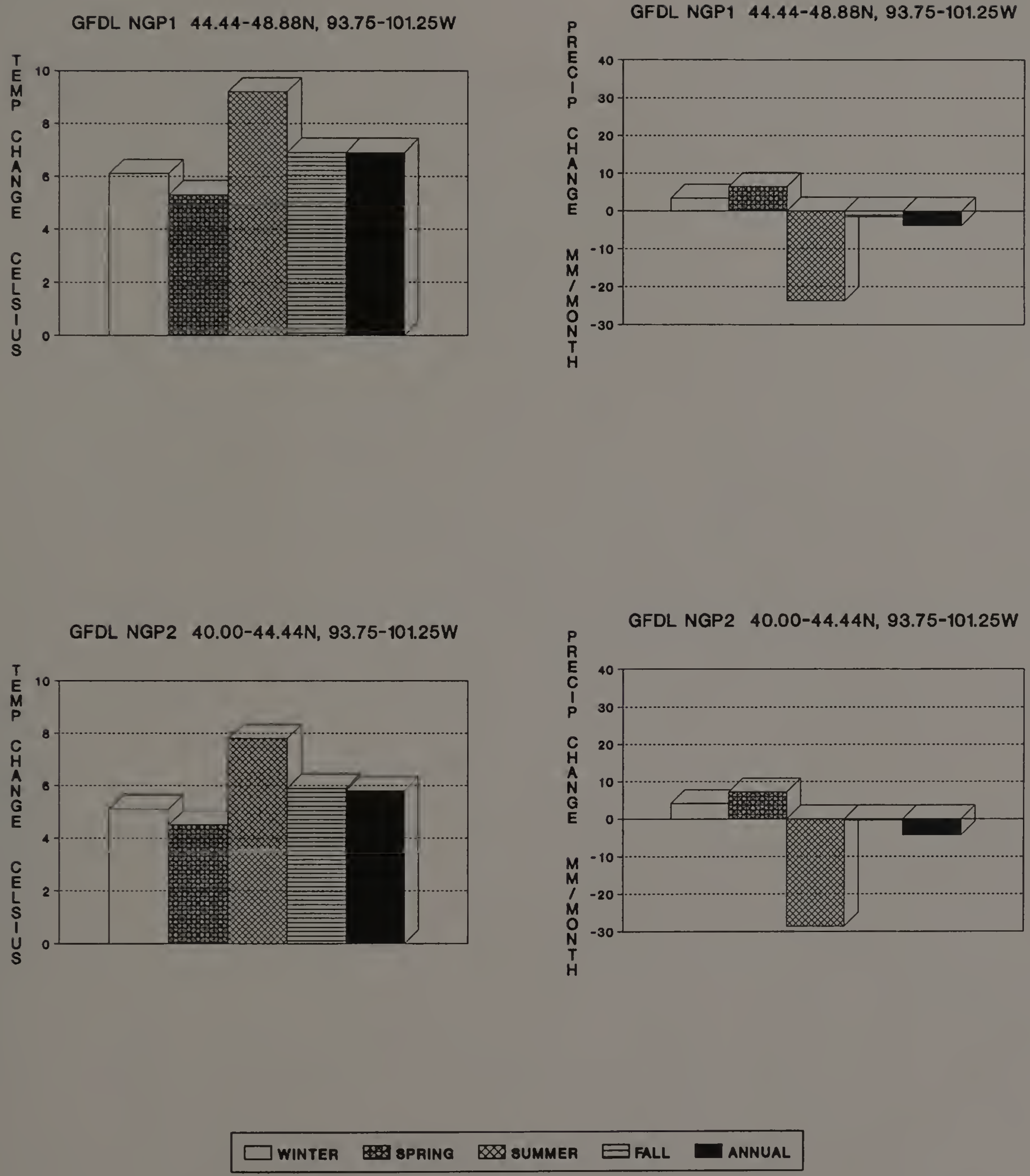

Continued, next page

Figure 5.3 Continued

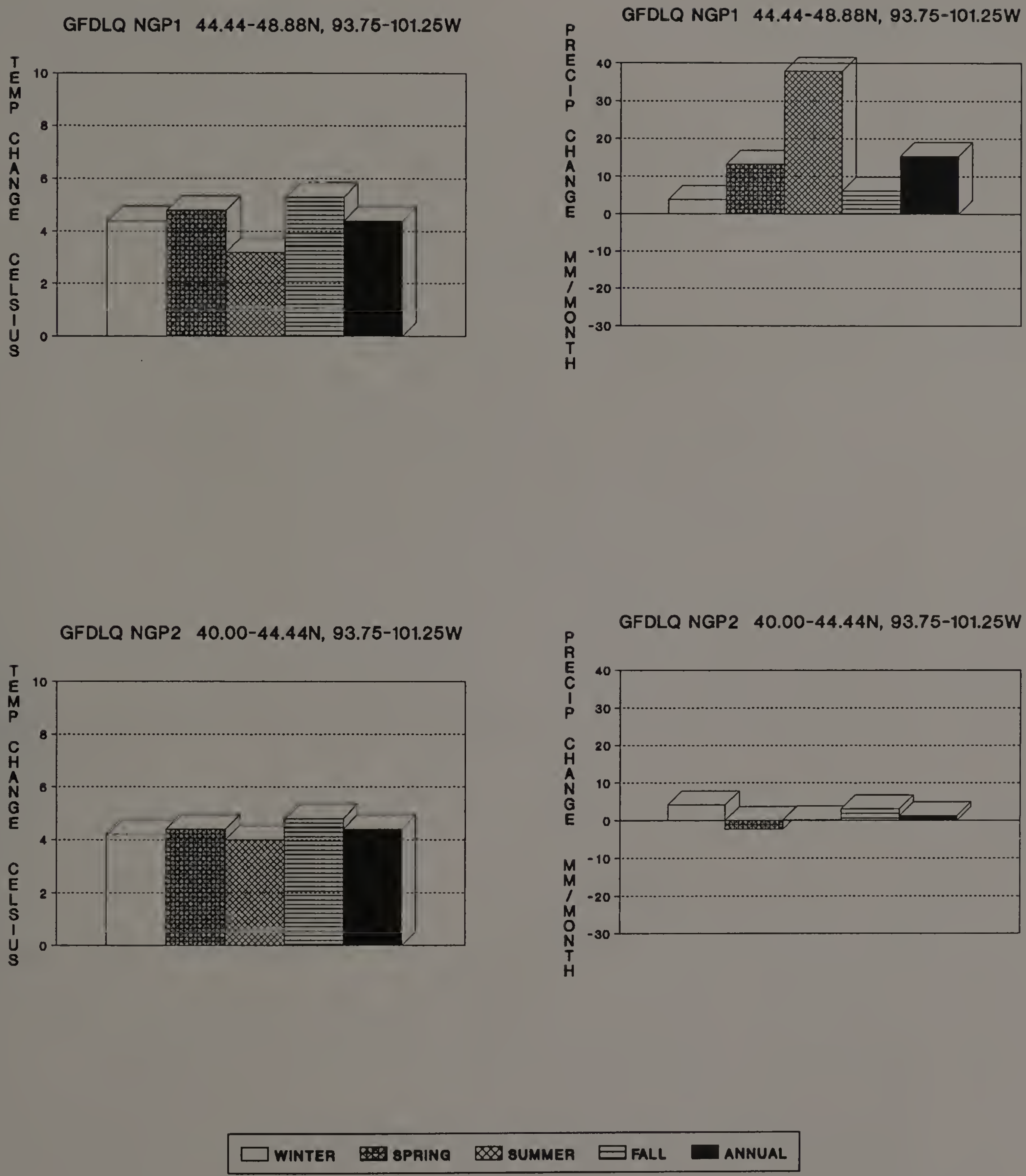

Mean winter wheat yields were consistently higher than spring wheat yields in the baseline simulations, but there were more winter wheat crop failures due to winterkill (Table 5.1). Crop failures of winter wheat decreased in all three climate change scenarios. In the spring wheat simulations, the only crop failures that occurred were caused by water stress in the GFDL climate change scenario.

In the simulations done with the GISS scenario, dryland winter wheat yields decreased (Table 5.2), even though there were fewer crop failures in the warmer climate. Irrigated yields were higher in two locations with the GISS scenario. Maturity dates were earlier and crop water stress coefficients were higher, both contributing to lower yields in the dryland simulations. Simulated spring wheat yields were consistently lower with the GISS scenarios than with baseline climate and there were no crop failures in either case.

In almost every case simulated, the GFDL climate change scenario caused large decreases in both winter and spring wheat under both dryland and irrigated conditions. If climate change of this severity occurs, both winter and spring wheat production would be curtailed in the Northern Great Plains.

At the two sites in North Dakota, simulated dryland yields of both spring and winter wheat were larger with the GFDL QFLUX climate change scenario than they were with the

Table 5.1 CERES-Wheat crop failures at Northern Great Plains study sites for 29 simulation years.

a) CERES-WHEAT 2XCO_2 DRYLAND

Crop	Site	Base	GISS	GFDL	GFDL GFLUX
Winter wheat	Bismark, ND	3	1	1	0
	Fargo, ND	3	2	2	2
	Pierre, SD	2	0	1	0
Spring wheat	Bismark, ND	0	0	7	0
	Fargo, ND	0	0	3	0
	Pierre,SD	0	0	2	0

b) CERES-WHEAT 2XCO_2 IRRIGATED

Crop	Site	Base	GISS	GFDL	GFDL GFLUX
Winter wheat	Bismark, ND	3	1	1	0
	Fargo, ND	3	0	0	1
	Pierre,SD	2	0	0	0
Spring wheat	Bismark, ND	0	0	0	0
	Fargo, ND	0	0	0	0
	Pierre,SD	0	0	0	0

Table 5.2 Change in CERES-Wheat yield for GISS, GFDL, and GFDL QFLUX $2XCO_2$ climate change scenarios at Northern Great Plains study sites.

a) CERES-WHEAT $2XCO_2$ DRYLAND

	GISS		GFDL		GFDL QFLUX	
Site	Yield	sd	Yield	sd	Yield	sd
	%Δ	%Δ	%Δ	%Δ	%Δ	%Δ
WINTER WHEAT						
Bismark, ND	-19.3	18.6	-59.7*	14.6	32.9	19.9
Fargo, ND	-33.0	16.6	-77.6*	13.7	25.4	17.7
Pierre, SD	-22.0	15.2	-34.4*	14.9	-40.6*	14.3
SPRING WHEAT						
Bismark, ND	-42.2*	20.7	-88.2*	18.0	24.8	21.6
Fargo, ND	-42.2	-87.4*	-87.4*	13.1	16.4	14.8
Pierre, SD	-4.7	20.9	-76.5*	16.5	-29.8	20.1

b) CERES-WHEAT $2XCO_2$ IRRIGATED

	GISS		GFDL		GFDL QFLUX	
Site	Yield	sd	Yield	sd	Yield	sd
WINTER WHEAT						
Bismark, ND	2.9	7.9	-20.0*	7.9	3.0	7.0
Fargo, ND	-3.1	6.4	-28.2*	6.3	-9.2	7.1
Pierre, SD	13.4	6.8	5.3	6.7	17.3	17.3
SPRING WHEAT						
Bismark, ND	-43.0*	4.2	-88.4*	3.8	-46.8	4.1
Fargo, ND	-31.6*	3.9	-70.2*	3.7	-33.8*	3.7
Pierre, SD	-19.7*	4.5	-47.8*	4.3	-22.4*	4.6

*Greater than two times the st. dev. of percent change.

baseline climate. Evidently, in those sites the moderately warmer temperatures and increases in precipitation in the winter and spring of the climate change scenario improved conditions for wheat growth. Not only were yields higher, there were fewer crop failures as well. In contrast, at the more southern site in Pierre, South Dakota, both spring and winter wheat yields declined with the GFDL QFLUX scenario and there were no crop failures in either the baseline or climate change simulations.

To summarize, winter wheat fared better than spring wheat in the climate change simulations at most of the Northern Great Plains sites. Simulated winter wheat yields even improved in the relatively benign GFDL QFLUX scenario. These results suggest that winter wheat production would be likely to expand and that spring wheat production would decline in the area.

5.1.2 Southern Great Plains

When the mean winter wheat yield changes at northern sites were compared to those at Southern Great Plains sites (Table 5.3), the average simulated yield decreases in the north approximately equaled or exceeded the mean yield changes in the south for the GISS and GFDL scenarios (simulations were not made with the GFDL QFLUX scenario in the Southern Great Plains). The only exception to this was a slight increase (4%) in Northern Great Plains irrigated

Table 5.3 Mean change in CERES-Wheat yield for GISS and GFDL $2XCO_2$ climate change scenarios in the Southern and Northern Great Plains.

a) CERES-WHEAT $2XCO_2$ DRYLAND

Site	GISS Yield	GFDL Yield
	(%Δ)	(%Δ)
N. GREAT PLAINS		
Winter wheat	-25	-57
Spring wheat	-30	-84
S. GREAT PLAINS		
Winter wheat	-30	-33

b) CERES-WHEAT $2XCO_2$ IRRIGATED

Site	GISS Yield	GFDL Yield
N. GREAT PLAINS		
Winter wheat	+4	-14
Spring wheat	-31	-69
S. GREAT PLAINS		
Winter wheat	-10	-15

yields over a 10% decrease in irrigated yields in the south. Given the GISS and GFDL projections of future climate, it does not appear, therefore, that wheat production in the northern part of the U.S. Great Plains may be benefited by climate change relative to more southern regions of the Great Plains.

5.2 Comparison to Drought Years of the 1930s

Mean maximum and minimum temperature and precipitation data for the decade of the 1930s are graphed in Figure 5.4 for stations nearby 11 of the 14 study sites in the Southern Great Plains. These 1930s data were compared to monthly temperature and precipitation of the baseline years 1951-1980 by calculating the mean monthly differences (1951-1980 monthly means minus 1930s monthly means), standard deviations of the differences, and Z scores (Table 5.4). The Z scores indicate that while the temperatures in the 1930s were significantly higher than the later thirty-year period at most sites, annual precipitation for the decade was not significantly lower. Individual months at many sites were significantly lower, however (See Appendix E).

To put the predictions of trace gas-induced climate change into perspective, the magnitudes of temperature and precipitation changes from the GFDL scenario were compared to a selected set of the observations shown in Figure 5.4, namely the observations of temperature and precipitation

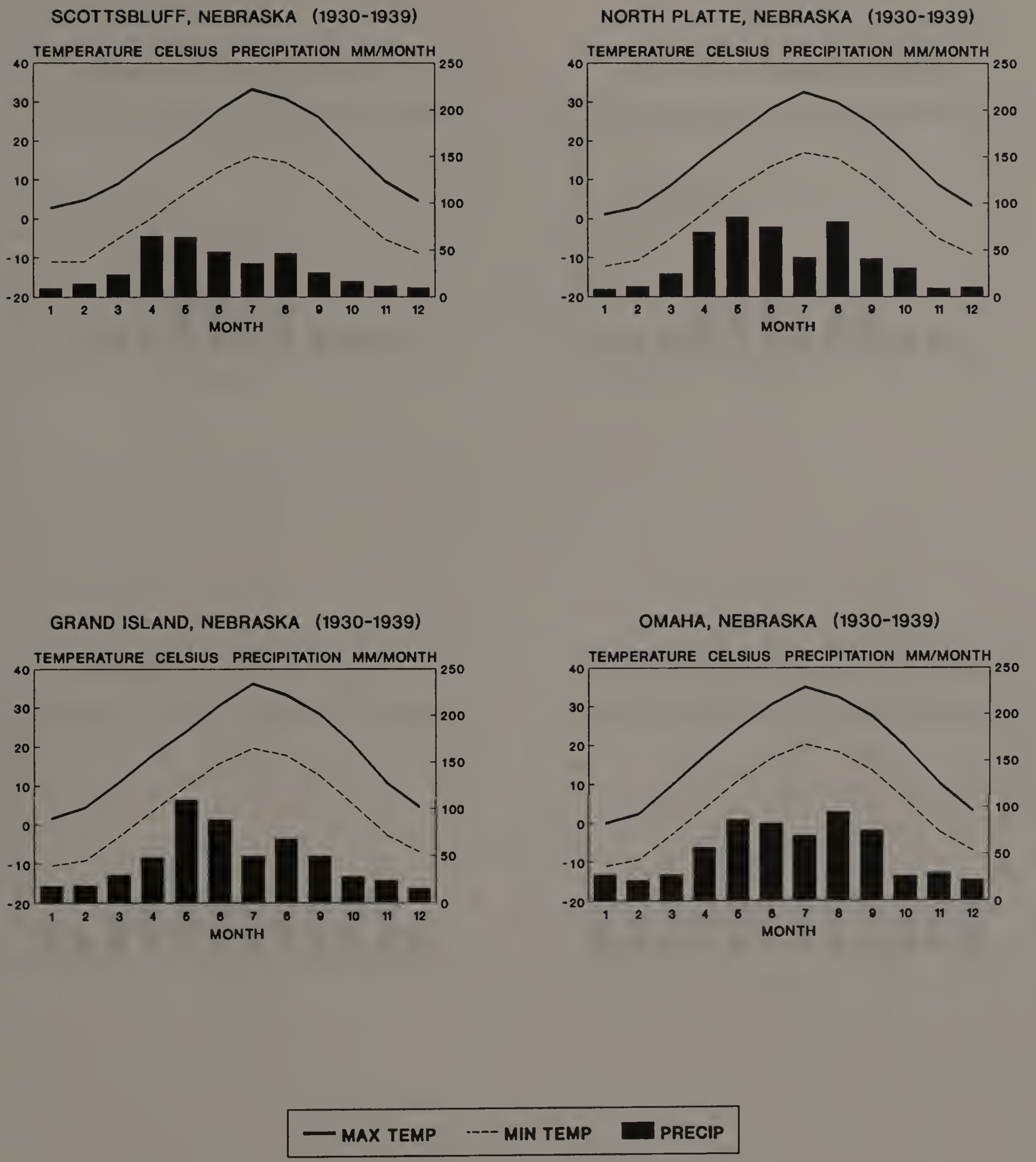

Continued, next page

Figure 5.4 Observed mean monthly maximum and minimum temperature and precipitation at Southern Great Plains sites (1930-1939).

Figure 5.4 Continued

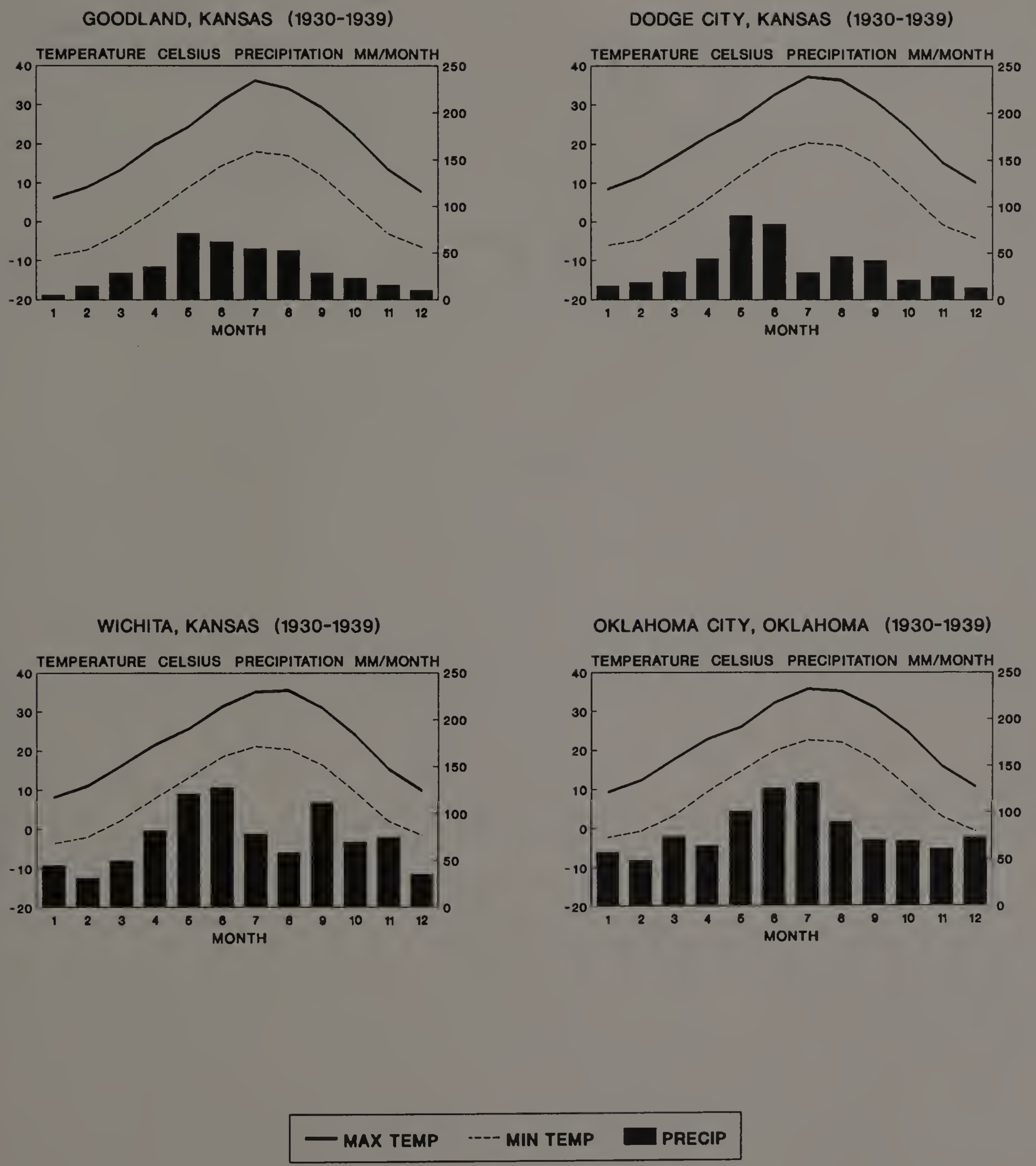

Continued, next page

Figure 5.4 Continued

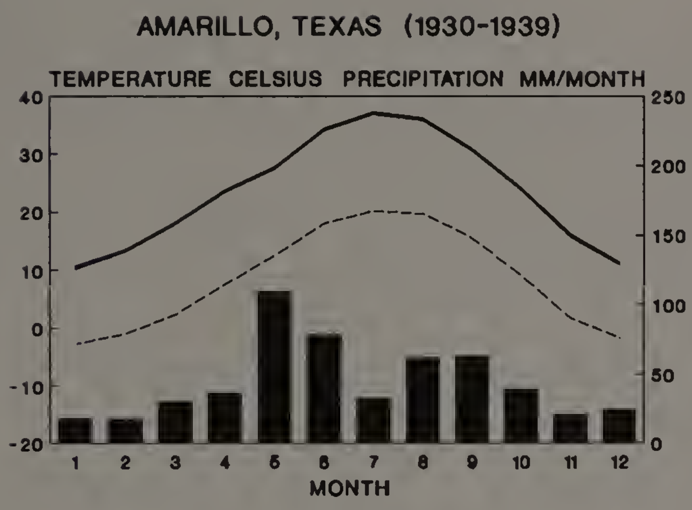

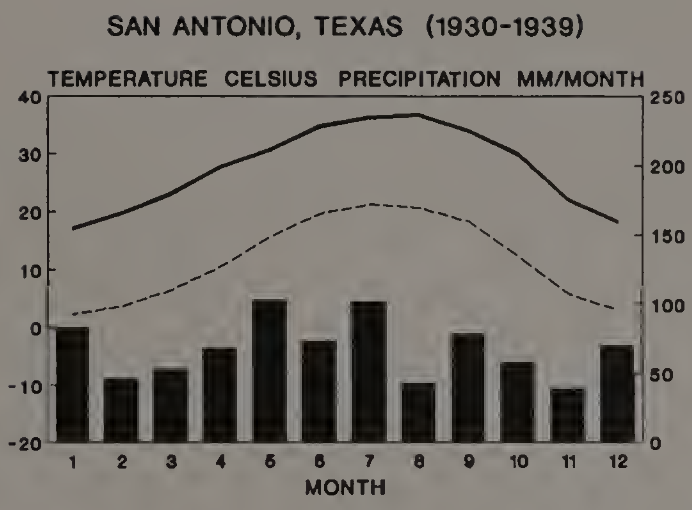

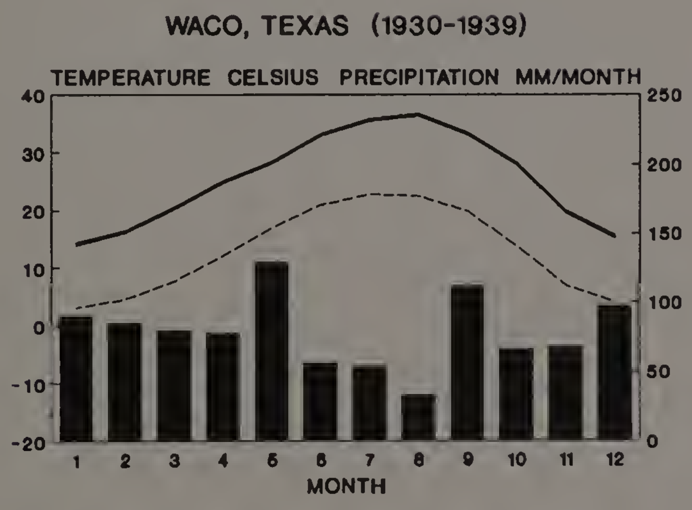

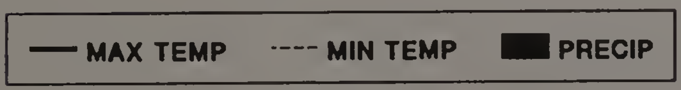

Table 5.4 Differences and Z scores of temperature and precipitation (1951-1980 monthly means minus 1930-1939 monthly means) in S. Great Plains.

Site	TEMP Dif. (°C)	TEMP sd (°C)	TEMP Z	PRECIP Dif. (mm)	PRECIP sd (mm)	PRECIP Z
NEBRASKA						
Grand Island	-1.542	0.301	-5.11*	4.042	3.844	1.05
Scottsbluff	-0.100	0.254	0.39	0.033	2.572	0.13
Omaha	-0.608	0.290	-2.10*	12.783	4.403	2.90*
North Platte	-0.300	0.280	-1.07	0.775	3.279	0.24
KANSAS						
Goodland	-1.950	0.242	-8.05*	1.233	2.939	0.42
Dodge City	-2.042	0.236	-8.65*	5.850	3.609	1.62
Wichita	-1.858	0.244	-7.62*	-12.150	5.220	-2.33*
OKLAHOMA						
Okla. City	-0.858	0.230	-3.73*	-14.875	6.715	-2.22*
TEXAS						
Amarillo	-2.000	0.212	-9.45*	-3.642	3.996	-0.91
Waco	0.208	0.201	1.04	-12.700	6.550	-1.94
San Antonio	0.758	0.196	3.87*	-6.158	6.000	-1.03

*Greater than two standard deviations.

from the worst years of the 1930s drought for the states of Nebraska and Kansas (Figure 5.5). This comparison showed that precipitation is predicted to decrease in the GFDL climate change scenario for those states by about the same amount as precipitation actually decreased during the most severe drought years (1934 and 1936). The comparison further showed that the climate change scenario temperatures are about 3°C higher than the average Dust Bowl temperatures. The question is whether these significantly higher temperatures, in addition to the lack of precipitation in some cases, are likely to cause extremely severe consequences to agricultural production in the region, creating a latter-day "Dust Bowl."

In order to answer this question, the CERES crop models were run with observed climate data from the decade of the 1930s at 9 of the study sites for wheat and at 11 of the study sites for corn. In the simulations, cultivars and management were specified as for current dryland conditions. The changes (from the baseline yields) in simulated crop yields generated with the 1930s data were compared to the changes generated with both the GISS and GFDL climate change scenarios.

5.2.1 Wheat

Results of the simulations indicate that the decade of the 1930s was not uniformly negative to wheat yields in the

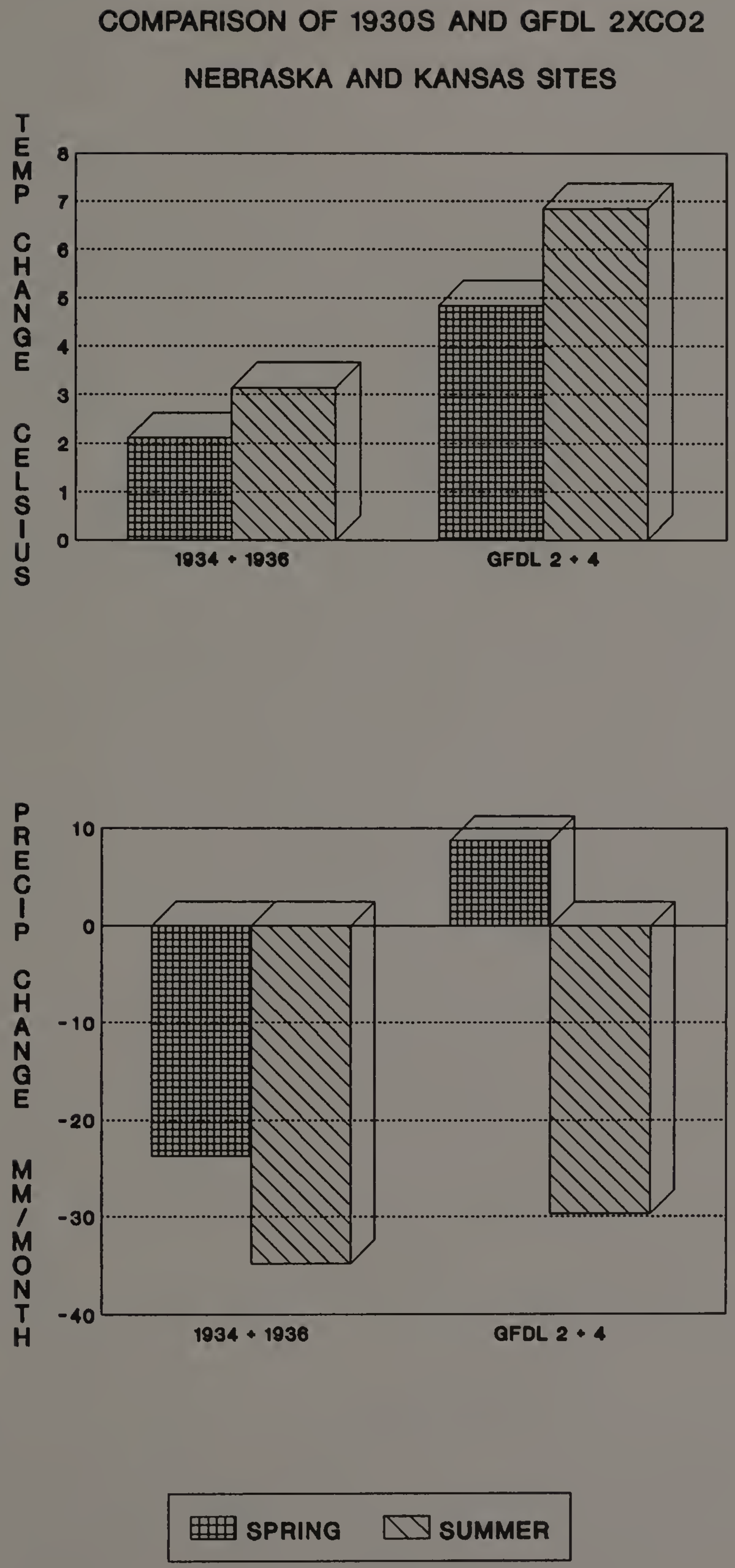

Figure 5.5 Comparisons of observed drought climate (mean of 1934 and 1936) and GFDL 2XCO_2 climate change scenario in Nebraska and Kansas.

Southern Great Plains. This occurred because drought and high temperature conditions were not equally severe at all locations, as shown in Table 5.4 and Appendix 5. In 4 out of the 9 locations, simulated 1930s yields were lower than baseline yields. Wheat yields in the 1930s simulations were especially low in Omaha, Nebraska and Goodland, Kansas. In the other 5 locations, mean yields for the 1930s simulations were actually higher than the baseline case, due to more favorable precipitation conditions during the growing season.

When these results were compared to results from the climate change runs, simulated dryland wheat yields were more negative in both the GISS and the GFDL climate change scenarios than in the 1930s simulations at most locations (Table 5.5), suggesting significant negative effects of climate change in the region.

5.2.2 Corn

The projection of future Dust Bowl conditions can be even more strongly inferred from the results of the corn simulations. Both historically and in the CERES simulations, the 1930s climate was more damaging to corn yields than to wheat yields (Table 5.6). This is not surprising because corn is more susceptible to both high temperature and drought injury than wheat. Grand Island and Omaha, Nebraska, Goodland and Dodge City, Kansas, and San

Table 5.5 Change in CERES-Wheat yield for GISS and GFDL $2XCO_2$ climate change scenarios and for 1930s observed climate.

Site	GISS (%Δ)	GFDL (%Δ)	1930s (%Δ)
NEBRASKA			
Grand Island	-17.1*-	-26.0*-	-13.0*
Scotts Bluff	25.9*-	-45.3*-	1.1
Omaha	-13.9*+	-20.1*+	-24.6*
North Platte	-27.7*-	-40.4*-	-1.4
KANSAS			
Goodland	-10.5 +	-46.9*-	-33.7*
Dodge City	-38.7*-	-12.3 -	2.6
Wichita	-33.6*-	-18.8*-	48.3*
OKLAHOMA			
Okla. City	-45.4*-	-26.9*-	15.8*
TEXAS			
Amarillo	-55.4*-	-55.1*-	35.4*

* Greater than two times the st. dev. of percent change.
\+ better than 1930s
\- worse than 1930s

Table 5.6 Change in CERES-Maize yield for GISS and GFDL $2XCO_2$ climate change scenarios and for 1930s observed climate.

Site	GISS (%Δ)	GFDL (%Δ)	1930s (%Δ)
NEBRASKA			
Grand Island	-19.8*+	-74.5*-	-37.9*
Scotts Bluff	-33.2 -	-83.4*-	25.9
Omaha	-24.5*+	-63.4*-	-28.8*
North Platte	-4.0 -	-66.8*-	2.4
KANSAS			
Goodland	-26.7 -	-90.1*-	-13.9
Dodge City	-42.9*+	-66.7*-	-58.4*
Wichita	-26.6*-	-42.7*-	13.2*
OKLAHOMA			
Okla. City	-12.6*-	-8.2 -	4.0
TEXAS			
Amarillo	-12.5 -	-38.1*-	-2.9
Waco	-5.4 -	-18.2*-	16.6*
San Antonio	-3.5 +	-12.2 +	-41.0*

* Greater than two times the st. dev. of percent change.
\+ better than 1930s
\- worse than 1930s

Antonio, Texas had particularly negative corn yield changes in the 1930s simulations. However, as was demonstrated in the statistical analysis of the 1930s climate data, the drought of the 1930s was not uniformly present throughout the Southern Great Plains for the duration of the entire decade, and corn yields under simulated 1930s conditions were still greater than the baseline yields in 5 locations.

When comparing the effects of the climate change scenarios with those of the 1930s on CERES corn yields, the GISS climate change scenario had consistently negative effects on corn yields and these negative effects were more severe than the 1930s effects in 6 out of the 11 locations. With the hotter and drier GFDL climate change scenario, the yield changes at all except a few sites were much more negative than the 1930s yield changes, again implying potentially serious consequences for the region.

5.3 Possible Adaptations

Farmers may adjust management variables to attempt to mitigate negative effects or to take advantage of beneficial effects of the projected climate changes. If farmers find that crop production is declining because of changed or changing climate, they will not react passively and continue to grow their crops in the same ways. They are likely to adopt or develop practices appropriate for optimal crop production, given the new climatic conditions. For example, farmers may alter the amounts and timing of irrigation, or establish new irrigation systems; they may plant their crops earlier or later according to changes in the length of the growing season; and they may switch to crop cultivars that are more adapted to the new climatic regimes. As part of this study, three possible adaptations to climate change — modifications of irrigation, planting date, and cultivar — were tested with the CERES models.

5.3.1 Changes in Irrigation

Irrigated simulations were carried out in order to study the relative changes in yield, applied irrigation water, and yield stability compared to dryland simulations. Results are described in the sections below.

5.3.1.1 Effects on Yield

Dryland and irrigated yields for the 30 years of the CERES baseline and climate change simulations are shown in Figures 5.6 and 5.7 for wheat in Amarillo, Texas, and corn in Grand Island, Nebraska. The model results indicate that the high temperatures of the climate change scenarios have a negative effect on crop yields, even under irrigated conditions. The decreases in irrigated crop yields, which occur even when an adequate amount of water is constantly available for crop growth, are due to the shortening of crop growth stages, especially the duration of the grain filling

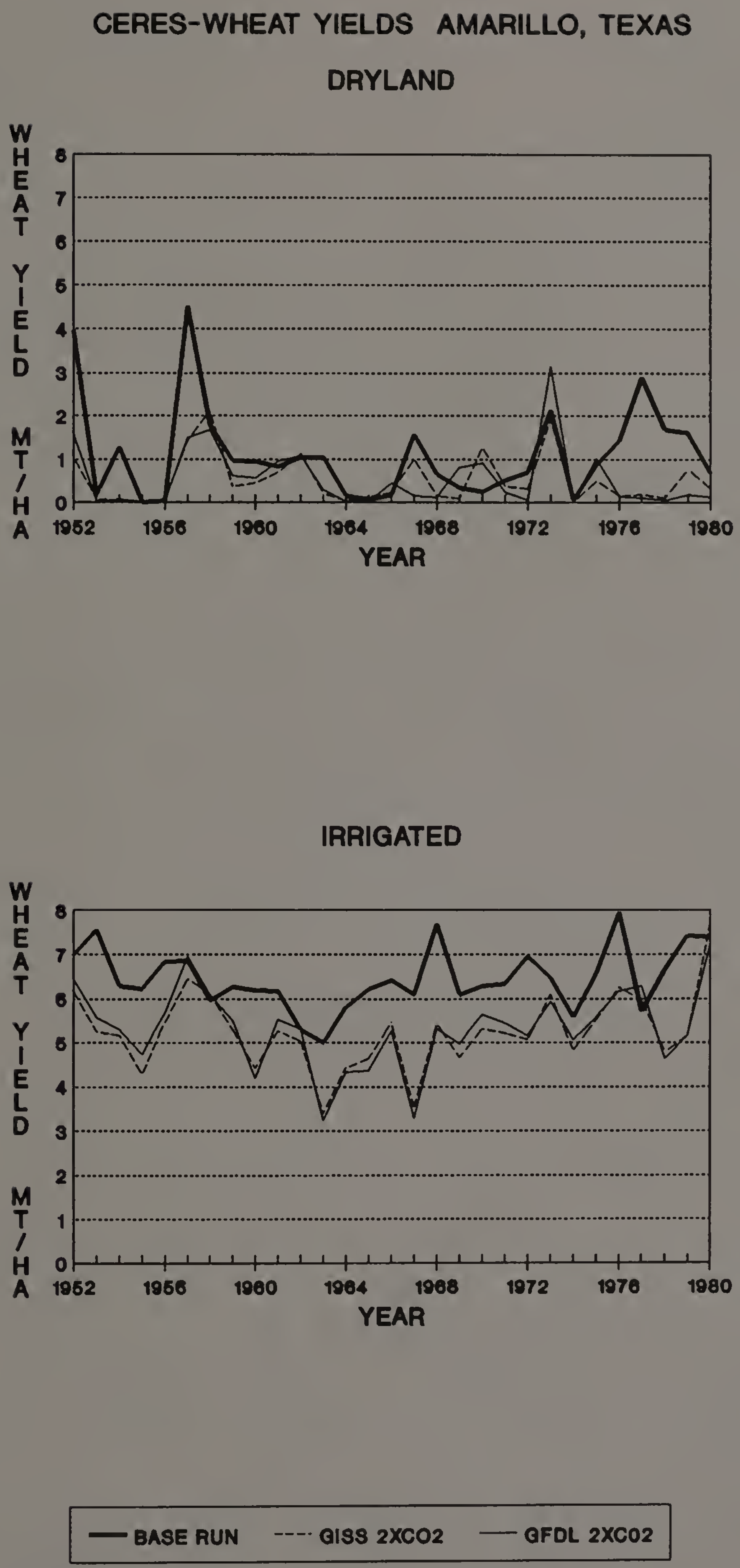

Figure 5.6 CERES-Wheat dryland and irrigated yields for Amarillo, Texas for baseline, GISS and GFDL $2XCO_2$ climate change scenarios.

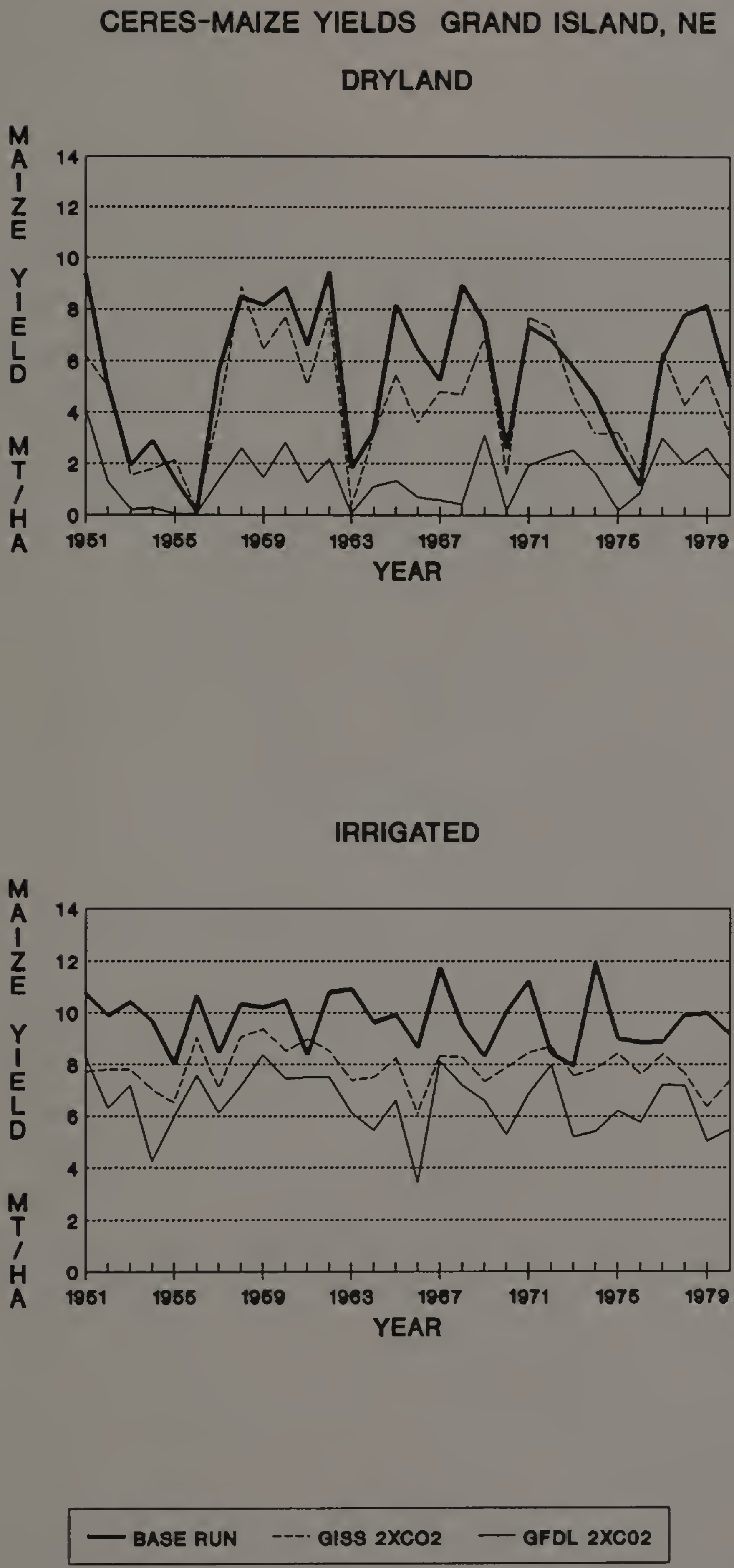

Figure 5.7 CERES-Maize dryland and irrigated yields for Grand Island, Nebraska with baseline, GISS and GFDL $2XCO_2$ climate change scenarios.

period. The irrigated yield results further indicate, however, that simulated irrigated yields in the climate change scenarios were maintained at acceptable production levels and are less variable than the simulated dryland yields (see Table 4.3). This suggests that new irrigation systems may be required to maintain adequate production levels in the region given a greenhouse climate.

5.3.1.2 Water Use

For Great Plains farmers who already irrigate, the amount of water required for crop irrigation may increase under climate change. In the CERES-Wheat simulations for the GISS climate change scenario, the amount of water applied for irrigation (water added to the soil profile in the automatic irrigation simulations is summed over each growing season) remained essentially the same at the sites in Nebraska and increased by up to 50% at most sites in Kansas, Oklahoma, and Texas (Table 5.7).

These increases in water applied for irrigation occurred even though total crop evapotranspiration generally decreased (implying more water in the soil profile), because water applied for irrigation depends on modeled soil moisture, which in turn depends not only on evapotranspiration but on precipitation as well. This can be seen in the results from the central and southern GISS gridboxes where precipitation decreases in the climate change scenario (see

Table 5.7 Change in CERES-Wheat water applied for irrigation with GISS and GFDL $2XCO_2$ climate change scenarios.

	CERES-WHEAT $2XCO_2$ IRRIGATED			
	GISS		GFDL	
Site	Ir H_2O	sd	Ir H_2O	sd
	(%Δ)	(%Δ)	(%Δ)	(%Δ)
NEBRASKA				
Norfolk	-2.5	3.9	14.6*	4.2
Grand Island	2.0	4.2	13.6*	4.3
Scottsbluff	3.2	3.4	21.2*	3.6
Omaha	-6.8	5.2	2.8	5.2
North Platte	9.4*	3.7	22.8	3.9
KANSAS				
Goodland	-0.8	3.3	17.4*	3.2
Dodge City	16.5*	2.6	5.9	3.4
Wichita	20.0*	5.1	-2.3	5.3
OKLAHOMA				
Tulsa	49.2*	8.1	-2.3	7.4
Oklahoma City	31.8*	5.2	12.4*	5.2
TEXAS				
Amarillo	17.9*	3.3	13.2*	3.4
Brownsville	-4.1	4.1	-3.4	4.1
Mean	11.3		9.7	

*Greater than two times the st. dev. of percent change.

Figure 3.5) and water applied for irrigation in the CERES-Wheat simulation increased at most sites. With the GFDL scenario, significant increases in water applied for irrigation occurred at half of the study sites, especially in the northern gridboxes where precipitation decreases greatly during the growing season (Table 5.7).

In the CERES-Maize simulations, water applied for irrigation increases significantly at half the study sites in the GISS scenario, and at almost all the sites in the GFDL scenario, in one location by over 100% (Table 5.8). The severe summer dryness in the GFDL scenario contributed to an average increase of 50% in water applied for irrigation of corn over all sites. In contrast, wheat irrigation water increased only about 10% on average in the GFDL scenario. This marked summer dryness affected the irrigation water applied to corn far more than it did the irrigation water applied to wheat because wheat is harvested earlier in the season, thus escaping the severe summer droughts.

When the CERES crop models were run with both the climate change scenarios and the modifications for the physiological effects of CO_2, the effects of increased stomatal resistance described in Section 4.5.3. were reflected in the amount of crop irrigation water applied. Less irrigation water was needed because of the water savings caused by increased stomatal resistance (Table 5.9).

Table 5.8 Change in CERES-Maize water applied for irrigation with GISS and GFDL $2XCO_2$ climate change scenarios.

	CERES-MAIZE $2XCO_2$ IRRIGATED			
	GISS		GFDL	
Site	Ir H_2O	sd	Ir H_2O	sd
	(%Δ)	(%Δ)	(%Δ)	(%Δ)
NEBRASKA				
Norfolk	12.0*	4.1	87.3*	4.7
Grand Island	7.1	3.6	78.9*	4.6
Scottsbluff	6.9	3.7	73.0*	4.1
Omaha	14.2*	4.8	107.2*	5.8
North Platte	7.6	4.5	64.8*	5.3
KANSAS				
Goodland	14.9*	3.3	68.4*	3.6
Dodge City	28.1*	4.6	47.9*	4.8
Wichita	29.4*	6.1	51.9*	6.6
OKLAHOMA				
Tulsa	15.7*	5.0	40.7*	5.1
Oklahoma City	20.5*	5.2	10.7*	5.1
TEXAS				
Amarillo	28.1*	3.7	48.8*	4.3
Waco	4.0	4.1	8.1	4.2
San Antonio	-4.7	4.7	7.8	4.8
Brownsville	-3.6	3.6	6.7	3.6
Mean	12.9		50.2	

*Greater than two times the st. dev. of percent change.

Table 5.9 CERES-Wheat and CERES-Maize change in water applied for irrigation with GISS and GFDL $2XCO_2$ climate change scenarios with physiological CO_2 effects.

	WHEAT		MAIZE	
	GISS	GFDL	GISS	GFDL
SITE	Ir. H_2O		Ir. H_2O	
	(%Δ)	(%Δ)	(%Δ)	(%Δ)
NEBRASKA				
Norfolk	-13.3*	3.1	-30.1*	34.1*
Grand Island	-9.0*	0.3	-28.5*	32.5
Scotts Bluff	-5.0*	12.7*	-27.9*	26.1*
Omaha	-17.9*	-9.6	-25.6*	52.3*
North Platte	0.4	13.0*	-27.0*	21.6*
KANSAS				
Goodland	-7.3*	8.3*	-21.4*	26.9
Dodge City	9.5*	-2.1	-7.8	9.9*
Wichita	12.4*	-8.6	-11.5	9.3
OKLAHOMA				
Tulsa	39.4*	-15.9*	-24.7*	-3.1
Okla. City	21.9*	2.5	-15.9*	-25.2*
TEXAS				
Amarillo	7.2*	2.3	-8.7*	7.2
Waco	-	-	-29.5*	-23.2*
San Antonio	-	-	-32.1*	-22.2*
Brownsville	-7.9	-9.7*	-28.3*	-19.3*
Mean	2.5	-0.3	-22.8	9.1

*Greater than two times the st. dev. of percent change.

Patterns of changes in wheat irrigation water simulated with the combined effects were similar to those projected with the climate scenarios alone. For example, decreases in water used to irrigate wheat occurred in northern sites where precipitation increases in the GISS scenario, and the reverse, increases in irrigation in the more central and southern sites, occurred where precipitation decreases.

In the corn simulations, water applied for irrigation decreased everywhere when the GISS scenario was combined with the physiological effects of CO_2 (Table 5.9). Both the increased stomatal resistance and the shortening of the growing season contributed to this beneficial result. These two factors are, for the most part, unable to overcome the effects of the hotter and drier GFDL scenario. Water applied for irrigation in CERES-Maize with the GFDL scenario increases significantly over the baseline in the northern and central portions of the study area, even when the water-saving physiological effect of increased CO_2 is taken into account.

These results imply that if climate change is severe, regional demand will rise for water from irrigation systems currently in place.

5.3.2 Changes of Planting Date

One manifestation of global warming in temperate regions, present in both the GISS and GFDL climate change scenarios, is a lengthening of the growing season, defined as the number of days between the last frost of the spring and the first frost in the fall. Farmers may adjust planting dates of their crops in response to these changes, planting later in the fall for winter crops or earlier in the spring for summer crops. When choosing planting dates for wheat, farmers seek to establish enough growth to maintain a viable dormant period over the winter, but to avoid excessive growth before the onset of cold weather that could reduce yields. For planting dates of corn, temperatures must be warm enough for germination and early growth. Changes in planting dates were tested in simulations with the CERES models for both wheat and corn, to learn whether such changes could mitigate some of the damaging effects of the predicted climate change scenarios on yields.

5.3.2.1 Wheat

To simulate an adaptation to later fall frosts, planting dates of dryland winter wheat were delayed in simulations with the GISS doubled-CO_2 climate change scenario. The planting dates were delayed according to the average change in the first frost in the fall at each location. (Infestations of the Hessian fly (<u>Phytophaga destructor</u>), which damage wheat sown too early in the fall in some parts of the Great Plains, were not considered.) This adaptation to the GISS doubled CO_2 climate improved wheat yields in only a few cases under both dryland and irrigated growing conditions (Table 5.10), a result that suggests that early planting was not a primary cause of the modeled yield decreases in the GISS climate change scenario.

5.3.2.2 Corn

In another simulation, planting dates of CERES-Maize were advanced between 20 and 30 days, according to average changes in last spring frosts in the GISS climate change scenario. When planting dates in CERES-Maize were set earlier, decreases in dryland corn yields were ameliorated slightly in some locations, but overall yield declines were still large (up to 32%) in most locations (Table 5.11). The overall effect of the additional 20 to 30 days of growth on corn yields was small probably because solar radiation and temperatures, both important factors in crop growth, are relatively low early in the spring.

The results of these simulations suggest that changing planting dates in response to changes in length of growing season may not be a highly effective adaptation to global warming in the Southern Great Plains.

5.3.3 Changes of Cultivar

Farmers may also adjust to climate change by switching to cultivars that are better adapted to the new climate.

Table 5.10 Change in CERES-Wheat yield in GISS 2XCO_2 adjustment experiment.

Site	CC		CC + PD		CC + PD + C	
	(%Δ)	(%Δ)	(%Δ)	(%Δ)	(%Δ)	(%Δ)
a) CERES-WHEAT 2XCO2 DRYLAND						
NEBRASKA						
NONE	-10.5	6.0	-33.4*	3.1	-13.8*	3.7
GINE	-17.1*	6.0	-38.7*	3.2	-19.4*	4.0
SBNE	-25.9*	9.6	-15.3	9.4	13.6	10.6
OMNE	-13.9*	4.3	-11.8*	4.2	6.7	5.5
NPNE	-27.7*	8.4	-7.1	8.6	27.2*	9.8
KANSAS						
GOKS	-10.5	16.1	-2.0	16.6	20.9	19.0
DCKS	-38.7*	11.7	-37.8*	11.6	25.4	14.4
WIKS	-33.6*	6.9	-28.6*	6.7	9.1	6.7
OKLAHOMA						
TUOK	-33.9*	3.3	-32.4*	3.2	18.8*	4.0
OKOK	-45.4*	5.9	-45.9*	5.9	2.1	7.6
TEXAS						
AMTX	-55.4*	12.3	-50.8*	12.3	152.7*	20.8
BRTX	-45.3*	4.1	-48.4*	3.9	-30.2*	4.4
b) CERES-WHEAT 2XCO_2 DRYLAND						
NEBRASKA						
NONO	-3.2	2.4	-9.9*	1.2	-2.5	3.9
GINE	-3.7	2.0	-8.4*	1.5	2.0	4.2
SBNE	6.1*	1.8	-8.7*	1.3	3.2	3.4
OMNE	-11.6*	2.4	-10.5*	1.3	-6.8	5.2
NPNE	6.5*	2.8	-3.0*	1.4	9.4*	3.7
KANSAS						
GOKS	0.8	1.9	-8.3*	1.2	-0.8	3.3
DCKS	-6.9*	2.0	-0.3*	1.2	16.5*	2.6
WIKS	-10.7*	2.0	-2.5*	1.2	20.0*	5.1
OKLAHOMA						
TUOK	-21.5*	2.0	2.7	1.4	49.2*	8.1
OKOK	-19.6*	2.1	3.1*	1.2	31.8*	5.2
TEXAS						
AMTX	-18.3*	1.8	3.8*	1.4	17.9*	3.3
BRTX	-48.3*	3.3	-11.2*	2.3	-4.1	4.1

* Greater than 2 x SD% change.

CC = Climate change alone

CC+PD = Climate change plus change in planting date

CC+PD+C = Climate change plus change in planting date plus change in cultivar

Table 5.11 Dryland CERES-Maize yield in GISS $2XCO_2$ adjustment experiment for planting date.

CERES-MAIZE $2XCO_2$ DRYLAND

	CC		CC + PD	
Site	Yield	sd	Yield	sd
	%Δ	%Δ	%Δ	%Δ
NEBRASKA				
Norfolk	-18.6*	7.7	-15.2	7.8
Grand Island	-19.8*	7.2	-11.0	7.4
Scotts Bluff	-33.2	22.3	-28.0	22.5
Omaha	-24.5*	3.1	-18.9*	3.5
North Platte	-4.0	12.8	-4.2	12.8
KANSAS				
Goodland	-26.7	20.6	-30.8	20.2
Dodge City	-42.9*	14.7	-32.0*	15.6
Wichita	-26.6*	7.4	-20.0*	7.4
OKLAHOMA				
Tulsa	-10.5*	3.7	-7.4*	3.6
Okla. City	-12.6*	5.3	0.1	5.7
TEXAS				
Waco	-5.4	5.9	-4.5	5.9
San Antonio	-3.5	7.4	-4.7	7.8

*Greater than two times the st. dev. of percent change.

CC = Climate change alone
CC + PD = Climate change plus change in planting date

Described below are results of CERES-Wheat and CERES-Maize simulations with a range of such cultivars.

5.3.3.1 Wheat

To test the effect of such an adjustment on modeled crop yields, new cultivars were chosen for CERES-Wheat simulations with the GISS climate change scenario on the basis of vernalization requirement and photoperiod sensitivity. Since winter wheat cultivars with high vernalization requirements need cold temperatures to induce reproductive growth (Evans et al., 1975), warmer temperatures in the winter in the GCM climate change scenarios would allow shifts to cultivars with intermediate or no vernalization requirements. Cultivars with no vernalization requirements are spring wheats.

Wheat cultivars also vary in photoperiod sensitivity, i.e., the need for long hours of daylight to flower (Evans et al., 1975). Cultivars adapted to high latitudes tend to display greater photoperiod sensitivity, hastening flowering in those regions. Since the warmer temperatures of the doubled-CO_2 climate change scenarios tend to hasten wheat growth in the spring, cultivars with lower photoperiod sensitivity would be needed to delay flowering and to extend the growing season as long as possible.

Results of the adjustment simulation show that a cultivar better adapted to the changed climate caused wheat yields to be equal to or greater than baseline levels at two-thirds of the dryland sites (Table 5.10). In the irrigated runs, yields equal to or higher than baseline yields occurred at more than half of the locations. At two sites, Amarillo (dryland) and Grand Island (irrigated), the change in cultivar resulted in very large increases in yields, although this may be caused by poorly specified cultivars in the baseline simulation.

These results indicate that some wheat cultivars appear to be available for adaptation to climate change. However, these cultivars may not be efficacious at all locations. Furthermore, these simulations were performed with the GISS climate change scenario, which is the less severe of the two scenarios used in this study. It is likely that the cultivar adaptations would be less successful in mitigating the effects of the more severe GFDL climate change scenario.

5.3.3.2 Corn

Similar results were observed when tropical corn cultivars were substituted for currently grown cultivars in the climate change simulations at all the sites in the Southern Great Plains. Cultivars were chosen on the basis of higher growing degree requirements for phenological growth stages and lower photoperiod sensitivity. While the more climatically appropriate corn cultivars did mitigate the effects of the climate change at the more southern sites, they were not able to compensate for the yield declines at the more northern locations.

The adaptation experiments with dryland CERES-Wheat and CERES-Maize and the GISS climate change scenario are compared in Table 5.12. Planting date had very little effect on mean yield changes in both crops. Shifts in cultivar improved the range of wheat yield changes across all sites, while tropical corn cultivars improved yields over baseline at San Antonio, but not at Dodge City.

Table 5.12 Comparison of CERES-Wheat and CERES-Maize adaptation experiments.

ADAPTATIONS

PLANTING DATE		GISS Dryland	
Wheat	$2XCO_2$	-30%	mean
	20-30 d later	-29%	mean
Corn	$2XCO_2$	-19%	mean
	20-30 d early	-15%	mean

CULTIVAR & PLANTING DATE		GISS Dryland	
Wheat	$2XCO_2$	-55 - -11%	range
	low vern. req.	-30 - +27%	range
	low phot. sen.		
Corn	$2XCO_2$	-44%	Dodge City
	tropical cult.	-55%	Dodge City
Corn	$2XCO_2$	-5%	San Antonio
	tropical cult.	+16%	San Antonio

CHAPTER 6

DISCUSSION

6.1 Physiological Effects of CO_2

Relatively few experimental studies have examined the interactive effects of CO_2, water, nutrients, light, and temperature on crop growth and development. So it is important to note that this study is based on limited data in regard to the physiological effects of CO_2. As more experimental work is done, improved simulations will be possible.

This study is also limited because the doubled CO_2 climate may occur before the 660 ppm level of CO_2 used in the combined simulations. This is because other radiatively active trace gases, such as methane, nitrous oxide, and CFCs, are increasing in the atmosphere as well as CO_2, but without the beneficial physiological effects. Further simulations should test the effects of doubled CO_2 climate change scenarios with 555 ppm CO_2 on crop growth and yield, a more realistic estimate of atmospheric CO_2 level to associate with the equivalent doubled CO_2 climate (Hansen et al., 1988b).

While the physiological effects of CO_2 are undoubtedly beneficial, the relative importance of these effects compared to the magnitude of the projected climate change is in doubt. While the positive effects of CO_2 compensated for negative climate effects on yields in some simulations in some areas, these compensations were not universal, especially when the projected climate change was severe as to both heat and water regimes.

There are other reasons why the beneficial effects of increasing CO_2 may be relatively small. First, uncertainty exists concerning the extent to which the beneficial effects will be seen in crops growing in variable, windy, and pest-infected (weeds, insects, and diseases) fields under climate change conditions. Homeostatic mechanisms, raised leaf temperatures, and sink limitations may further dampen the most dramatic positive effects seen in controlled environment experiments.

Finally, changes in patterns of agricultural productivity are likely to occur regardless of these beneficial effects. An optimistic estimation of yield increases caused by higher levels of CO_2 does not preclude significant changes in regional agriculture in the future, as regions respond differentially to simultaneous changing yet differing thermal and water regimes.

6.2 Shift from Corn to Wheat Production

A comparison of wheat and corn simulation results suggests that wheat production may be more adapted to future conditions in the Great Plains than corn production, and that there may be a shift to greater wheat production if global warming occurs. Particularly if climate change as predicted by the GFDL GCM comes to pass, corn production may be severely limited in the Southern Great Plains. In many simulations, the lower photosynthetic response of corn, a C4 crop, to CO_2 (10% compared to 25% for wheat, a C3 crop) (Cure, 1985), did not compensate for the shortening of the corn growing period caused by the higher temperatures of the climate change scenarios. This led to decreases in corn crop yields even with the beneficial effects of CO_2. Furthermore, because corn requires more water than wheat (400-750 mm compared to 300-450 mm (Doorenbos and Pruitt, 1977)), any decrease in precipitation or increase in evaporative demand will likely be more damaging to corn production than to wheat production.

6.3 Stress on Water Resources

The simulation results pertaining to irrigation imply that regional demand for irrigation water would likely rise in response to the predicted climate changes for two reasons. First, more acreage would be irrigated as high temperatures and changed hydrologic regimes decrease yield levels and increase yield variability. Increased acreage under irrigation would be needed to ensure acceptable and stable yield levels. Second, crops currently irrigated would require more water where precipitation decreases and evaporative demand increases with higher temperatures and greater atmosphere drying. The beneficial physiological effects of CO_2 may not compensate fully in this regard, especially if climate change is as severe as predicted by the GFDL GCM.

Heightened demand for irrigation could place stress on the already partially depleted Ogallala Aquifer and other water resources especially in the southern part of the region studied. Many of the problems associated with intensive irrigation, e.g., water depletion and soil degradation (Hillel, 1987), could be exacerbated by global warming. Streamflows also may slacken if more surface water is diverted for irrigation, thereby aggravating water quality problems, and in turn harming fish, wildlife, and recreational activities. Furthermore, availability of and competition for water supplies may also change with climate change. The need for irrigation systems in new locations and increasing capacity in currently irrigated areas may entail high costs, especially under changed regional water regimes. However, actual implementation of expanded irrigation systems depends on the hydrology and economics of each local situation and further study is needed to permit realistic projections.

6.4 Agriculture in the Great Plains

The results of this study should be interpreted as the potential sensitivity of the modeled crops, wheat and corn, in the Great Plains to a range of climate change and CO_2

conditions. However, given the projections of a virtually unidirectional warming trend driven by increasing concentrations of atmospheric trace gases and the potential for increased drought stress caused by higher temperatures and/or insufficient precipitation, it appears that agriculture may become more marginal and environmentally damaging in areas such as the Great Plains. The simulation results, from both the wheat and corn simulations, imply a trend toward "Dust Bowl" conditions possibly even worse than the 1930s for future agricultural production in many parts of the Great Plains, if climate change occurs as predicted.

While many critical uncertainties remain about the magnitude and timing of future climate change, agriculture as it is practiced now in the southern Great Plains is likely to become more difficult to sustain. If the higher temperatures that are predicted by global climate models come to pass, changes in regional crop yields, crop irrigation requirements, and heat and drought stress (see Appendix D) will ensue. If the climate change is relatively mild, farmers may be able to make some adjustments by planting summer crops earlier in the season, substituting better-adapted crop varieties, and increasing the use of irrigation. If, however, it is more severe, climate change will cause greater declines in yields, potentially leading to economic consequences to farmers and other members of rural communities in the region.

6.5 Further Research

Many assumptions and simplifications are embedded in the crop and climate models used in this study, leading to directions for further research on climate change impacts on agriculture. On the experimental side, longterm studies of the physiological effects of CO_2 on crops in realistic settings are needed to predict accurately the combined effects of changed atmospheric concentration and climatic factors. Other future stresses on crop yields, including pollutants such as tropospheric ozone and acid rain, should also be studied interactively with CO_2.

In the area of simulation, models of crop growth are needed which are both physiologically detailed and validated for wide areas. These improved models should be used to study a full range of adjustments in both management techniques and cultivars. Since the Great Plains extends beyond the United States' border, extension of the study sites northward into Canada would give a fuller picture of possible effects on the entire region. Finally, potential changes in climate variability, especially in drought frequency are also critical factors to be addressed. Such changes could affect crop yields considerably. However, future changes in variability cannot yet be predicted with confidence by the GCMs.

The results of this study also suggest that development of heat- and drought-tolerant cultivars should be included in plant-breeding objectives for the region, to ensure the availability of a broad range of cultivars under climate change conditions.

CHAPTER 7

SUMMARY AND CONCLUSIONS

7.1 The CERES Crop Models

This study has shown that the CERES models simulate current crop yields in the Great Plains reasonably well. The modifications that were made in the models account for the primary effects of increasing atmospheric CO_2 on crop growth, i.e., increases in photosynthetic rate and stomatal resistance. Thus, the CERES models appear to be suitable to project the separate and combined effects of changed climate and increased CO_2 on wheat and corn in the Great Plains.

7.2 The Role of Temperature Increases

Higher temperature was the major cause of simulated yield reductions in both wheat and corn in the southern and central parts of the region. In most cases, increases in temperature during the growing season caused a shortening of the crop life cycle, particularly the grain filling period. In general, the smaller temperature increases of the GISS scenario caused smaller yield reductions compared to the GFDL scenario.

7.3 The Role of Precipitation Changes

Precipitation changes were largely less important than temperature changes in causing simulated yield decreases, especially in wheat. This somewhat surprising result may be accounted for primarily by the difference in crop calendars of wheat and corn and by the nature of the climate change scenarios.

7.3.1 Wheat

Changes in precipitation had a relatively minor effect on simulated wheat yields in the Great Plains. Because wheat is a winter annual and grows to maturity in the early part of the growing season, a wheat crop growing in the field can take full advantage of the replenishment of soil moisture that occurs throughout the winter. Lower incoming solar radiation in winter also causes potential and actual evapotranspiration to be lower. The CERES-Wheat model captures these effects by accumulating soil moisture over the period from winter dormancy to spring green-up and by calculating evapotranspiration with the physically realistic Priestly-Taylor equation which includes solar radiation as a driving variable. Furthermore, wheat is primarily a dryland crop and has lower water requirements than corn.

7.3.2 Corn

Changes in precipitation did affect simulated corn yields in some locations, particularly in Nebraska and Kansas. The largest yield reductions of the entire set of simulations occurred when CERES-Maize was run with the GFDL climate scenario. This scenario predicts very high temperature rises (up to 7.8°C in Nebraska during the summer) and pronounced summer dryness (decreases of 34 mm month^{-1}), to which corn, a summer crop, is sensitive, particularly during flowering and grain filling.

While changes in precipitation did not affect yields greatly, they did influence the amount of water applied in the irrigation simulations of both wheat and corn, because of the ensuing changes in soil moisture that triggered the application of irrigation water.

7.4 The Role of CO_2

If atmospheric CO_2 continues to rise without accompanying climate changes, crop yields would benefit, according to simulations carried out with the CERES models. These benefits would accrue because of the dual effects of stimulation of photosynthesis and reduction of transpiration on a per unit leaf area basis. Under baseline (1951-1980) climate conditions, wheat yields simulated with 660 ppm CO_2 were enhanced by about 28% compared to yields simulated with 330 ppm CO_2. Simulated corn yields were raised by about 70% under dryland conditions and by 6% under irrigated conditions. The simulated maize effects are unrealistically high, compared to experimental results.

These results for both crops, however, which are based on modifications of the CERES models, are not to be taken as definitive because they are in turn based on limited experimental results from controlled environments. As more experimental work is done, improved simulations will be possible.

This study may also have over-estimated the potential beneficial effects of CO_2 because the crop models do not capture the highly variable, windy, and pest-infected conditions that exist (and will continue to exist) in farmers' fields.

7.5 Combined Climate and Physiological Effects

When the combined climatic and physiological effects of CO_2 were simulated with the CERES models, the physiological effects of CO_2 compensated for and even overcame negative climate change impacts in many, but not all, locations. In particular, the physiological effects were not able to compensate for the severe decreases in yield caused by the GFDL scenario, which has higher temperatures and less precipitation in some locations. In that scenario, simulated yields of both corn and wheat decreased significantly under dryland conditions, even with the beneficial physiological effects of CO_2.

The positive effects of CO_2, however, may be overestimated in this study because the entire greenhouse effect was attributed to a concentration of 660 ppm CO_2, ignoring the actual increase in other radiatively active gases. These other gases, including methane, nitrous oxide, and the chlorofluorocarbons, are likely to raise temperature without any accompanying effects on plant physiology, such as enhancing photosynthesis and improving water use efficiency. A warming equivalent to doubled-CO_2 may occur when atmospheric concentration is only about 550 ppm, given current emissions growth rates.

7.6 Comparison of Great Plains Subregions

Winter wheat may replace spring wheat in Northern Great Plains regions, because of fewer crop failures caused by winterkill and lower relative yield changes. The simulations showed that climate change may not cause southern areas of the United States to become less productive for wheat growth relative to northern areas. The high latitude warming in the GISS and GFDL scenarios caused yield decreases of winter wheat to be as great as or higher than the decreases in the Southern Great Plains.

7.7 Comparison to Drought Years of the 1930s

In most locations, simulated wheat and corn yields were more negative in both the GISS and the GFDL climate change scenarios than in the 1930s simulations. This implies a trend toward "Dust Bowl" conditions possibly even worse than the 1930s for future agricultural production in many parts of the Great Plains. Particularly if climate change as predicted by the GFDL GCM comes to pass, corn production may be severely limited in the Southern Great Plains.

7.8 Possible Adaptations

Farmers may adjust to climate change by increasing their irrigation applications, altering planting dates, and sowing climatically adapted crop cultivars or species. Of these adjustments, irrigation and change of cultivar appear to be possible, but not fully effective, adaptations to climate change as projected by the GISS and GFDL GCMs.

7.8.1 Changes in Irrigation

Simulated irrigated yields in the climate change scenarios were maintained at acceptable production levels and appeared to be less variable than the simulated dryland yields. These results suggest that demand for water may increase in presently irrigated acreage and that new irrigation systems may be required to maintain adequate production levels in the Southern Great Plains. More acreage would be irrigated as high temperatures and changed hydrologic regimes decrease yield levels and increase yield variability. Increased irrigation would be needed to ensure acceptable and stable yield levels. Crops currently irrigated would require more water where precipitation decreases. The beneficial physiological effects of CO_2 may not compensate fully in this regard, especially if climate change is as severe as predicted by the GFDL GCM.

Heightened demand for irrigation could place stress on the already depleted Ogallala Aquifer and other water resources in the region.

7.8.2 Changes of Planting Date

Changing planting dates in response to changes in length of growing season had little effect on simulated wheat and corn yields. Although wheat is planted in the fall and lies dormant over the winter, yield is primarily determined by factors operative in the following growing season. In corn, the effect of earlier planting date is small probably because solar radiation and temperature, both important factors in crop growth, are relatively low early in the spring. Results of simulations with both crops suggest that changing planting dates in response to changes in length of growing season may not be a highly effective adaptation to global warming in the Southern Great Plains.

7.8.3 Changes of Cultivar

The results of this study indicate that some cultivars of both wheat and corn appear to be available for adaptation to climate change, but that these cultivars may not be efficacious at all locations. The wheat simulations with changed cultivar were performed with the GISS climate change scenario, which is the less severe of the two scenarios used in this study. Wheat cultivar adaptations may be less successful in mitigating the effects of the more severe GFDL climate change scenario, and a similar inference may be drawn from the results of the corn cultivar simulations. These results also suggest that development of heat- and drought-tolerant cultivars should be included in plant-breeding objectives for the region, to ensure the availability of a broad range of cultivars under climate change conditions.

7.9 Shift from Corn to Wheat Production

In general, simulated corn yields were more adversely affected by the climate change scenarios than simulated wheat yields. This suggests that wheat may be more adapted to future conditions in the Great Plains than corn and that there may be a shift to greater wheat production if global warming occurs.

7.10 Agriculture in the Great Plains

If the higher temperatures that are predicted by global climate models come to pass, agriculture as practiced in both the Southern and the Northern Great Plains is likely to become more difficult to sustain. Beneficial physiological crop response to CO_2 may compensate for negative climate change up to certain thresholds and farmers may be able to adjust by substituting better-adapted crop varieties, by increasing the use of irrigation, and by shifting to greater wheat production. If, however, climate change is more severe, it will cause greater declines in both wheat and corn yields, leading to greater consequences to farmers throughout the entire region.

Many critical uncertainties remain about the magnitude and timing of future climate change, as well as about the nature of crop responses to higher levels of atmospheric CO_2. As prediction of climate change and understanding of crop physiological mechanisms advance, the methods devised for this study may be iterated, leading to improved regional projections of future agricultural impacts.

APPENDICES

APPENDIX A

STUDY SITES

1. Climate station, tape ID#, latitude and longitude, county, Land Resource Region (LRR), Major Land Resource Area (MLRA), generic soil types* and soil ID numbers for sites used in Great Plains study.

Grand Island, NE 14935 40.58N 98.19W Hall H 71
- H. deep silt loam, #6
- M. deep sandy loam, #9
- L. med. silt loam, #5

Norfolk, NE 14941 41.59N 97.26W Madison M 102B
- H. deep silty clay, #3
- M. deep silt loam, #6
- L. med. silt loam, #5

N. Platte, NE 24023 41.08N 100.41W Lincoln G 65, H 72
- H. deep silty clay, #3
- M. deep silt loam, #6
- L. deep sand, #12

Omaha, NE 14942 41.18N 95.54W Douglas M 106,107
- H. deep silty clay, #3
- M. deep silt loam, #6
- L. deep sandy loam, #9

Scotts Bluff, NE 24028 41.52N 103.36W S. Bluff G 67
- H. med. silty clay, #2
- M. deep silt loam, #6
- L. deep sandy loam, #9

Dodge City, KS 13985 37.46N 99.58W Ford H 73
- H. shallow silty clay, #1
- M. med. silt loam, #5
- L. deep sand, #12

---

* H = Generic soil with highest drained upper limit of plant extractable water of agricultural soils present in production area/or MLRA.
  M = Generic soil with medium water-holding capacity of agricultural soils present at site in production area/or MLRA.
  L = Generic soil with lowest water-holding capacity of agricultural soils present in production area/or MLRA.

Goodland, KS 23065 39.22N 101.42W Sherman H 72
    H. shallow silty clay, #1
    M. deep silt loam, #6
    L. deep sandy loam, #9

Wichita, KS 3928 37.39N 97.25W Sedgwick H 75,80A
    H. deep silty clay, #3
    M. deep silt loam, #6
    L. med. silt loam, #5

Okla. City, OK 13967 35.24N 97.36W Oklahoma H 80A
    H. deep silty clay, #3
    M. deep silt loam, #6
    L. deep sand, #12

Tulsa, OK 13968 36.12N 95.54W Tulsa M 112
    H. deep silty clay, #3
    M. deep silt loam, #6
    L. med. silt loam, #5

Amarillo, TX 23047 35.14N 101.42W Potter H 77
    H. deep silty clay, #3
    M. deep sandy loam, #9
    L. med. silt loam, #5

Brownsville, TX 12919 25.54N 97.26W Cameron I 83D
    H. deep silty clay, #3
    M. deep silt loam, #6
    L. deep sandy loam, #9

San Antonio, TX 12921 29.32N 98.28W Bexar I 81, J 86,87
    H. deep sandy loam, #9
    M. med. silt loam, #5
    L. med. sandy loam, #8

Waco, TX 13959 31.37N 97.13W McLennon J 85,86
    H. deep silty clay, #3
    M. deep silt loam, #6
    L. deep sandy loam, #9

Bismarck, ND 46.46N 100.45W Burleigh F 53B
    A. deep silt loam, #6

Fargo, ND 46.54N 96.58W Cass F 55B,56
    A. deep silty clay, #3

Pierre, SD 44.23N 100.17W Hughes F 53C, G 63A
    A. deep silt loam #6

2. Land resource regions (LRR) and Major Land Resource Areas (MLRA) of sites in Great Plains Study.

D	Western Range and Irrigated Region
42	Southern Desertic Basins, Plains, and Mountains
F	Northern Great Plains Spring Wheat Region
53B	Central Dark Brown Glaciated Plains
53C	Southern Dark Brown Glaciated Plains
55B	Central Black Glaciated Plains
56	Red River Valley of the North
G	Western Great Plains Range and Irrigated Region
63A	Northern Rolling Pierre Shale Plains
65	Nebraska Sand Hills
67	Central High Plains
H	Central Great Plains Winter Wheat and Range Region
71	Central Nebraska Loess Hills
72	Central High Tableland
73	Rolling Plains and Breaks
75	Central Loess Plains
77	Southern High Plains
78	Central Rolling Red Plains
80A	Central Rolling Red Prairies
I	Southwest Plateaus and Plains Range and Cotton Region
81	Edwards Plateau
83D	Lower Rio Grande Valley
J	Southwestern Prairies Cotton and Forage Region
85	Grand Prairie
86	Texas Blackland Prairie
87	Texas Claypan Area

M Central Feed Grains and Livestock Region

102B Loess Uplands and Till Plains
106 Nebraska and Kansas Loess-Drift Hills
107 Iowa and Missouri Deep Loess Hills
112 Cherokee Prairies

Source: USDA, Soil Conservation Services, 1981: Land Resource Regions and Major Land Resource Areas of the United States. Agriculture Handbook 296.

APPENDIX B

GENERIC SOIL TYPES

```
Format line #1 of soil
     IDUMSL  1X,I2   # assigned to a soil type
     PEDON   1X,A12  SCS pedon number
     TAXON   1X,A60  Soil classification


Format line #2
     SALB    F6.2    Bare soil albedo
     U       1X,F5.2 Upper limit stage 1 evaporation, mm
     SWCON   1X,F6.2 Soil H2O drainage constant fraction drained per day
     CN2     1X,F6.2 SCS curve # used to calculate daily runoff
     TAV     1x,F5.1 Annual ave. ambient temperature C
     AMP     1X,F5.1 Annual amplitude in mean monthly temperature C
     DMOD    1X,F3.1 Soil mineralization factor (Default = 1)
     SWCON1  1X,E9.2 Coefficient in steady state solution
               (Default=.00267)
     SWCON2  1X,F6.1 Coefficient in steady state solution (Default=58)
     SWCON3  1X,F5.2 Coefficient in steady state solution (Default=6.68)
     RWUMX   1X,F5.2 Maximum daily root water uptake (Default=0.03)
     PHFAC3  1X,F4.2 Variable to reduce apparent photosynthesis
               (Default=1)


Format line #3
     DLAYR(L) F6.0   Thickness of soil layer L, cm
     LL(L)   1X,F6.3 Lower limit of plant-extractable H2O cm**3/cm**3
     DUL(L)  1x,F6.3 Drained upper limit soil H2O content for layer L
     SAT(L)  1X,F6.3 Saturated H2O content for layer L cm**3/cm**3
     SW(L)   1X,F6.3 Default soil H2O for layer L cm**3/cm**3
     WR(L)   1x,F6.3 Weighting factor for soil depth L to determine root
             growth distribution, no units
     BD(L)   1X,F5.2 Moist bulk density of soil in layer L g/c**3
     OC(L)   1X,F5.2 Organic carbon concentration in layer L %
     NH4(L)  1X,F4.1 Default ammonium in layer L, mg elemental N/kg soil
     NO3(L)  1X,F4.1 Default nitrate in layer L, mg elemental N/kg soil
     PH(L)   1X,F4.1 Default Ph in layer L in 1:1 soil: water slurry


  1             SHALLOW SILTY CLAY
   .11  6.00    .10  89.00    6.9  13.9 1.0   .27E-02   58.0  6.68   .03
1.00
   10.   .513   .680   .760   .680  1.000  1.35  1.74  2.5  3.3  6.5
   15.   .513   .679   .759   .679   .819  1.36  1.66  2.4  3.2  6.5
   15.   .514   .679   .759   .679   .607  1.36  1.45  2.2  3.0  6.5
   20.   .516   .677   .757   .677   .449  1.36  1.16  2.1  2.7  6.5
   -1.
  2             MEDIUM SILTY CLAY
   .11  6.00    .20  87.00    6.9  13.9 1.0   .27E-02   58.0  6.68   .03
1.00
   10.   .513   .680   .760   .680  1.000  1.35  1.74  2.5  3.3  6.5
   15.   .513   .679   .759   .679   .819  1.36  1.66  2.4  3.2  6.5
   20.   .514   .679   .759   .679   .607  1.36  1.45  2.2  3.0  6.5
   25.   .516   .677   .757   .677   .407  1.37  1.12  2.0  2.7  6.5
   30.   .518   .676   .756   .676   .247  1.37   .73  1.8  2.3  6.5
   30.   .520   .674   .754   .674   .135  1.38   .37  1.5  1.9  6.5
   -1.
```

```
  3              DEEP SILTY CLAY
   .11  6.00    .30  85.00    6.9  13.9 1.0   .27E-02   58.0  6.68   .03
1.00
   10.   .513   .680   .760   .680  1.000  1.35  1.74  2.5  3.3  6.5
   15.   .513   .679   .759   .679   .819  1.36  1.66  2.4  3.2  6.5
   25.   .514   .679   .759   .679   .607  1.36  1.45  2.2  3.0  6.5
   30.   .516   .677   .757   .677   .368  1.37  1.09  2.0  2.6  6.5
   30.   .519   .675   .755   .675   .202  1.38   .65  1.7  2.2  6.5
   30.   .521   .674   .754   .674   .111  1.38   .29  1.4  1.8  6.5
   30.   .522   .673   .753   .673   .061  1.39   .09  1.1  1.3  6.5
   30.   .522   .673   .753   .673   .033  1.39   .01   .8   .9  6.5
   -1.
  4              SHALLOW SILT LOAM
   .12  6.00    .20  81.00    6.9  13.9 1.0   .27E-02   58.0  6.68   .03
1.00
   10.   .106   .262   .362   .262  1.000  1.37  1.16  2.5  3.3  6.5
   15.   .106   .262   .362   .262   .819  1.37  1.10  2.4  3.2  6.5
   15.   .107   .262   .362   .262   .607  1.37   .97  2.2  3.0  6.5
   20.   .108   .261   .361   .261   .449  1.38   .77  2.1  2.7  6.5
   -1.
  5              MEDIUM SILT LOAM
   .12  6.00    .30  79.00    6.9  13.9 1.0   .27E-02   58.0  6.68   .03
1.00
   10.   .106   .262   .362   .262  1.000  1.37  1.16  2.5  3.3  6.5
   15.   .106   .262   .362   .262   .819  1.37  1.10  2.4  3.2  6.5
   20.   .107   .262   .362   .262   .607  1.37   .97  2.2  3.0  6.5
   25.   .108   .261   .361   .261   .407  1.38   .75  2.0  2.7  6.5
   30.   .110   .260   .360   .260   .247  1.38   .49  1.8  2.3  6.5
   30.   .111   .259   .359   .259   .135  1.39   .24  1.5  1.9  6.5
   -1.
  6              DEEP SILT LOAM
   .12  6.00    .40  77.00    6.9  13.9 1.0   .27E-02   58.0  6.68   .03
1.00
   10.   .106   .262   .362   .262  1.000  1.37  1.16  2.5  3.3  6.5
   15.   .106   .262   .362   .262   .819  1.37  1.10  2.4  3.2  6.5
   25.   .107   .262   .362   .262   .607  1.37   .97  2.2  3.0  6.5
   30.   .108   .261   .361   .261   .368  1.38   .72  2.0  2.6  6.5
   30.   .110   .260   .360   .260   .202  1.38   .43  1.7  2.2  6.5
   30.   .111   .259   .359   .259   .111  1.39   .20  1.4  1.8  6.5
   30.   .112   .258   .358   .258   .061  1.39   .06  1.1  1.3  6.5
   30.   .112   .258   .358   .258   .033  1.39   .01   .8   .9  6.5
   -1.
  7              SHALLOW SANDY LOAM
   .13  6.00    .40  74.00    6.9  13.9 1.0   .27E-02   58.0  6.68   .03
1.00
   10.   .086   .220   .320   .220  1.000  1.61   .70  2.5  3.3  6.5
   15.   .086   .220   .320   .220   .819  1.61   .66  2.4  3.2  6.5
   15.   .086   .220   .320   .220   .607  1.61   .58  2.2  3.0  6.5
   20.   .087   .219   .319   .219   .449  1.61   .46  2.1  2.7  6.5
   -1.
  8              MEDIUM SANDY LOAM
   .13  6.00    .50  70.00    6.9  13.9 1.0   .27E-02   58.0  6.68   .03
1.00
   10.   .086   .220   .320   .220  1.000  1.61   .70  2.5  3.3  6.5
   15.   .086   .220   .320   .220   .819  1.61   .66  2.4  3.2  6.5
   20.   .086   .220   .320   .220   .607  1.61   .58  2.2  3.0  6.5
   25.   .087   .219   .319   .219   .407  1.61   .45  2.0  2.7  6.5
   30.   .088   .219   .319   .219   .247  1.62   .29  1.8  2.3  6.5
   30.   .089   .218   .318   .218   .135  1.62   .15  1.5  1.9  6.5
   -1.
```

```
  9              DEEP SANDY LOAM
   .13  6.00    .50  68.00   6.9  13.9 1.0   .27E-02   58.0  6.68   .03
1.00
   10.   .086   .220   .320   .220  1.000  1.61   .70  2.5  3.3  6.5
   15.   .086   .220   .320   .220   .819  1.61   .66  2.4  3.2  6.5
   25.   .086   .220   .320   .220   .607  1.61   .58  2.2  3.0  6.5
   30.   .087   .219   .319   .219   .368  1.61   .43  2.0  2.6  6.5
   30.   .088   .218   .318   .218   .202  1.62   .26  1.7  2.2  6.5
   30.   .089   .218   .318   .218   .111  1.62   .12  1.4  1.8  6.5
   30.   .089   .218   .318   .218   .061  1.62   .04  1.1  1.3  6.5
   30.   .089   .217   .317   .217   .033  1.62   .01   .8   .9  6.5
   30.   .089   .217   .317   .217   .018  1.62   .00   .5   .5  6.5
   -1.
 10              SHALLOW SAND
   .15  4.00    .40  75.00   6.9  13.9 1.0   .27E-02   58.0  6.68   .03
1.00
   10.   .032   .107   .267   .107  1.000  1.66   .29  2.5  3.3  6.5
   15.   .032   .107   .267   .107   .819  1.66   .28  2.4  3.2  6.5
   15.   .032   .107   .267   .107   .607  1.66   .24  2.2  3.0  6.5
   20.   .032   .107   .267   .107   .449  1.66   .19  2.1  2.7  6.5
   -1.
 11              MEDIUM SAND
   .15  4.00    .50  70.00   6.9  13.9 1.0   .27E-02   58.0  6.68   .03
1.00
   10.   .032   .107   .267   .107  1.000  1.66   .29  2.5  3.3  6.5
   15.   .032   .107   .267   .107   .819  1.66   .28  2.4  3.2  6.5
   20.   .032   .107   .267   .107   .607  1.66   .24  2.2  3.0  6.5
   25.   .032   .107   .267   .107   .407  1.66   .19  2.0  2.7  6.5
   30.   .033   .106   .266   .106   .247  1.66   .12  1.8  2.3  6.5
   -1.
 12              DEEP SAND
   .15  4.00    .60  65.00   6.9  13.9 1.0   .27E-02   58.0  6.68   .03
1.00
   10.   .032   .107   .267   .107  1.000  1.66   .29  2.5  3.3  6.5
   15.   .032   .107   .267   .107   .819  1.66   .28  2.4  3.2  6.5
   25.   .032   .107   .267   .107   .607  1.66   .24  2.2  3.0  6.5
   30.   .032   .107   .267   .107   .368  1.66   .18  2.0  2.6  6.5
   30.   .033   .106   .266   .106   .202  1.66   .11  1.7  2.2  6.5
   30.   .033   .106   .266   .106   .111  1.66   .05  1.4  1.8  6.5
   30.   .033   .106   .266   .106   .061  1.66   .01  1.1  1.3  6.5
   30.   .033   .106   .266   .106   .033  1.66   .00   .8   .9  6.5
   -1.
```

APPENDIX C

PERCENT CHANGE STATISTICS

1. Individual run

	BASELINE YIELD	$2xCO_2$ YIELD	YIELD DIF. 2xCO2-BASE
	1	1	1
	.	.	.
	.	.	.
	.	.	.
	n_a	n_b	n_c
Observed mean	μ_a	μ_b	μ_c

Observed standard deviation σ_a σ_b

Standard deviation of observed mean

$$\sigma_{\mu_a} = \frac{\sigma_a}{\sqrt{n_a}}, \quad \sigma_{\mu_b} = \frac{\sigma_b}{\sqrt{n_b}}$$

Observed mean yield difference

$$\mu_c = \mu_b - \mu_a$$

Observed standard deviation of mean yield difference

$$\sigma_{\mu_c} = \sqrt{\sigma^2_{\mu_a} + \sigma^2_{\mu_b}}$$

Mean and uncertainty of percent change

$$\left(\frac{\mu_c \pm \sigma_{\mu_c}}{\mu_a}\right) \times 100$$

2. Summary of 3 soils at one site

$$\left(\frac{\mu_{cL} + \mu_{cM} + \mu_{cH} \pm \sqrt{\sigma^2_{\mu_{cL}} + \sigma^2_{\mu_{cM}} + \sigma^2_{\mu_{cH}}}}{\mu_{aL} + \mu_{aM} + \mu_{aH}}\right) \times 100$$

Summary mean and uncertainty of change over all soils; L, M, H = low, medium, and high production capacity

APPENDIX D

POTENTIAL FOR INCREASED PLANT STRESS

Predictions of global warming caused by increasing trace gases, potential increases in UV-B radiation from stratospheric ozone depletion, and increasing levels of tropospheric ozone, acid precipitation, and air pollution all raise the possibility that certain combinations of plant stresses may be even more prevalent in the coming decades, than they are today. In particular, high temperature and drought stress may occur much more often and in combination with other stresses, if global warming becomes a reality.

D.1 High Temperature Stress

The threshold for high temperature stress on most crop plants lies between 45 and 65°C (Levitt, 1980). Rapid rates of warming cause protein to coagulate, leading to cell rupture; gradual rates of warming break down proteins, releasing toxic ammonia (Salisbury and Ross, 1978). Elevated temperatures also cause respiration rate to increase and photosynthesis to decrease. At temperatures above 40°C, irreversible enzyme damage and uncoupling of photophos-phorylation occurs in wheat (Azcon-Bieto, 1983; Kobza and Edwards, 1987). Critical stages for high temperature injury include seedling emergence in most crops, silking and tasseling in corn (Shaw, 1983), grain filling in wheat (Johnson and Kanemasu, 1983), and flowering in soybeans (Mederski, 1983).

Highest and lowest maximum temperatures in March, April, and May from baseline climate and three GCMs (GISS, GFDL, and Oregon State University (OSU) (Schlesinger and Zhao, 1988) are shown in Table A4.1 for southern and northern Great Plains sites. Maximum temperatures are consistently higher in the climate change scenarios than in the baseline climate. The highest maximum temperatures are greater than 40°C in all but six cases. In the warmer GISS and GFDL scenarios, maximum temperatures reach temperatures 45°C, the threshold for high temperature stress, or higher at several sites in the spring season. Average highest maximum temperatures in the spring range between 31 and 35°C in the baseline climate and 34 and 39, 35 and 42, and 34 and 38°C in the GISS, GFDL, and OSU scenarios respectively (Table A4.2).

Similar maximum temperature statistics for June, July, and August are shown in Table A4.3. While baseline climate has three out of 21 sites with high maximum temperatures of 45°C, the GISS and OSU climate change scenarios have 19 sites each and the GFDL scenario, 20 sites with temperatures above the heat stress threshold. The highest temperature in any of the climate change scenarios is 54°C, occurring in Norfolk, Nebraska and Pierre, South Dakota. Average highest maximum temperatures in the Great Plains for all the scenarios are above 40°C in every case and are frequently over 45°C in the GFDL scenario (Table A4.4).

These results suggest that climate change as predicted by three GCMs holds the potential for increased heat stress on crops in the Great Plains, particularly in the summer months, and, to a lesser degree, in the spring.

D.2 Drought Stress

The anticipated greenhouse warming has led to concern about future water availability, because, in the past, warmer summers have been correlated with reduced precipitation. A variety of research approaches have been used to explore the question of future drought, with some results showing decreases in runoff (Revelle and Waggoner, 1983) and others, summer drying (Manabe and Wetherald, 1987). Because precipitation changes are not consistent in GCM doubled-CO_2 experiments, use of soil moisture as drought predictor has produced mixed results (Kellogg and Zhao, 1988).

A drought index which uses the difference between potential evaporation (the atmospheric demand for water) and precipitation (the atmospheric supply for water) has been calculated for the transient climate change simulations of the GISS GCM (Rind et al., 1990). Given current exponential emissions growth rates, drought begin to increase in frequency in the 1990s, and severe drought, which only occur 5% of the time in the current climate, occur about 50% of the time by the 2050s. Droughts of this frequency could have severe consequences on agriculture, and research on climate change and drought is critical prioroty for further study.

Table D.1 Highest and lowest maximum temperatures in March, April, and May for observed (1951-1980) climate and GISS, GFDL, and OSU climate change scenarios.

SITE	OBSERVED RANGE OF MAX TEMPS	GISS 2XCO2 RANGE OF MAX TEMPS	GFDL 2XCO2 RANGE OF MAX TEMPS	OSU 2XCO2 RANGE OF MAX TEMPS
	(°C)	(°C)	(°C)	(°C)
NPNE	-14 – 36	-8 – 40	-9 – 40	-11 – 39
NONE	-14 – 39	-9 – 44	-10 – 44	-11 – 43
GINE	-12 – 38	-7 – 42	-7 – 42	-9 – 41
OMNE	-13 – 36	-8 – 40	-8 – 40	-10 – 39
SBNE	-14 – 35	-8 – 39	-9 – 40	-12 – 38
GOKS	-13 – 37	-8 – 41	-9 – 44	-11 – 39
DCKS	-13 – 39	-8 – 42	-9 – 45	-11 – 41
WIKS	-13 – 38	-8 – 41	-9 – 44	-10 – 40
TUOK	-8 – 39	-3 – 44	-4 – 44	-4 – 43
OKOK	-8 – 38	-3 – 43	-4 – 43	-5 – 42
AMTX	-8 – 39	-5 – 42	-2 – 46	-6 – 41
SATX	3 – 38	7 – 43	8 – 44	7 – 42
BRTX	8 – 39	12 – 43	12 – 45	11 – 42
WATX	2 – 38	7 – 44	6 – 43	5 – 43
BIND	-21 – 36	-15 – 40	-14 – 40	-17 – 39
FAND	-20 – 38	-15 – 43	-14 – 44	-17 – 41
MIND	-24 – 37	-18 – 41	-18 – 41	-21 – 41
RSCD	-18 – 37	-12 – 41	-13 – 42	-15 – 40
PISD	-17 – 41	-12 – 45	-12 – 45	-14 – 44
HUSD	-18 – 37	-12 – 41	-13 – 41	-14 – 40
SFSD	-16 – 38	-10 – 42	-11 – 42	-13 – 41

Table D.2 Average highest and lowest maximum temperatures in March, April, and May for observed (1951-1989) climate and GISS, GFDL, and OSU climate change scenarios.

SITE	OBSERVED RANGE OF MAX TEMPS	GISS 2XCO2 RANGE OF MAX TEMPS	GFDL 2XCO2 RANGE OF MAX TEMPS	OSU 2XCO2 RANGE OF MAX TEMPS
	(°C)	(°C)	(°C)	(°C)
NPNE	-6 – 32	0 – 36	-1 – 36	-2 – 35
NONE	-7 – 33	-1 – 37	-2 – 37	-3 – 36
GINE	-6 – 33	0 – 37	-1 – 37	-2 – 36
OMNE	-4 – 33	2 – 37	1 – 37	-1 – 36
SBNE	-5 – 32	1 – 36	0 – 37	-2 – 34
GOKS	-4 – 33	1 – 37	0 – 39	-2 – 35
DCKS	-2 – 34	3 – 38	2 – 40	1 – 37
WIKS	-1 – 33	5 – 37	4 – 39	3 – 36
TUOK	3 – 33	8 – 38	7 – 39	6 – 36
OKOK	3 – 33	8 – 37	7 – 39	6 – 37
AMTX	1 – 35	6 – 38	5 – 42	4 – 37
SATX	11 – 35	15 – 38	16 – 40	15 – 38
BRTX	15 – 35	19 – 39	19 – 40	18 – 38
WATX	8 – 34	14 – 39	13 – 41	12 – 38
BIND	-11 – 31	-5 – 35	-4 – 36	-7 – 34
FAND	-12 – 31	-6 – 35	-5 – 36	-8 – 35
MIND	-13 – 31	-8 – 34	-6 – 35	-9 – 34
RSCD	-8 – 31	-3 – 36	-3 – 37	-5 – 35
PISD	-8 – 33	-3 – 37	-3 – 37	-5 – 36
HUSD	-8 – 32	-3 – 36	-3 – 36	-5 – 35
SFSD	-8 – 32	-2 – 36	-3 – 36	-4 – 35

Table D.3 Highest and lowest maximum temperatures in June, July, and August for observed (1951-1980) climate and GISS, GFDL, and OSU climate change scenarios.

SITE	OBSERVED RANGE OF MAX TEMPS	GISS 2XCO2 RANGE OF MAX TEMPS	GFDL 2XCO2 RANGE OF MAX TEMPS	OSU 2XCO2 RANGE OF MAX TEMPS
	(°C)	(°C)	(°C)	(°C)
NPNE	10 - 44	14 - 48	18 - 53	14 - 48
NONE	11 - 45	14 - 49	19 - 54	15 - 49
GINE	12 - 43	15 - 47	20 - 51	15 - 47
OMNE	13 - 43	17 - 47	21 - 52	17 - 47
SBNE	7 - 43	10 - 47	14 - 52	10 - 46
GOKS	11 - 42	14 - 47	17 - 50	14 - 46
DCKS	11 - 43	14 - 48	17 - 49	14 - 47
WIKS	14 - 45	18 - 50	20 - 51	18 - 49
TUOK	14 - 44	18 - 49	20 - 50	18 - 48
OKOK	17 - 43	20 - 48	20 - 47	20 - 47
AMTX	13 - 42	17 - 46	17 - 49	16 - 46
SATX	22 - 41	27 - 46	25 - 45	26 - 46
BRTX	26 - 39	29 - 44	28 - 42	29 - 42
WATX	20 - 44	23 - 50	23 - 48	23 - 48
BIND	7 - 43	11 - 47	17 - 53	11 - 47
FAND	8 - 41	12 - 46	17 - 51	12 - 46
MIND	8 - 41	11 - 44	18 - 50	12 - 44
RSCD	3 - 43	6 - 47	10 - 52	6 - 47
PISD	7 - 45	10 - 49	15 - 54	10 - 49
HUSD	8 - 44	12 - 48	17 - 53	12 - 48
SFSD	12 - 42	15 - 47	20 - 50	16 - 47

Table D.4 Average highest and lowest maximum temperatures in June, July, and August for observed (1951-1980) climate and GISS, GFDL, and OSU climate change scenarios.

SITE	OBSERVED RANGE OF MAX TEMPS	GISS 2XCO2 RANGE OF MAX TEMPS	GFDL 2XCO2 RANGE OF MAX TEMPS	OSU 2XCO2 RANGE OF MAX TEMPS
	(°C)	(°C)	(°C)	(°C)
NPNE	16 – 39	20 – 43	24 – 47	20 – 43
NONE	17 – 39	21 – 43	25 – 48	21 – 43
GINE	17 – 40	21 – 44	25 – 48	21 – 43
OMNE	19 – 39	23 – 43	27 – 47	23 – 43
SBNE	15 – 39	18 – 43	22 – 47	18 – 42
GOKS	16 – 40	19 – 44	22 – 47	19 – 44
DCKS	19 – 40	22 – 45	24 – 46	22 – 44
WIKS	20 – 41	24 – 45	26 – 46	24 – 44
TUOK	22 – 40	26 – 45	27 – 45	25 – 44
OKOK	22 – 40	26 – 45	25 – 43	25 – 44
AMTX	19 – 39	23 – 43	25 – 45	23 – 43
SATX	26 – 38	30 – 43	29 – 42	30 – 43
BRTX	28 – 36	32 – 41	31 – 40	31 – 40
WATX	26 – 40	29 – 45	29 – 44	29 – 44
BIND	15 – 39	19 – 43	24 – 48	19 – 43
FAND	15 – 37	19 – 41	24 – 46	19 – 41
MIND	14 – 37	17 – 40	23 – 47	17 – 41
RSCD	14 – 39	18 – 44	21 – 48	17 – 43
PISD	16 – 41	20 – 46	24 – 50	20 – 45
HUSD	16 – 39	20 – 44	24 – 47	20 – 43
SFSD	16 – 38	20 – 42	24 – 46	20 – 42

APPENDIX E

COMPARISON OF 1951-80 & 1930-39 CLIMATE DATA

Table E.1 Mean difference, standard deviations, and Z scores of mean monthly temperature (1951-80 minus 1930-39).

		MDIF	SDN	SD30S	SDDIF	ZMON	MDIF	SDDIF	ZANN
NPNE	1	-.4000	.5842	1.7076	1.8048	-.2216			
NPNE	2	1.2000	.5660	1.7076	1.7990	.6670			
NPNE	3	-.2000	.4747	.6641	.8163	-.2450			
NPNE	4	.0000	.3104	.4743	.5669	.0000			
NPNE	5	-.5000	.3104	.9171	.9682	-.5164			
NPNE	6	-.7000	.3286	.7589	.8270	-.8464			
NPNE	7	-1.5000	.2739	.3795	.4680	-3.2053			
NPNE	8	-.3000	.2373	.4111	.4747	-.6320			
NPNE	9	-.7000	.3286	.5692	.6573	-1.0650			
NPNE	10	.4000	.3469	.6325	.7213	.5545			
NPNE	11	-.3000	.3286	.4111	.5263	-.5700			
NPNE	12	-.6000	.4747	.5692	.7412	-.8095			
NPNE	ANN						-.3000	.2804	-1.0697

		MDIF	SDN	SD30S	SDDIF	ZMON	MDIF	SDDIF	ZANN
GINE	1	-2.0000	.4930	1.8341	1.8992	-1.0531			
GINE	2	-.4000	.6390	1.7709	1.8826	-.2125			
GINE	3	-1.8000	.5477	.8222	.9879	-1.8220			
GINE	4	-.7000	.3286	.5060	.6033	-1.1602			
GINE	5	-.8000	.3104	.9171	.9682	-.8263			
GINE	6	-1.4000	.3104	.8222	.8788	-1.5930			
GINE	7	-3.1000	.3104	.4743	.5669	-5.4687			
GINE	8	-1.9000	.2556	.5060	.5669	-3.3518			
GINE	9	-2.4000	.2921	.6641	.7255	-3.3081			
GINE	10	-1.1000	.3286	.6957	.7694	-1.4297			
GINE	11	-1.1000	.2921	.5692	.6398	-1.7193			
GINE	12	-1.8000	.4747	.6957	.8422	-2.1372			
GINE	ANN						-1.5417	.3014	-5.1151

		MDIF	SDN	SD30S	SDDIF	ZMON	MDIF	SDDIF	ZANN
OMNE	1	-1.1000	.4382	1.6760	1.7323	-.6350			
OMNE	2	.8000	.6025	1.7393	1.8407	.4346			
OMNE	3	-.5000	.5660	.7589	.9467	-.5281			
OMNE	4	.5000	.3286	.4427	.5514	.9068			
OMNE	5	-.3000	.3469	.9171	.9805	-.3060			
OMNE	6	-.9000	.2921	.6641	.7255	-1.2405			
OMNE	7	-2.3000	.2739	.4743	.5477	-4.1992			
OMNE	8	-1.3000	.2373	.6325	.6755	-1.9244			
OMNE	9	-1.7000	.2921	.6957	.7545	-2.2530			
OMNE	10	.0000	.3834	.6957	.7944	.0000			
OMNE	11	.1000	.3286	.4743	.5771	.1733			
OMNE	12	-.6000	.4747	.6957	.8422	-.7124			
OMNE	ANN						-.6083	.2896	-2.1007

Continued, next page

Table E.1 Continued

		MDIF	SDN	SD30S	SDDIF	ZMON	MDIF	SDDIF	ZANN
SBNE	1	-.2000	.5295	1.4230	1.5183	-.1317			
SBNE	2	2.0000	.4747	1.3598	1.4403	1.3886			
SBNE	3	.1000	.4382	.6325	.7694	.1300			
SBNE	4	.1000	.3651	.5692	.6763	.1479			
SBNE	5	.1000	.2739	.8538	.8967	.1115			
SBNE	6	-.4000	.3286	.6325	.7127	-.5612			
SBNE	7	-1.2000	.2556	.3795	.4575	-2.6228			
SBNE	8	-.7000	.1826	.3479	.3929	-1.7818			
SBNE	9	-1.3000	.3834	.6957	.7944	-1.6365			
SBNE	10	.4000	.3286	.6008	.6848	.5841			
SBNE	11	.1000	.3286	.5060	.6033	.1657			
SBNE	12	-.2000	.4747	.7273	.8685	-.2303			
SBNE ANN							-.1000	.2544	-.3930

		MDIF	SDN	SD30S	SDDIF	ZMON	MDIF	SDDIF	ZANN
GOKS	1	-1.4000	.4930	1.4230	1.5060	-.9296			
GOKS	2	-1.0000	.5112	1.2017	1.3059	-.7658			
GOKS	3	-2.4000	.4747	.7906	.9221	-2.6027			
GOKS	4	-1.9000	.3104	.3479	.4662	-4.0756			
GOKS	5	-1.7000	.2921	.7589	.8132	-2.0904			
GOKS	6	-1.8000	.3469	.5376	.6398	-2.8134			
GOKS	7	-2.7000	.2556	.3795	.4575	-5.9013			
GOKS	8	-2.5000	.2191	.5376	.5805	-4.3065			
GOKS	9	-2.7000	.3286	.5060	.6033	-4.4752			
GOKS	10	-1.8000	.3286	.5692	.6573	-2.7386			
GOKS	11	-1.9000	.2921	.4111	.5043	-3.7675			
GOKS	12	-1.6000	.4017	.7589	.8587	-1.8633			
GOKS ANN							-1.9500	.2422	-8.0519

		MDIF	SDN	SD30S	SDDIF	ZMON	MDIF	SDDIF	ZANN
DCKS	1	-2.6000	.5112	1.2333	1.3350	-1.9475			
DCKS	2	-2.0000	.5660	1.2017	1.3283	-1.5057			
DCKS	3	-2.8000	.5112	.8222	.9682	-2.8921			
DCKS	4	-1.6000	.3286	.3795	.5020	-3.1873			
DCKS	5	-1.5000	.3286	.6325	.7127	-2.1046			
DCKS	6	-1.5000	.3286	.5376	.6301	-2.3807			
DCKS	7	-2.2000	.3104	.3479	.4662	-4.7191			
DCKS	8	-2.3000	.2556	.4427	.5112	-4.4991			
DCKS	9	-2.6000	.3104	.5376	.6208	-4.1885			
DCKS	10	-1.5000	.3469	.6008	.6938	-2.1621			
DCKS	11	-1.7000	.3104	.5376	.6208	-2.7386			
DCKS	12	-2.2000	.3469	.7273	.8058	-2.7302			
DCKS ANN							-2.0417	.2360	-8.6507

Continued, next page

Table E.1 Continued

		MDIF	SDN	SD30S	SDDIF	ZMON	MDIF	SDDIF	ZANN
WIKS	1	-3.6000	.5112	1.3598	1.4527	-2.4781			
WIKS	2	-2.9000	.5477	1.0752	1.2066	-2.4034			
WIKS	3	-2.6000	.4747	.9171	1.0326	-2.5178			
WIKS	4	-1.3000	.3286	.4427	.5514	-2.3578			
WIKS	5	-.7000	.3286	.4427	.5514	-1.2696			
WIKS	6	-.4000	.3104	.5376	.6208	-.6444			
WIKS	7	-.8000	.3651	.4427	.5739	-1.3940			
WIKS	8	-1.4000	.2556	.6008	.6529	-2.1441			
WIKS	9	-2.2000	.3469	.7273	.8058	-2.7302			
WIKS	10	-1.6000	.3286	.6325	.7127	-2.2449			
WIKS	11	-1.9000	.3104	.6008	.6763	-2.8096			
WIKS	12	-2.9000	.3469	.6641	.7492	-3.8707			
WIKS ANN							-1.8583	.2438	-7.6230

		MDIF	SDN	SD30S	SDDIF	ZMON	MDIF	SDDIF	ZANN
OKOK	1	-1.4000	.4747	1.2965	1.3807	-1.0140			
OKOK	2	-1.0000	.4930	.9803	1.0973	-.9114			
OKOK	3	-1.0000	.4564	.8854	.9962	-1.0039			
OKOK	4	-.5000	.3286	.4427	.5514	-.9068			
OKOK	5	-.1000	.2556	.4427	.5112	-.1956			
OKOK	6	-1.1000	.2556	.5060	.5669	-1.9405			
OKOK	7	-1.4000	.2921	.3479	.4542	-3.0821			
OKOK	8	-1.3000	.2373	.6325	.6755	-1.9244			
OKOK	9	-1.2000	.3104	.8222	.8788	-1.3655			
OKOK	10	-.6000	.3104	.5376	.6208	-.9666			
OKOK	11	-.1000	.3286	.5376	.6301	-.1587			
OKOK	12	-.6000	.3286	.5692	.6573	-.9129			
OKOK ANN							-.8583	.2303	-3.7267

		MDIF	SDN	SD30S	SDDIF	ZMON	MDIF	SDDIF	ZANN
AMTX	1	-2.0000	.4564	1.0752	1.1680	-1.7123			
AMTX	2	-2.0000	.4564	1.0436	1.1390	-1.7559			
AMTX	3	-2.2000	.4199	.7906	.8952	-2.4576			
AMTX	4	-1.9000	.3286	.4427	.5514	-3.4460			
AMTX	5	-1.5000	.3104	.4743	.5669	-2.6461			
AMTX	6	-2.4000	.2739	.3795	.4680	-5.1285			
AMTX	7	-2.7000	.2556	.2846	.3825	-7.0582			
AMTX	8	-2.9000	.2191	.4743	.5225	-5.5503			
AMTX	9	-2.2000	.2556	.6008	.6529	-3.3694			
AMTX	10	-1.5000	.3104	.5692	.6483	-2.3136			
AMTX	11	-1.5000	.3834	.3795	.5394	-2.7806			
AMTX	12	-1.2000	.3104	.6957	.7618	-1.5752			
AMTX ANN							-2.0000	.2116	-9.4539

Continued, next page

Table E.1 Continued

		MDIF	SDN	SD30S	SDDIF	ZMON	MDIF	SDDIF	ZANN
SATX	1	.5000	.4017	.9171	1.0012	.4994			
SATX	2	.7000	.4199	.7273	.8398	.8335			
SATX	3	1.7000	.3834	.8854	.9649	1.7619			
SATX	4	1.8000	.2739	.5376	.6033	2.9835			
SATX	5	1.0000	.2008	.4111	.4575	2.1857			
SATX	6	.4000	.1826	.3479	.3929	1.0182			
SATX	7	.4000	.1826	.2214	.2869	1.3940			
SATX	8	.2000	.1826	.1897	.2633	.7596			
SATX	9	.1000	.2373	.4743	.5304	.1885			
SATX	10	.1000	.3286	.6957	.7694	.1300			
SATX	11	1.2000	.3286	.6957	.7694	1.5596			
SATX	12	1.0000	.3104	.6641	.7330	1.3642			
SATX	ANN						.7583	.1958	3.8730

		MDIF	SDN	SD30S	SDDIF	ZMON	MDIF	SDDIF	ZANN
WATX	1	-.9000	.4564	.9171	1.0244	-.8786			
WATX	2	-.2000	.4199	.8538	.9515	-.2102			
WATX	3	.5000	.4017	.9171	1.0012	.4994			
WATX	4	.9000	.3286	.4111	.5263	1.7100			
WATX	5	.8000	.2191	.4427	.4940	1.6196			
WATX	6	.7000	.2191	.2530	.3347	2.0917			
WATX	7	.7000	.2556	.2846	.3825	1.8299			
WATX	8	.3000	.2191	.2530	.3347	.8964			
WATX	9	-.3000	.2556	.4743	.5388	-.5568			
WATX	10	-.5000	.3104	.6957	.7618	-.6563			
WATX	11	.5000	.3651	.6641	.7578	.6598			
WATX	12	.0000	.3286	.6325	.7127	.0000			
WATX	ANN						.2083	.2007	1.0379

Table E.2 Mean differences, standard deviations, and Z scores of mean monthly precipitation (1951-80 minus 1930-39).

		MDIF	SD30	SD10	SDDIF	Z	MDIF	SDDIF	ZANN
NPNE	1	2.1000	1.4606	1.9922	2.4703	.8501			
NPNE	2	3.0000	2.5013	1.7709	3.0647	.9789			
NPNE	3	3.6000	4.0349	5.3126	6.6712	.5396			
NPNE	4	-21.9000	5.0938	14.9576	15.8011	-1.3860			
NPNE	5	.3000	8.8001	12.2064	15.0478	.0199			
NPNE	6	19.6000	9.9868	11.8585	15.5036	1.2642			
NPNE	7	33.7000	8.2889	7.4946	11.1747	3.0157			
NPNE	8	-31.2000	5.7146	13.2183	14.4007	-2.1666			
NPNE	9	1.7000	6.8830	9.7082	11.9006	.1428			
NPNE	10	-7.5000	3.2316	16.3174	16.6343	-.4509			
NPNE	11	5.2000	2.7021	3.0042	4.0406	1.2869			
NPNE	12	.7000	1.5701	1.6760	2.2966	.3048			
NPNE	ANN						.7750	3.2794	.2363

		MDIF	SD30	SD10	SDDIF	Z	MDIF	SDDIF	ZANN
GINE	1	-5.1000	1.7162	6.1981	6.4313	-.7930			
GINE	2	2.2000	3.3776	3.1939	4.6486	.4733			
GINE	3	10.0000	6.6092	6.4194	9.2136	1.0854			
GINE	4	19.2000	6.1710	11.6688	13.2001	1.4545			
GINE	5	-15.0000	9.0192	24.2230	25.8477	-.5803			
GINE	6	6.2000	11.7395	13.4081	17.8211	.3479			
GINE	7	19.3000	9.0009	11.8585	14.8876	1.2964			
GINE	8	-1.8000	8.3802	11.7637	14.4434	-.1246			
GINE	9	14.6000	10.5710	9.1706	13.9945	1.0433			
GINE	10	.0000	4.4183	7.6527	8.8366	.0000			
GINE	11	-3.0000	3.9801	8.3168	9.2201	-.3254			
GINE	12	1.9000	2.8299	4.7434	5.5234	.3440			
GINE	ANN						4.0417	3.8437	1.0515

		MDIF	SD30	SD10	SDDIF	Z	MDIF	SDDIF	ZANN
OMNE	1	-8.4000	2.2457	7.8108	8.1272	-1.0336			
OMNE	2	1.4000	3.6150	6.0400	7.0391	.1989			
OMNE	3	20.7000	6.2988	7.8424	10.0588	2.0579			
OMNE	4	17.9000	6.0067	11.9534	13.3778	1.3380			
OMNE	5	23.9000	10.0416	17.4558	20.1380	1.1868			
OMNE	6	21.7000	9.7495	16.0644	18.7914	1.1548			
OMNE	7	22.7000	10.6441	17.4241	20.4181	1.1118			
OMNE	8	9.8000	11.1918	20.7445	23.5710	.4158			
OMNE	9	14.3000	12.2142	16.2225	20.3066	.7042			
OMNE	10	27.0000	7.1569	5.8502	9.2437	2.9209			
OMNE	11	4.5000	5.0025	9.9928	11.1750	.4027			
OMNE	12	-2.1000	2.6291	5.9451	6.5005	-.3231			
OMNE	ANN						12.7833	4.4031	2.9032

Continued, next page

Table E.2 Continued

		MDIF	SD30	SD10	SDDIF	Z	MDIF	SDDIF	ZANN
SBNE	1	2.1000	1.6067	2.3717	2.8647	.7331			
SBNE	2	-4.8000	1.3145	2.7512	3.0491	-1.5742			
SBNE	3	.7000	3.3776	4.2058	5.3942	.1298			
SBNE	4	-28.4000	3.3776	15.3687	15.7354	-1.8048			
SBNE	5	4.1000	7.0108	13.7875	15.4676	.2651			
SBNE	6	26.3000	7.3030	6.2929	9.6402	2.7281			
SBNE	7	13.9000	5.9154	6.8621	9.0599	1.5342			
SBNE	8	-21.7000	3.0125	9.2655	9.7429	-2.2273			
SBNE	9	1.4000	5.4225	7.3049	9.0975	.1539			
SBNE	10	2.4000	2.9029	5.6605	6.3614	.3773			
SBNE	11	1.2000	2.0813	3.6682	4.2176	.2845			
SBNE	12	3.2000	1.7892	2.2136	2.8463	1.1243			
SBNE	ANN						.0333	2.5719	.0130

		MDIF	SD30	SD10	SDDIF	Z	MDIF	SDDIF	ZANN
GOKS	1	4.4000	1.3693	1.4546	1.9977	2.2025			
GOKS	2	-5.2000	1.8805	4.1426	4.5494	-1.1430			
GOKS	3	-2.0000	3.8341	7.8424	8.7295	-.2291			
GOKS	4	-5.5000	3.1950	5.7870	6.6104	-.8320			
GOKS	5	3.2000	7.1204	11.3526	13.4008	.2388			
GOKS	6	7.4000	8.2706	10.7834	13.5898	.5445			
GOKS	7	7.3000	6.1528	13.4397	14.7811	.4939			
GOKS	8	-3.1000	5.4225	13.4713	14.5217	-.2135			
GOKS	9	8.0000	6.9013	6.1664	9.2549	.8644			
GOKS	10	.1000	4.3818	12.5226	13.2671	.0075			
GOKS	11	-.2000	2.5560	5.1861	5.7818	-.0346			
GOKS	12	.4000	1.6979	2.7512	3.2330	.1237			
GOKS	ANN						1.2333	2.9389	.4197

		MDIF	SD30	SD10	SDDIF	Z	MDIF	SDDIF	ZANN
DCKS	1	-4.0000	1.7527	4.3007	4.6441	-.8613			
DCKS	2	-4.3000	2.5926	8.7911	9.1654	-.4692			
DCKS	3	7.7000	8.3984	10.2458	13.2480	.5812			
DCKS	4	3.1000	6.8465	10.3406	12.4018	.2500			
DCKS	5	-7.0000	8.7636	19.5745	21.4467	-.3264			
DCKS	6	-4.1000	9.1287	16.1909	18.5870	-.2206			
DCKS	7	49.3000	9.8042	6.8621	11.9671	4.1196			
DCKS	8	17.9000	8.4714	9.4552	12.6951	1.4100			
DCKS	9	5.6000	7.1934	9.4236	11.8553	.4724			
DCKS	10	11.5000	5.6050	5.7237	8.0111	1.4355			
DCKS	11	-5.5000	4.0349	9.9296	10.7180	-.5132			
DCKS	12	.0000	2.2457	2.4350	3.3124	.0000			
DCKS	ANN						5.8500	3.6087	1.6211

Continued, next page

Table E.2 Continued

		MDIF	SD30	SD10	SDDIF	Z	MDIF	SDDIF	ZANN
WIKS	1	-27.5000	2.8847	6.2929	6.9226	-3.9725			
WIKS	2	-8.9000	3.2133	3.9845	5.1187	-1.7387			
WIKS	3	3.3000	8.6905	11.8269	14.6766	.2248			
WIKS	4	-19.2000	6.8830	11.0363	13.0068	-1.4761			
WIKS	5	-22.7000	10.8084	17.4874	20.5580	-1.1042			
WIKS	6	-25.1000	11.9038	25.4563	28.1021	-.8932			
WIKS	7	15.2000	11.6300	18.2147	21.6109	.7033			
WIKS	8	14.8000	9.5851	14.9260	17.7386	.8343			
WIKS	9	-23.8000	12.0682	24.0333	26.8931	-.8850			
WIKS	10	-5.9000	8.1611	14.0405	16.2400	-.3633			
WIKS	11	-36.5000	6.2623	18.9104	19.9203	-1.8323			
WIKS	12	-9.5000	3.4507	8.6646	9.3265	-1.0186			
WIKS	ANN						-12.1500	5.2198	-2.3277

		MDIF	SD30	SD10	SDDIF	Z	MDIF	SDDIF	ZANN
OKOK	1	-33.8000	3.5419	12.2696	12.7706	-2.6467			
OKOK	2	-16.2000	3.7063	10.2458	10.8955	-1.4868			
OKOK	3	-21.8000	6.2258	24.1914	24.9797	-.8727			
OKOK	4	10.1000	6.9196	9.4868	11.7422	.8601			
OKOK	5	39.1000	12.3968	12.1748	17.3754	2.2503			
OKOK	6	-26.7000	11.5935	23.6538	26.3422	-1.0136			
OKOK	7	-53.5000	10.6258	48.3828	49.5359	-1.0800			
OKOK	8	-28.2000	6.9013	14.4516	16.0149	-1.7609			
OKOK	9	16.5000	11.7578	21.9462	24.8974	.6627			
OKOK	10	-.5000	9.7495	19.1318	21.4727	-.0233			
OKOK	11	-21.5000	6.2258	16.7917	17.9087	-1.2005			
OKOK	12	-42.0000	3.9436	18.0566	18.4822	-2.2725			
OKOK	ANN						-14.8750	6.7150	-2.2152

		MDIF	SD30	SD10	SDDIF	Z	MDIF	SDDIF	ZANN
AMTX	1	-6.0000	2.2639	7.3365	7.6778	-.7815			
AMTX	2	-2.6000	2.0631	7.8108	8.0787	-.3218			
AMTX	3	-8.0000	4.6374	4.8383	6.7018	-1.1937			
AMTX	4	-9.3000	3.8158	7.2732	8.2134	-1.1323			
AMTX	5	-38.5000	8.9644	21.4402	23.2389	-1.6567			
AMTX	6	10.6000	12.4516	21.3138	24.6844	.4294			
AMTX	7	36.4000	8.7270	6.2613	10.7408	3.3889			
AMTX	8	13.2000	7.3943	10.3723	12.7381	1.0363			
AMTX	9	-19.0000	6.2623	16.1592	17.3302	-1.0963			
AMTX	10	-3.5000	5.8424	12.7124	13.9906	-.2502			
AMTX	11	-5.5000	2.7934	7.3049	7.8207	-.7033			
AMTX	12	-11.5000	3.7610	8.0006	8.8405	-1.3008			
AMTX	ANN						-3.6417	3.9956	-.9114

Continued, next page

Table E.2 Continued

		MDIF	SD30	SD10	SDDIF	Z	MDIF	SDDIF	ZANN
SATX	1	-43.1000	8.2158	15.4319	17.4827	-2.4653			
SATX	2	1.8000	6.3718	6.9570	9.4340	.1908			
SATX	3	-18.9000	4.8747	9.3920	10.5817	-1.7861			
SATX	4	1.0000	10.3520	15.7798	18.8723	.0530			
SATX	5	-9.9000	12.2142	26.7845	29.4380	-.3363			
SATX	6	4.2000	10.6076	17.0447	20.0759	.2092			
SATX	7	-53.3000	11.0457	21.0291	23.7536	-2.2439			
SATX	8	25.8000	12.4881	11.7637	17.1562	1.5038			
SATX	9	17.2000	15.8292	31.2117	34.9962	.4915			
SATX	10	15.4000	10.1694	22.6735	24.8497	.6197			
SATX	11	20.9000	8.2889	7.8108	11.3892	1.8351			
SATX	12	-35.0000	5.1303	13.9773	14.8891	-2.3507			
SATX	ANN						-6.1583	6.0004	-1.0263

		MDIF	SD30	SD10	SDDIF	Z	MDIF	SDDIF	ZANN
WATX	1	-46.5000	5.8424	16.7917	17.7790	-2.6154			
WATX	2	-32.6000	5.2581	16.3174	17.1436	-1.9016			
WATX	3	-28.2000	6.5179	15.9063	17.1899	-1.6405			
WATX	4	19.0000	13.2001	13.8824	19.1563	.9918			
WATX	5	-8.1000	16.1578	26.7212	31.2266	-.2594			
WATX	6	10.3000	11.8125	18.2463	21.7363	.4739			
WATX	7	-7.7000	11.5569	19.0685	22.2974	-.3453			
WATX	8	16.8000	9.6764	7.1784	12.0483	1.3944			
WATX	9	-30.0000	9.7495	39.9396	41.1123	-.7297			
WATX	10	12.5000	11.0275	23.8752	26.2989	.4753			
WATX	11	-10.6000	7.6133	13.3448	15.3638	-.6899			
WATX	12	-47.3000	7.4308	11.9534	14.0748	-3.3606			
WATX	ANN						-12.7000	6.5502	-1.9389

BIBLIOGRAPHY

Ackerson, R.C., U.D. Havelka, and M.G. Boyle. 1984. CO_2-enrichment effects on soybean physiology. II. Effects of stage-specific CO_2 exposure. Crop Sci. 24:1150-1154.

Acock, B. and L.H. Allen, Jr. 1985. Crop responses to elevated carbon dioxide concentrations. In B.R. Strain and J.D. Cure (eds.). Direct Effects of Increasing Carbon Dioxide on Vegetation, DOE/ER-0238, US Dept. of Energy, Washington, D.C. pp. 53-97.

Adams, R.M., J.D. Glyer, and B.A. McCarl. 1989. The economic effects of climate change on U.S. agriculture: A preliminary assessment. In J.B. Smith and D. Tirpak (eds.). The Potential Effects of Global Climate Change on the United States. Report to Congress. Appendix C-1. EPA-230-05-89-053. U.S. Environmental Protection Agency. Washington, D.C. pp. 4-1 - 4-56.

Allen, L.H., Jr., P. Jones, and J.W. Jones. 1985. Rising atmospheric CO_2 and evapotranspiration. In Advances in Evapotranspiration. Proceedings of the National Conference on Advances in Evapotranspiration. December 16-17, 1985. American Society of Agricultural Engineers. St. Joseph, Michigan. pp. 13-27.

Azcon-Bieto, J. 1983. Inhibition of photosynthesis by carbohydrates in wheat leaves. Plant Physiol. 73:681-686.

Bach, W. 1988. Development of climatic scenarios: A. From general circulation models. In M.L. Parry, T.R. Carter, and N.T. Konijn. (eds.). 1988. The Impact of Climatic Variations on Agriculture. Volume 1. Assessment in Cool Temperate and Cold Regions. Kluwer Academic Publishers. Dordrecht. pp. 125-157.

Baker, J.T., L.H. Allen, Jr., K.J. Boote, P. Jones, and J.W. Jones. 1989. Response of soybean to air temperature and carbon dioxide concentration. Crop Sci. 29:98-105.

Barnola, J.M., D. Raynaud, Y.S. Korotkevich, and C. Lorius. 1987. Vostok ice core provides 160,000-year record of atmospheric CO_2. Nature 329:408-414.

Bazzaz, F.A. 1990. The response of natural ecosystems to the rising global CO_2 levels. Ann. Rev. Ecol. Syst. 21:167-196.

Blake, D.R. and F.S. Rowland. 1988. Continuing worldwide increase in tropospheric methane, 1978-1987. Science 239:1129-1131.

Blasing, T.J. and A.M. Solomon. 1983. Response of the North American Corn Belt to Climatic Warming. U.S. Department of Energy. DOE/NBB-0040. 27 pp.

Boden, T.A., P. Kanciruk, and M.P. Farrell. 1990. Trends '90: A Compendium of Data on Global Change. ORNL/CDIAC-36. Carbon Dioxide Information Analysis Center, Oak Ridge National Laboratory, Oak Ridge, Tennessee, 286 pp.

Bradley, R.S., H.F. Diaz, J.K. Eischeid, P.D. Jones, P.M. Kelly, and C.M. Goodess. 1987. Precipitation fluctuations over Northern Hemisphere land areas since the mid-19th century. Science 237:171-175.

Budyko, M.I. 1974. Climate and Life. Academic Press. New York.

Chandrasekhar, S. 1960. Radiative Transfer. Dover Publications, Inc. New York. 393 pp.

Charles-Edwards, D.A. 1982. Physiological Determinants of Crop Growth. Academic Press. New York. 161 pp.

Chaudhuri, U.N., R.B. Burnett, E.T. Kanemasu, M.B. Kirkham. 1986. Effect of Elevated Levels of CO_2 on Winter Wheat under Two Moisture Regimes. 029 in series: Response of Vegetation to Carbon Dioxide. U.S. Department of Energy. 71 pp.

Cure, J.D. 1985. Carbon dioxide doubling responses: A crop survey. In B.R. Strain and J.D. Cure (eds.). Direct Effects of Increasing Carbon Dioxide on Vegetation, DOE/ER-0238, US Dept. of Energy, Washington, D.C. pp. 99-116.

Delmas, R.J., J.M. Ascencio, and M. Legrand. 1980. Polar ice evidence that atmospheric CO_2 20,000 yr-BP was 50% of present. Nature 284:155-157.

Diaz, H.F., R.S. Bradley, and J.K. Eischeid. 1989. Precipitation fluctuations over global land areas since the late 1800s. J. Geophys. Res. 94:1195-1210.

Doorenbos, J. and A.H. Kassam. 1979. Yield Response to Water. FAO Irrigation and Drainage Paper 33. United Nations Food and Agriculture Organization. Rome. 193 pp.

Emmett, E.E. 1986. Health effects of ultraviolet radiation. In J.G. Titus (ed.) Effects of Changes in Stratospheric Ozone and Global Climate. Volume 1: Overview. U.S. Environmental Protection Agency. Washington, D.C. pp. 129-145.

Evans, L.T., I.F. Wardlaw, and R.A. Fischer. 1975. Wheat. In L.T. Evans (ed.). Crop Physiology. Cambridge University Press. Cambridge. pp. 101-149.

Fitter, A.H. and R.K.M. Hay. 1987. Environmental Physiology of Plants. 2nd ed. Academic Press. London. 423 pp.

France, J. and J.H.M. Thornley. 1984. Mathematical Models in Agriculture. Butterworths. Boston. 335 pp.

Frazier, I. 1989. Great Plains. Penguin Books. New York. 292 pp.

Frederick, K.D. and J.C. Hanson. 1982. Water for Western Agriculture. Resources for the Future. Washington, D.C. 241 pp.

Gedzelman, S.D. 1980. The Science and Wonders of the Atmosphere. John Wiley & Sons. New York. 535 pp.

Glantz, M.H. and J.H. Ausubel. 1984. The Ogallala Aquifer and carbon dioxide: Comparison and convergence. Environmental Conservation 11(2):123-31.

Grotch, S.L. 1988. Regional Intercomparisons of General Circulation Model Predictions and Historical Climate Data. DOE/NBB-0084. U.S. Department of Energy. Washington, D.C. 291 pp.

Hansen, J., D. Johnson, A. Lacis, S. Lebedeff, P. Lee, D. Rind, and G. Russell. 1981. Climate impact of increasing atmospheric carbon dioxide. Science 213:957-966.

Hansen, J., G. Russell, D. Rind, P. Stone, A. Lacis, S. Lebedeff, R. Ruedy, and L. Travis. 1983. Efficient three-dimensional global models for climate studies: Models I and II. Monthly Weather Review 111(4):609-662.

Hansen, J.E., A. Lacis, D. Rind, G. Russell, P. Stone, I. Fung, R. Ruedy, and J. Lerner. 1984. Climate sensitivity: Analysis of feedback mechanisms. In W.C. Clark (ed.). Climate Processes and Climate Sensitivity. Series 5. Clarendon Press. New York. pp. 284-286.

Hansen, J. and S. Lebedeff. 1987. Global trends of measured surface air temperature. J. Geophys. Res. 92:13345-13372.

Hansen, J. and S. Lebedeff. 1988. Global surface temperatures: update through 1987. Geophys. Res. Letters. 15:323-326.

Hansen, J., I. Fung, A. Lacis, S. Lebedeff, D. Rind, R. Ruedy, G. Russell, and P. Stone. 1988a. Prediction of near-term climate evolution: What can we tell decision-makers now? In Preparing for Climate Change. Proceedings of the First North American Conference on Preparing for Climate Change: A Cooperative Approach. October 27-29, 1987. Climate Institute. Washington, D.C. pp. 35-47.

Hansen, J., I. Fung, A. Lacis, D. Rind, S. Lebedeff, R. Ruedy, and G. Russell. 1988b. Global climate changes as forecast by Goddard Institute for Space Studies three-dimensional model. J. Geophys. Res. 93(D8):9341-9364.

Hansen, J., D. Rind, A. DelGenio, A. Lacis, S. Lebedeff, M. Prather, R. Ruedy. 1989. Regional greenhouse climate effects. In J. Topping (ed.). Coping with Climate Change., Proceedings of the Second North American Conference on Preparing for Climate Change: A Cooperative Approach. December 6-8, 1988. Climate Institute, Washington, DC. pp. 68-81.

Henderson-Sellers, A. and K. McGuffie. A Climate Modelling Primer. John Wiley & Sons. Chichester. 217 pp.

High Plains Associates. 1982. Six-State High Plains Ogallala Aquifer Regional Resources Study: Summary. Camp Dresser and McKee. Austin, TX.

Hillel, D. 1987. The Efficient Use of Water in Irrigation. The World Bank. World Bank Technical Paper Number 64. Washington, D.C. 107 pp.

Hillel, D. 1990. Role of irrigation in agricultural systems. In Irrigation of Agricultural Crops. ASA-CSSA-SSSA. Agronomy Monograph no. 30. pp. 5-30.

Hillel, D. and C. Rosenzweig. 1989. The Greenhouse Effect and Its Implications Regarding Global Agriculture. Massachusetts Agricultural Experiment Station. Research Bulletin Number 724. Amherst. 36 pp.

Hodges, Tom. 1991. Predicting Crop Phenology. CRC Press. Boca Raton. 233 pp.

Hodges, T., V. French, and S. LeDuc. 1985. Yield Model Development: Estimating Solar Radiation for Plant Simulation Models. YM-15-00403 JSC-20239. AgRISTARS.

Hoffman, J.S., D. Keyes, and J.G. Titus. 1983. Projecting Future Sea Level Rise, Methodology, Estimates to the Year 2100, and Research Needs. EPA 230-09-007. U.S. Environmental Protection Agency. Washington, D.C. 121 pp.

Houghton, R.A., R.D. Boone, J.R. Fruci, J.E. Hobbie, J.M. Melillo, C.A. Palm, B.J. Peterson, G.R. Shaver, G.M. Woodwell, B. Moore, D.L. Skole, and N. Myers. 1987. The flux of carbon from terrestrial ecosystems to the atmosphere in 1980 due to changes in land use: Geographic distribution of the global flux. Tellus 39B:122-139.

Huber, S.C., H.H. Rogers, and F.L. Mowray. 1984. Effects of water stress on photosynthesis and carbon partitioning in soybean (Glycine max [L.] Merr.) plants grown in the field at different CO_2 levels. Plant Physiol., 76:244-249.

Hurt, R.D. 1981. The Dust Bowl. Nelson-Hall. Chicago. 214 pp.

Idso, S.B., B.A. Kimball, and J.R. Mauney. 1987a. Atmospheric carbon dioxide enrichment effects on cotton midday foliate temperature: Implications for plant water use and crop yield. Agron. J. 79:667-672.

Idso, S.B., B.A. Kimball, M.G. Anderson, and J.R. Mauney. 1987: Effects of atmospheric CO_2 enrichment on plant growth: the interactive role of air temperature. Agriculture, Ecosystems and Environment. 20:1-10.

Intergovernmental Panel on Climate Change. 1990. Climate Change: The IPCC Scientific Assessment. J.T. Houghton, G.J. Jenkins, and J.J. Ephraums (eds.). World Meteorological Organization and United Nations Environmental Program. Cambridge University Press. Cambridge. 365 pp.

Johnson, R.C. and E.T. Kanemasu. 1983. Yield and development of winter wheat at elevated temperatures. Agron. J. 75:561-565.

Jones, C.A. and J.R. Kiniry. 1986. CERES-Maize: A Simulation Model of Maize Growth and Development. Texas A&M Press. College Station. 194 pp.

Jones, P. L.H. Allen, Jr., J.W. Jones, K.J. Boote, and W.J. Campbell. 1984. Soybean canopy growth, photosynthesis, and transpiration responses to whole-season carbon dioxide enrichment. Agron. J. 76:633-637.

Jones, P., L.H. Allen, Jr., and J.W. Jones. 1985. Responses of soybean canopy photosynthesis and transpiration to whole-day temperature changes in different CO_2 environments. Agron. J. 77:242-249.

Joyce, L.A. and R.N. Kickert. 1987. Applied plant growth models for grazing lands, forests, and crops. In K. Wisiol and J.D. Hesketh (eds.). Plant Growth Modeling for Resource Management Volume I Current Models and Methods. CRC Press, Inc. Boca Raton, Florida. pp. 17-55.

Jurik, T.W., J.A. Weber, and D.M. Gates. 1984. Short-term effects of CO_2 on gas exchange of leaves of bigtooth aspen (Populus grandidentata) in the field. Plant Physiol. 75:1022-1026.

Kellogg, W.W. and Z.-C. Zhao. 1988. Sensitivity of soil moisture to doubling of carbon dioxide in climate model experiments, I, North America. J. Clim. 1:348-366.

Kimball, B.A. 1983. Carbon dioxide and agricultural yield: an assemblage and analysis of 430 prior observations. Agron. J. 75:779-788.

Kimball, B.A., J.R. Mauney, G. Guinn, F.S. Nakayama, P.J. Pinter, Jr., K.L. Clawson, S.B. Idso, G.D. Butler, and J.R. Radin. 1984. Effects of increasing atmospheric CO_2 on the yield and water use of crops. 023 in series: Response of Vegetation to Carbon Dioxide. U.S. Departments of Energy and Agriculture. 60 pp.

Kimball, B.A., J.R. Mauney, J.W. Radin, F.S. Nakayama, S.B. Idso, D.L. Hendrix, D.H. Akey, S.G. Allen, M.G. Anderson, and W. Hartung. 1986. Effects of increasing atmospheric CO_2 on the growth, water relations, and physiology of plants grown under optimal and limiting levels of water and nitrogen. 039 in series: Response of Vegetation to Carbon Dioxide. U.S. Departments of Energy and Agriculture. 125 pp.

King, K.M. and D.H. Greer. 1986. Effects of carbon dioxide enrichment and soil water on maize. Agron. J. 78:515-521.

Kobza, J. and G.E. Edwards. 1987. Influence of leaf temperature on photosynthetic carbon metabolism in wheat. Plant Physiol. 83:69-74.

Kondratyev, K. Ya. 1972. Radiation Processes in the Atmosphere. WMO - No. 309. World Meteorological Organization. 214 pp.

Larcher, W. 1980. Physiological Plant Ecology. 2nd edition. Springer-Verlag. Berlin. 303 pp.

Lashof, D.A. and D.A. Tirpak (eds.). 1989. Policy Options for Stabilizing Global Climate. U.S. Environmental Protection Agency Draft Report to Congress. Washington, D.C.

Lemon, E.R. (ed.). 1983. CO_2 and Plants: AAAS Selected Symposium 84. Westview Press, Inc. Boulder, Colorado. 280 pp.

Levitt, J. 1980. Responses of Plants to Environmental Stresses. Vol. I. Chilling, Freezing, and High Temperature Stresses. Academic Press. New York. 497 pp.

Liverman, D.M., W.H. Terjung, J.T. Hayes, and L.O. Mearns. 1986. Climatic change and grain corn yields in the North American Great Plains. Climatic Change 9:327-347.

Lockeretz, W. 1978. The lessons of the Dust Bowl. American Scientist 66(5):560-569.

Loomis, R.S., R. Rabbinge, and E. Ng. 1979. Explanatory models in crop physiology. Annu. Rev. Plant Physiol. 30:339.

MacCracken, M.C. and F.M. Luther (eds.). 1985. Projecting the Climatic Effects of Increasing Carbon Dioxide. U.S. Department of Energy. DOE/ER-0237. Washington, D.C. 381 pp.

Manabe, S. and R. Wetherald. 1987. Large-scale changes of soil wetness induced by an increase in atmospheric carbon dioxide. J. Atmos. Sci. 44:1211-1236.

Mearns, L.O., R.W. Katz, and S.H. Schneider. 1984. Extreme high temperature events: Changes in their probabilities with changes in mean temperature. Journal of Climate and Applied Meteorology 23:1601-1613.

Mederski, H.J. 1983. Effects of water and temperature stress on soybean plant growth and yield in humid temperate climates. In C.D. Raper and P.J. Kramer (eds.). Crop Reactions to Water and Temperature Stresses in Humid, Temperate Climates. Westview press. Boulder. pp. 35-48.

Mitchell, J.F.B., C.A. Wilson, and W.M. Cunnington. 1987. On CO_2 climate sensitivity and model dependence of results. Q.J.R. Meteorol. Soc.: 113:293-322.

Mitchell, J.F.B. 1989. The "greenhouse" effect and climate change. Reviews of Geophysics 27(1):115-139.

Mitchell, J.F.B., S. Manabe, T. Tokioka and V. Meleshko. 1990. Equilibrium climate change -- and its implications for the future. In J.T. Houghton, G.J. Jenkins and J.J. Ephraums (eds.). Climate Change: The IPCC Scientific Assessment. World Meteorological Organization and United Nations Environmental Program.Cambridge University Press. Cambridge. pp. 131-172.

Montreal Protocol on Substances that Deplete the Ozone Layer, adopted and opened for signature Sept. 16, 1987, reprinted in 26 I.L.M. 1541 (1987) (entered into force Jan. 1, 1989).

Morison, J.I.L. and R.M. Gifford. 1983. Stomatal sensitivity to carbon dioxide and humidity. A comparison of two C3 and two C4 grass species. Plant Physiol. 71:789-796.

Morison, J.I.L. and R.M. Gifford. 1984. Plant growth and water use with limited water supply in high CO_2 concentrations. I. Leaf area, water use and transpiration. Austral. J. Plant Physiol. 11:361-374.

National Research Council. 1983. Changing Climate. National Academy Press. Washington, D.C. 496 pp.

Neftel, A., H. Oeschger, R.J. Schwander, B. Stauffer, and R. Zumbrunn. 1982. Ice core sample measurements give atmospheric CO_2 content during the past 40,000 years. Nature 295:220-223.

Otter-Nacke, S., D.C. Godwin, and J.T. Ritchie. 1986. Testing and Validating the CERES-Wheat Model in Diverse Environments. YM-15-00407 JSC 20244. AgRISTARS. Earth Resources Applications Division. Lyndon B. Johnson Space Center. Houston, Texas 77058. 147 pp.

Parry, M.L. and T.R. Carter. 1985. The effect of climatic variations on agricultural risk. Climatic Change 7:95-110.

Parry, M.L., T.R. Carter, and N.T. Konijn. (eds.). 1988. The Impact of Climatic Variations on Agriculture. Volume 1. Assessment in Cool Temperate and Cold Regions. Kluwer Academic Publishers. Dordrecht. 876 pp.

Peart, R.M., J.W. Jones, R.B. Curry, K. Boote, and L.H. Allen, Jr. 1989. Impact of climate change on crop yield in the southeastern U.S.A. In J.B. Smith and D. Tirpak (eds.). The Potential Effects of Global Climate Change on the United States. Report to Congress. Appendix C-1. EPA-230-05-89-053. U.S. Environmental Protection Agency. Washington, D.C. pp. 2-1 - 2-54.

Prinn, R.G. 1988. How have the atmospheric concentrations of the halocarbons changed? In F.S. Rowland and I.S.A. Isaksen (eds.). The Changing Atmosphere. John Wiley & Sons Ltd. pp. 33-48.

Ramanathan, V., R.J. Cicerone, H.B. Singh, and J.T. Kiehl. 1985. Trace gas trends and their potential role in climate change. J. Geophys. Res. 90(D3):5547-5566.

Ramanathan, V. 1988. The radiative and climatic consequences of the changing atmospheric composition of trace gases. In F.S. Rowland and I.S.A. Isaksen (eds.). The Changing Atmosphere. John Wiley & Sons, Ltd. pp. 159-186.

Revelle, R.R. and P.E. Waggoner. 1983. Effects of the carbon dioxide induced climatic change on water supplies in the western United States. In Changing Climate: Report of the Carbon Dioxide Assessment Committee. National Academy Press. Washington, DC.

Richardson, C.W. and D.A. Wright. 1984. WGEN: A Model for Generating Daily Weather Variables. ARS-8. U.S. Department of Agriculture. Agricultural Research Service. 83 pp.

Riebsame, W.E. 1990. The Great Plains. In B.L. Turner II and W.B. Meyer (eds.). The Earth as Transformed by Human Action. Cambridge University Press. Cambridge, UK.

Rimmington, G.M. and D.A. Charles-Edwards, 1987. Mathematical descriptions of plant growth and development. In K. Wisiol and J.D. Hesketh (eds.). Plant Growth Modeling for Resource Management Volume I Current Models and Methods. CRC Press, Inc. Boca Raton. pp. 3-15.

Rind, D., R. Goldberg, J. Hansen, C. Rosenzweig, and R. Ruedy. 1990. Potential evapotranspiration and the likelihood of future drought. J. Geophys. Res. 95(D7):9983-10,004.

Ritchie, J.T., B.D. Baer, and T.Y. Chou. 1989. Effect of global climate change on agriculture: Great Lakes region. In J.B. Smith and D. Tirpak (eds.). The Potential Effects of Global Climate Change on the United States. Report to Congress. Appendix C-1. EPA-230-05-89-053. U.S. Environmental Protection Agency. Washington, D.C. pp. 1-1 - 1-30.

Ritchie, J.T. and S. Otter. 1985. Description and performance of CERES-Wheat: A user-oriented wheat yield model. In W.O. Willis (ed.). ARS Wheat Yield Project. ARS - 38. USDA-ARS. pp. 159-175.

Robertson, T., V.W. Benson, J.R. Williams, C.A. Jones, and J.R. Kiniry. 1987. Impacts of climate change on yields and erosion for selected crops in the southern United States. In M. Meo (ed.) Proceedings of the Symposium on Climate Change in the Southern United States: Future Impacts and Present Policy Issues. Science and Public Policy Program. University of Oklahoma. Norman, OK. pp. 73-88.

Rogers, H.H., G.E. Bingham, J.D. Cure, J.M Smith, and K.A. Surano. 1983. Responses of selected plant species to elevated carbon dioxide in the field. J. Environ. Qual. 12:569-574.

Rose, E. 1989. Direct (physiological) effects of increasing CO_2 on crop plants and their interactions with indirect (climatic) effects. In J.B. Smith and D. Tirpak (eds.). The Potential Effects of Global Climate Change on the United States. Report to Congress. Appendix C-2. EPA-230-05-89-053. U.S. Environmental Protection Agency. Washington, D.C. pp. 7-1 - 7-37.

Rosenzweig, C. 1985. Potential CO_2-induced climate effects on North American wheat-producing regions. Climatic Change 7:367-389.

Sahrawat, K.L. and D.R. Keeney. 1986. Nitrous oxide emissions from soils. Advances in Soil Science 4:103-148.

Salisbury, F.B. and C.W. Ross. 1978. Plant Physiology. Wadsworth Publishing Company, Inc. Belmont, CA. 422 pp.

Santer, B. 1985. The use of general circulation models in climate impact analysis - A preliminary study of the impacts of a CO_2-induced climatic change on Western European agriculture. Climatic Change 7:71-93.

Schönfeld, R.C. Johnson, and D.M. Ferris. 1989. Development of winter wheat under increased atmospheric CO_2 and water limitation at tillering. Crop Sci. 29:1083-1086.

Schlesinger, M. and Z. Zhao. 1988. Seasonal climate changes induced by doubled CO_2 simulated by the OSU atmospheric GCM/mixed layer ocean mode. Oregon State University, Climate Research Institute. Corvallis, OR.

Sellers, William D. 1965. Physical Climatology. The University of Chicago Press. Chicago. 272 pp.

Shaw, R.H. 1983. Estimates of yield reductions in corn caused by water and temperature stress. In C.D. Raper and P.J. Kramer (eds.). Crop Reactions to Water and Temperature Stresses in Humid, Temperate Climates. Westview press. Boulder. pp. 49-66.

Smit, B., M. Brklacich, R.B. Stewart, R. McBride, M. Brown, and D. Bond. 1989. Sensitivity of crop yields and land resource potential to climatic change in Ontario, Canada. Climatic Change 14:153-174.

Smit, B., L. Ludlow, and M. Brklacich. 1988. Implications of a global climatic warming for agriculture: A review and appraisal. J. Environ. Qual. 17(4):519-527.

Smith, J.B. and D. Tirpak (eds.). 1989. The Potential Effects of Global Climate Change on the United States. Report to Congress. EPA-230-05-89-050. U.S. Environmental Protection Agency. Washington, D.C. 423 pp.

Stewart, R.B. 1986. Climatic change: Implications for the Prairies. Trans. Roy. Soc. Can. Series V/I:67-96.

Stouffer, R.J., S. Manabe, and K. Bryan. 1989. Interhemispheric asymmetry in climate response to a gradual increase of atmospheric CO_2. Nature 342:660-662.

Tandon, J.P. 1985. Wheat improvement programs for the hotter parts of India. In Wheats for More Tropical Environments, A Proceedings of the International Symposium. CIMMYT. El Batan, Mexico. pp. 63-67.

Terjung, W.H., D.M. Liverman, and J.T. Hayes. 1984. Climatic change and water requirements for grain corn in the North American Great Plains. Climatic Change 6:193-220.

Thomas, J.F. and C.N. Harvey. 1983. Leaf anatomy of four species grown under continuous CO_2 enrichment. Bot. Gaz. 144:303-309.

Tolbert, N.E. and I. Zelitch. 1983. Carbon metabolism. In E.R. Lemon (ed.) 1983. CO_2 and Plants: AAAS Selected Symposium 84. Westview Press, Inc. Boulder, Colorado. pp. 21-64.

U.S. Department of Agriculture. 1981. Land Resource Regions and Major Land Resource Areas of the United States. Agricultural Handbook #296. Soil Conservation Service. Washington, D.C.

U.S. Department of Commerce. 1984. 1982 Census of Agriculture. Volume 1. Geographic Area Series. Part 51. United States Summary and State Data. Washington, D.C.

Wall, G.W. and D.N. Baker. 1987. Effects of temperature and elevated carbon dioxide concentrations on the phenology of spring wheat. Agron. Abstr. 1987. p.18.

Warrick, R.A. and M.J. Bowden. 1981. The changing impacts of drought in the Great Plains. In M.P. Lawson and M.E. Baker (eds.). The Great Plains: Perspectives and Prospects. University of Nebraska Press. Lincoln. pp. 111-137.

Warrick, R.A. 1984. The possible impacts on wheat production of a recurrence of the 1930s drought in the U.S. Great Plains. Climatic Change 6:5-26.

Washington, W. and G. Meehl. 1989. Climate sensitivity due to increased CO_2: experiments with a coupled atmosphere and ocean general circulation model. Clim. Dynamics 4:1-38.

Watson, R.T. 1986. Atmospheric ozone. In J.G. Titus (ed.) Effects of Changes in Stratospheric Ozone and Global Climate. Volume 1: Overview. U.S. Environmental Protection Agency. Washington, D.C. pp. 69-82.

Wigley, T.M.L. 1985. Impact of extreme events. Nature 316:106-107.

Wigley, T.M.L., J. Angell, and P.D. Jones. 1985. Analysis of the temperature record. In M.C. MacCracken and F.M. Luther (eds.). Detecting the Climatic Effects of Increasing Carbon Dioxide. DOE/ER-0235. U.S. Dept. of Energy. Washington, D.C. pp. 55-90.

Wilhite, D.A. 1988. The Ogallala Aquifer and carbon dioxide: Are policy responses applicable? In M.H. Glantz (ed.). Societal Responses to Regional Climatic Change: Forecasting by Analogy. Westview Press. Boulder. pp. 353-373.

World Meteorological Organization, 1985. Report of the WMO/UNEP/ICSU-SCOPE Expert Meeting on the Reliability of Crop-Climate Models for Assessing the Impacts of Climatic Change and Variability. WCP-90. Geneva. 31 pp.

Worster, D. 1979. Dust Bowl: The Southern Plains in the 1930s. Oxford University Press. New York. 277 pp.